AD_____

Award Number: DAMD17-99-1-9126

TITLE: Photodynamic Therapy Oxidative Stress as a Molecular Switch Controlling Therapeutic Gene Expression for the Treatment of Locally Recurrent Breast Carcinoma

PRINCIPAL INVESTIGATOR: Charles J. Gomer, Ph.D.

CONTRACTING ORGANIZATION: Children's Hospital of Los Angeles
Los Angeles, California 90027

REPORT DATE: June 2002

TYPE OF REPORT: Final

PREPARED FOR: U.S. Army Medical Research and Materiel Command
Fort Detrick, Maryland 21702-5012

REPORT DOCUMENTATION PAGE

Form Approved
OMB No. 074-0188

1. AGENCY USE ONLY (Leave blank)	2. REPORT DATE	3. REPORT TYPE AND DATES COVERED
	June 2002	Final (1 Jun 99 - 31 May 02)

4. TITLE AND SUBTITLE
Photodynamic Therapy Oxidative Stress as a Molecular Switch Controlling Therapeutic Gene Expression for the Treatment of Locally Recurrent Breast Carcinoma

5. FUNDING NUMBERS
DAMD17-99-1-9126

6. AUTHOR(S)

Charles J. Gomer, Ph.D.

7. PERFORMING ORGANIZATION NAME(S) AND ADDRESS(ES)

Children's Hospital of Los Angeles
Los Angeles, California 90027

E-Mail: cgomer@chla.usc.edu

8. PERFORMING ORGANIZATION REPORT NUMBER

9. SPONSORING / MONITORING AGENCY NAME(S) AND ADDRESS(ES)

U.S. Army Medical Research and Materiel Command
Fort Detrick, Maryland 21702-5012

10. SPONSORING / MONITORING AGENCY REPORT NUMBER

11. SUPPLEMENTARY NOTES

12a. DISTRIBUTION / AVAILABILITY STATEMENT

Approved for Public Release; Distribution Unlimited

12b. DISTRIBUTION CODE

13. ABSTRACT ***(Maximum 200 Words)***

Photodynamic Therapy (PDT) is a developing therapeutic modality which continues to show promise in the clinical treatment of cancer, including locally recurrent breast carcinoma. Our application is directly related to using novel molecular technologies to improve the effectiveness of PDT for treating locally recurrent breast cancers. In PDT, properties of photosensitizer localization in tumor tissue and photochemical generation of reactive oxygen species are combined with precise delivery of laser-generated light to produce a procedure offering local tumoricidal activity. We have demonstrated that PDT-mediated oxidative stress is a strong transcriptional inducer of stress proteins belonging to the heat shock protein (hsp) and glucose regulated protein (grp) families. We have also shown that the hsp and grp promoters can drive inducible expression of heterologous genes following PDT mediated oxidative stress. Inducible expression and function of p53 as well as inducible expression, secretion and biological activity of TNF-α have been demonstrated in human tumor cells. We have also demonstrated PDT inducible expression of the suicide gene HSV-thymidine kinase and enhanced tumoricidal action when PDT is combined with inducible HSV-TK gene therapy. These studies address a critical problem associated with improving treatments for locally recurrent breast cancer using new approaches which will minimize systemic toxicity and maximize a patient's quality of life.

14. SUBJECT TERMS
breast cancer, photodynamic therapy (PDT), therapeutic modality, photosensitizer, photochemical, tumoricidal activity

15. NUMBER OF PAGES
37

16. PRICE CODE

17. SECURITY CLASSIFICATION OF REPORT	18. SECURITY CLASSIFICATION OF THIS PAGE	19. SECURITY CLASSIFICATION OF ABSTRACT	20. LIMITATION OF ABSTRACT
Unclassified	Unclassified	Unclassified	Unlimited

Table of Contents

Army Grant Progress Report

Introduction:

Photodynamic therapy (PDT) is a therapeutic modality which has recently obtained FDA approval for the treatment of solid tumors. This therapy continues to show progress in clinical trials for a variety of malignancies including locally recurring breast cancer. However, recurrences can occur following PDT treatment. Our research efforts have been directed at combining laser inducible gene therapy techniques with photodynamic therapy in an effort to improve the effectiveness of PDT for treating breast cancers. Photodynamic therapy involves the localization of photosensitizer within tumor tissue and the photochemical generation of reactive oxygen species such as singlet oxygen following the delivery of laser light specifically to the tumor tissue. The activating non-thermal light is normally generated by lasers and delivered via fiber optic cables. The procedure is highly localized and produces minimal systemic toxicity when compared to conventional chemotherapy or radiation therapy. Tumor responses following PDT have been positive but there remains considerable need for improvement in this therapy modality. At a molecular level photodynamic therapy mediated oxidative stress is a strong transcriptional inducer of variety of genes including those encoding stress proteins such as heat shock proteins (hsp) and glucose regulated proteins (grp). Elements within the promoter regions of genes encoding stress proteins can be used to efficiently drive inducible expression of therapeutic genes following photodynamic therapy. This is the type of combined treatment (PDT plus inducible gene therapy) observations that we wish to exploit in enhancing the therapeutic response of PDT for breast cancer. These studies address a critical problem associated with improving treatments for locally recurring breast cancer using new approaches which will minimize toxicity and maximize quality of life.

Body:

The two specific tasks outlined in the Statement of Work of our originally approved project were: 1) to transfect breast cancer cells with PDT inducible expression vectors and evaluate the gene expression, and 2) to determine the tumoricidal efficacy of photodynamic therapy in mice implanted with breast cancer cells containing PDT inducible expression vectors. Task #1 was further broken down to involve obtaining stably transfected cell lines, evaluation of the expression of therapeutic genes, and the production of tumors in mice containing cells stably transfected with the inducible gene expression vectors. In our initial work the efficacy of PDT to function as a molecular switch by initiating expression of heterologous genes ligated to the human heat shock promoter (hsp) promoter was examined (1). Selective and temporal reporter gene expression was documented after PDT in mouse cancer cells stably transfected with recombinant vectors containing an hsp promoter ligated to either the lac-z or CAT reporter genes as well as in transfected tumors grown in mice. Hyperthermia treatments were included as a positive control for the activation of the hsp promoter for all experiments. Expression vectors containing either human p53 or tumor necrosis factor (TNF)-$\propto$ cDNA under the control of the hsp promoter were also constructed and evaluated. A p53 null and TNF-$\propto$ resistant ovarian carcinoma (SKOV-3) cell line was

stably transfected with either the p53 or TNF-∝ constructs. Inducible expression and function of p53 as well as inducible expression, secretion, and biological activity of TNF-∝ were documented after PDT or hyperthermia in transfected SKOV cells (1). These results demonstrated for the first time that PDT-mediated oxidative stress could function as a molecular switch for the selective and temporal expression of heterologous genes in tumor cells containing expression vectors under the control of an hsp promoter.

We have also used a PDT inducible glucose regulated protein (grp) promoter for studies associated with Task #1 since we see enhanced inducible expression with this promoter. We have used the therapeutic thymidine kinase (TK) suicide gene for these experiments. Our studies show that inducible expression of the herpes simplex virus (HSV) thymidine kinase gene is observed in mammary carcinoma cells lines stably transfected with a G1NaGrpTK retroviral inducible gene expression vector. This inducible expression vector is selectable by G418 and the vector has been stably transduced into mammary carcinoma cells. Activation of the grp promoter in this vector can lead to expression of the herpes simplex virus thymidine kinase gene. Cell lysates of the stably transfected cells were assayed for thymidine kinase levels using Western immunoblot analysis following PDT treatments (2). Non-transduced parental cells do not exhibit TK thymidine kinase expression. Transduced cells which served as non-treated controls exhibited basal levels and transduced cells exposed to PDT showed significant expression of thymidine kinase.

At the cellular level, we found that the expression level of thymidine kinase was a function of photodynamic therapy treatment conditions (photosensitizer dose, light dose, incubation conditions) as well as the actual time intervals between light exposure and analysis. These studies have been evaluated utilizing Western Immunoblot analysis with a polyclonal HSV antibody. Our results have demonstrated that thymidine kinase expression occurs between 8 and 36 hours after photodynamic therapy treatment with maximal expression occurring between 12 to 24 hours after treatment. Minimal expression is observed immediately after photodynamic therapy. Likewise, the temporal nature of our PDT inducible gene expression system is evident by the fact that HSV thymidine kinase expression returns to background levels at 72 hours following treatment. In all cases, expression of the thymidine kinase protein was evaluated in direct comparison to actin expression. A second issue of considerable importance at the cellular level was to determine the actual PDT doses which were associated with maximal expression of thymidine kinase. In this regard, we observed that photodynamic therapy doses in the range of 315 to 420 J/cm^2 (with a 25 ug/ml Photofrin photosensitizer incubation) were associated with maximal thymidine kinase expression. Positive expression controls used the grp inducible calcium ionophor A23187. These data provide new and essential information regarding the parameters associated with effective inducible gene therapy initiated by photodynamic therapy.

The final set of Task #1 studies involved the in-vivo analysis of inducible gene expression parameters. Specifically, the questions of PDT dose and time intervals following treatment were analyzed using stably transfected mammary carcinoma cells transplanted as tumors in mice. The ability of in-vivo PDT treatments to induce

expression of thymidine kinase was fairly uniform. PDT light doses ranging from 50 J/cm^2 up to 300 J/cm^2 all appear to be effective in the expression of thymidine kinase within solid tumor masses when a 5 mg/kg Photofrin drug dose was used. Thymidine kinase expression diminished above a dose of 300 J/cm^2. We assume that this decrease in thymidine kinase expression correlates with a near complete killing of all tumor cells and/or disruption of protein synthesis apparatus within the treated tumor tissue. Our studies of PDT controlled induction of thymidine kinase expression within tumors also illustrated that the kinetics for thymidine kinase expression plateau approximately 12 hours following treatment and remained steady up to 36 hours. Time periods after 36 hours were not obtainable due to the minimal amount of viable cells that one could collect.

After we had positively demonstrated proof of principal that PDT can selectively induce HSV-TK expression in tumors, we next set out to examine whether this expression can actually modulate breast cancer treatment response as outlined in Task 2. Our results show that inducible gene therapy using the grp promoter to drive expression of the HSV-Tk suicide gene does enhance tumoricidal action of PDT (2). Treatment of mouse TSA G1NaGrpTK mammary tumors with a combination of PDT and systemic gancyclovir (GCV) resulted in increased tumor cures compared to PDT treatments alone. Balb-C mice with 6 mm diameter tumors received either PDT treatment plus gancyclovir (10 daily injections of GCV, 100 mg/kg per dose) beginning one hour prior to a single PDT treatment (200 J/cm sq), or PDT alone, or gancyclovir alone. Mice were monitored for tumor recurrences three times per week for 40 days. PDT treatments alone produced 50% tumor cures, while the PDT plus gancyclovir regimen produced 100% tumor cures. Gancyclovir by itself did not resulted in any tumor cures. Therefore, we believe we have successfully completed the research goals of this proposal.

We believe our work provides strong proof of principal regarding PDT activated molecular switches for the treatment of breast cancer. Future studies will now be required to evaluate methods to effectively deliver expression vectors to tumor tissue.

Key Research Accomplishments:

1. Stable transfection and function of stress inducible therapeutic genes in mammary cancer cells
2. Inducible expression of therapeutic genes following photodynamic therapy in cell grown in culture and in tumors growing in mice.
3. Quantitative information regarding in-vitro expression profiles of thymidine kinase following photodynamic therapy has been obtained.
4. The kinetics and treatment parameters associated with maximal inducible expression of thymidine kinase with in-vivo tumors have also been obtained.
5. Enhanced efficacy of photodynamic therapy when combined with inducible gene therapy

Reportable Outcomes:

Peer Reviewed Manuscripts:

1. Luna, M.C., Ferrario, A., Wong, S., Fisher, A.M., Rucker, N., Gomer, C.J.: Photodynamic therapy mediated oxidative stress as a molecular switch for the temporal expression of genes ligated to the human heat shock promoter. *Cancer Res* 60:1637-1644, 2000

2. Ferrario, A., von Tiehl, K.F., Rucker, N., Schwarz, M.A., Gill, P.S. and Gomer, C.J. Anti-angiogenic treatment enhances photodynamic therapy responsiveness in a mouse mammary carcinoma. *Cancer Res.*, 60, 4066-4069, 2000

3. Rucker, N., Ferrario, A. and Gomer, C.J. Constitutive overexpression of HSP-70 in thermal resistant tumor cells does not alter sensitivity to porphyrin, chlorin or purpurin mediated PDT. *J Porphyrins and Phthalocyanines*, 5:143-146, 2001.

4. Keshelava, N., Zuo, J.J., Chen, P., Waidyaratne, S.N., Luna, M.C., Gomer, C.J., Triche, T.J. and Reynolds, C.P. Loss of p53 function confers high level multidrug resistance in neuroblastoma cell lines. *Cancer Res.*, 61, 6185-6193, 2001

5. Luna, M.C., Chen, X., Wong, S., Tsui, J., Rucker, N., Lee, A.S., Gomer, C.J.: Enhanced Photodynamic Therapy Efficacy with Inducible Suicide Gene Therapy Controlled by the grp Promoter. *Cancer Res* 62:1458-1461, 2002.

List of Personnel:
Charles J. Gomer, Ph.D.
Anita Fisher

Patents and Licenses:
None

Degrees Obtained:
None

Development of Cell Line Tissues and Serum Repositories:
None

Databases:
None

Funding Applied For:
None

Employment and Research Opportunities:
None

Conclusions:
We have been successful in obtaining proof of principal that photodynamic therapy (PDT) inducible expression of therapeutic genes is both possible in breast cancer cells grown in culture as well as in breast cancer cells transplanted into mice. We have been

successful in obtaining quantitative information related to photodynamic therapy inducible expression of the herpes simplex thymidine suicide gene controlled by the grp promoter. Expression in breast cancer cells and tumors has been observed and the kinetics of expression and parameters of PDT treatment required for maximal expression have been identified. The information that we have obtained refines the combination PDT plus inducible gene therapy protocol. We have further shown that the inducible expression of thymidine kinase gene when combined with PDT and gancyclovir offers an enhanced effectiveness in treatment mammary carcinomas. The information that we have obtained indicates that laser mediated PDT can be an efficient and selective molecular switch for activation of therapeutic genes. Inducible gene therapy protocols have a number of advances over constitutive gene expression. The ability to control both the temporal and spatial activation of genes is of significant benefit especially when toxic gene products are being produced. Therefore, reproducible treatment parameters to control both the temporal and spatial activation of genes should be of significant benefit when the genes are expressed for therapeutic purposes.

References:

1. Luna, M.C., Ferrario, A., Wong, S., Fisher, A.M., Rucker, N., Gomer, C.J.: Photodynamic therapy mediated oxidative stress as a molecular switch for the temporal expression of genes ligated to the human heat shock promoter. *Cancer Research,* 60:1637-1644, 2000

2. Luna, M.C., Chen, X., Wong, S., Tsui, J., Rucker, N., Lee, A.S., Gomer, C.J.: Enhanced Photodynamic Therapy Efficacy with Inducible Suicide Gene Therapy Controlled by the grp Promoter. *Cancer Research,* 62:1458-1461, 2002.

Appendices:

Five original journal articles

[CANCER RESEARCH 60, 1637–1644, March 15, 2000]

Photodynamic Therapy-mediated Oxidative Stress as a Molecular Switch for the Temporal Expression of Genes Ligated to the Human Heat Shock Promoter[1]

Marian C. Luna, Angela Ferrario, Sam Wong, Anita M. R. Fisher, and Charles J. Gomer[2]

Clayton Center for Ocular Oncology [M. C. L., A. F., S. W., A. M. R. F., C. J. G.], Children's Hospital Los Angeles; and Departments of Pediatrics [C. J. G.], Radiation Oncology [C. J. G.], and Molecular Pharmacology and Toxicology [C. J. G.], University of Southern California, Los Angeles, California 90027

ABSTRACT

Oxidative stress associated with photodynamic therapy (PDT) is a transcriptional inducer of genes encoding stress proteins, including those belonging to the heat shock protein (hsp) family. The efficiency of PDT to function as a molecular switch by initiating expression of heterologous genes ligated to the human hsp promoter was examined in the present study. Selective and temporal reporter gene expression was documented after PDT in mouse radiation-induced fibrosarcoma cells stably transfected with recombinant vectors containing an hsp promoter ligated to either the *lac-z* or *CAT* reporter genes and in transfected radiation-induced fibrosarcoma tumors grown in C3H mice. Hyperthermia treatments were included as a positive control for all experiments. Expression vectors containing either human *p53* or *tumor necrosis factor (TNF)-α* cDNA under the control of an hsp promoter were also constructed and evaluated. A *p53* null and *TNF-α*-resistant human ovarian carcinoma (SKOV-3) cell line was stably transfected with either the *p53* or *TNF-α* constructs. Inducible expression and function of p53 as well as inducible expression, secretion, and biological activity of TNF-α were documented after PDT or hyperthermia in transfected SKOV cells. These results demonstrate that PDT-mediated oxidative stress can function as a molecular switch for the selective and temporal expression of heterologous genes in tumor cells containing expression vectors under the control of an hsp promoter.

INTRODUCTION

PDT[3] is in clinical trials for the treatment of a variety of solid tumors (1). The porphyrin photosensitizer, PH, recently received FDA approval for PDT treatment of esophageal and endobronchial carcinoma (2). This procedure is also being evaluated in the management of nonmalignant disorders, such as age-related macular degeneration and psoriasis (3). PDT-mediated cytotoxicity relies on the localized photochemical generation of reactive oxygen species, including singlet oxygen (1). This leads to a rapid tumoricidal response mediated by both direct tumor cell toxicity and photodamage to the involved microvasculature (4). A growing number of second generation photosensitizers are also undergoing clinical evaluation (2). These new compounds exhibit properties comparable or superior to PH, including chemical purity, increased photon absorption at longer wavelength, improved tumor tissue retention, rapid clearance from surrounding normal tissues, high quantum yields of reactive oxygen species, and minimal dark toxicity (5). One such photosensitizer, NPe6, is a water-soluble chlorin involved in Phase I and II clinical trials (6, 7). Direct tumor cytotoxicity and vascular stasis are induced by NPe6-mediated PDT (8). The most effective *in vivo* responses occur when a short time interval (<6 h) is used between NPe6 administration and light treatment (9).

In addition to the development of new photosensitizers, continued improvements in clinical PDT will come from the translation of information generated from studies examining basic mechanisms of this procedure. Biochemical analysis indicates a variety of subcellular PDT targets, including the mitochondria, plasma membrane, and lysosomes (1, 2, 10, 11). Apoptotic and necrotic pathways are both involved in PDT-mediated cell death (2, 12). An assortment of early response genes, genes associated with signal transduction pathways and cytokine expression, as well as stress response genes are activated by PDT (13–19). Stress proteins classified as HSPs are expressed following PDT, and this response is at the level of transcription (18, 19). HSPs are highly conserved throughout evolution and function as molecular chaperones of nascent proteins (20). HSPs are also involved in protecting cells from stress by binding to denatured proteins and assisting in proper refolding (21). Transcriptional regulation of heat shock gene expression involves HSF binding to specific HSEs. The hsp promoter has multiple copies of a conserved HSE containing contiguous inverted repeats of the 5-bp sequence nGAAn positioned upstream of the TATA box element (22). The transcription factor HSF is maintained in a monomeric form in the cytoplasm of nonstressed cells through direct binding to HSP-70. During cellular stress, HSP-70 binds to denatured protein and allows monomeric HSF to trimerize and migrate to the nucleus where it then binds to HSE. HSP transcription is initiated upon phosphorylation of the HSF trimer (22).

The hsp promoter has been used for over 10 years to selectively drive inducible expression of heterologous genes after hyperthermia (23–28). In the present study, we examined the effectiveness of PDT-mediated oxidative stress to initiate translation of heterologous genes ligated to the human hsp promoter. Clinically relevant photosensitizers were used in experiments designed to evaluate the efficiency of PDT to function as a molecular switch for the expression of reporter genes and cancer therapeutic genes in a selective and temporal manner.

MATERIALS AND METHODS

Photosensitizers. PH was a gift from Quadra Logics, Inc. (Vancouver, British Columbia, Canada) and was dissolved in 5% dextrose in water to make a 2.5-mg/ml working solution. NPe6 was a gift from Porphyrin Products (Logan, UT) and was dissolved in saline at 2.5 mg/ml.

Cell Lines. Mouse RIF cells were originally obtained from G. Hahn (Stanford University, Palo Alto, CA) and were grown in RPMI 1640 medium supplemented with 15% FCS and antibiotics (29). Human ovarian adenocarcinoma (SKOV-3) cells were obtained from W. McBride (University of California, Los Angeles, Los Angeles, CA) and were grown in Dulbecco's minimal essential medium supplemented with 10% FCS and antibiotics (30). The SKOV-3 cells have a homozygously deleted p53 gene (31) and exhibit resistance to recombinant TNF-α (32). Mouse fibrosarcoma (WEHI-13VAR) cells were obtained from American Type Culture Collection (Rockville, MD) and were grown in RPMI 1640 medium supplemented with 10% FCS. These

Received 10/12/99; accepted 1/19/00.

The costs of publication of this article were defrayed in part by the payment of page charges. This article must therefore be hereby marked *advertisement* in accordance with 18 U.S.C. Section 1734 solely to indicate this fact.

[1] This investigation was performed in conjunction with the Clayton Foundation for Research and was supported in part by USPHS Grant RO1-CA-31230 from the National Institutes of Health, Office of Naval Research Grant N000014-91-J-4047 from the Department of Defense, United States Army Medical Research Grant BC981102 from the Department of Defense, the Neil Bogart Memorial Fund of the T. J. Martell Foundation for Leukemia, Cancer, and AIDS Research, and the Las Madrinas Endowment for Experimental Therapeutics in Ophthalmology.

[2] To whom requests for reprints should be addressed, at Children's Hospital Los Angeles, Mail Stop 67, 4650 Sunset Boulevard, Los Angeles, CA 90027. Phone: (323) 669-2335; Fax: (323) 669-0742; E-mail: cgomer@hsc.usc.edu.

[3] The abbreviations used are: PDT, photodynamic therapy; CAT, chloramphenicol acetyl transferase; β-gal, β-galactosidase, NPe6, mono-l-aspartyl chlorin e6; hsp, heat shock protein; PH, Photofrin porfimer sodium; TNF, tumor necrosis factor; HSE, heat shock element; HSF, heat shock factor; EMSA, electrophorectic mobility shift assay; HBS, high binding site; RIF, radiation-induced fibrosarcoma; CMV, cytomegalovirus.

cells exhibit TNF-α sensitivity when treated in the presence of actinomycin D (33).

Expression Vectors. Plasmids p2500-CAT and p173OR (providing inducible expression of CAT or β-gal, respectively under the control of a 2.5-kb human hsp70 promoter fragment) were obtained from StressGen Biotech Corp. (Vancouver, British Columbia, Canada). Plasmid pMC1Neo (providing constitutive expression of the neomycin resistance gene under the control of the thymidine kinase promoter) was obtained from Stratagene (La Jolla, CA). Plasmid pCMV-neo-Bam-hp53 (providing constitutive expression of wt *p53* under the control of the CMV promoter and G418 selectivity) was obtained from Y. Fung (Children's Hospital Los Angeles, Los Angeles, CA, Ref. 34). Plasmid pHSP.3hp53 (providing inducible expression of human *p53* under the control of a human hsp promoter fragment together with G418 selectivity) was constructed by first removing the CMV promoter from pCMV-neo-Bam-hp53 and replacing it with a 0.3-kb fragment of the human hsp70 promoter from plasmid pD3SX, which was obtained from StressGen Biotech Corp. Plasmid pHSP.3hTNF (providing inducible expression of human *TNF-α* under the control of the 0.3-kb hsp promoter fragment together with G418 selectivity) was constructed by replacing p53 from pHSP.3hp53 with the 1.1-kb fragment of human *TNF-α* cDNA excised from pE4 (American Type Culture Collection). Plasmid p53-HBS was obtained from Y. Fung (Children's Hospital Los Angeles) and contains two copies of a 20-bp p53 HBS ligated upstream from a minimal thymidine kinase promoter linked to CAT. Reporter gene activation occurs when p53 binds to the HBS motif of this promoter (35). Plasmids were grown in supercompetent *Escherichia coli*, DH5-α (Life Technologies, Inc., Grand Island, NY), isolated, and purified using a Qiagen plasmid kit (Qiagen, Inc., Chatsworth, CA).

Reporter plasmids (p2500-CAT or p173OR) were transfected into RIF cells along with pMC1Neo (5:1 ratio) using calcium phosphate precipitation. Cells were grown in media containing 600 μg/ml G418, and resulting colonies were picked using cloning rings. G418-resistant clones were expanded and tested for β-gal or CAT activity using heat (45°C for 20 min) as a positive inducing treatment. Individual clones exhibiting positive β-gal expression (HB-3) or CAT expression (HC-2) were isolated and used in subsequent studies. Expression plasmids containing inducible human genes (pHSP.3-hp53 or pHSP.3hTNF) were transfected into SKOV-3 cells using calcium phosphate precipitation. Cells were grown in media containing 800 μg/ml G418, and resulting colonies were picked using cloning rings. G418-resistant clones were expanded and examined for p53 or TNF-α expression using heat (45°C for 20 min) as a positive inducer. Individual SKOV-3 cell clones exhibiting positive p53 expression (p53-S4) or TNF-α expression (TNF-S2) were isolated and used in subsequent studies.

***In Vitro* PDT and Hyperthermia Treatments.** Photosensitization protocols involved seeding cells into plastic Petri dishes (60-mm dishes for survival analysis or 100-mm dishes for gene expression assays) and incubating overnight in complete growth media to allow for cell attachment. The plating efficiency for the parental RIF and transfected HC-2 and HB-3 cells ranged from 40 to 60%. Plating efficiencies for the parental SKOV-3 and transfected p53-S4 and TNF-S2 cells ranged from 50 to 70%. PDT treatments were performed as reported previously (13). Briefly, cells were incubated in the dark at 37°C for either 1 or 16 h with either PH or NPe6 (25 μg/ml) in media containing either 1% or 5% FCS, respectively. Following the 1-h incubation protocol, cells were rinsed in media with serum and immediately exposed to graded doses of light. After the extended 16-h photosensitizer incubation, cells were rinsed for 30 min in growth media containing 15% FCS and then exposed to graded doses of light. Six hundred sixty-four-nm laser light delivered at a dose rate of 2 mW/cm^2 was used for cells incubated with NPe6. Broad spectrum red light (570–650 nm) generated by a parallel series of red milar-filtered 30-W fluorescent bulbs and delivered at a dose rate of 0.35 mW/cm^2 was used for cells incubated with Photofrin. Survival was measured using a standard clonogenic assay (29). *In vitro* hyperthermia involved seeding cells in T-25 or T-75 plastic flasks 24 h before exposure to warmed media and placement in a temperature-controlled water bath for specified time intervals (36). Inducible gene expression experiments were performed using PDT or hyperthermia treatments, which resulted in between 20 and 50% survival.

***In Vivo* PDT and Hyperthermia Treatments.** Female C3H/HeJ mice (8–12 weeks old) were injected s.c. in the right hind flank with 10^4 parental RIF, HC-2, or HB-3 cells. Hyperthermia and PDT treatments were performed as reported previously on tumors measuring 6–7 mm in diameter and 3 mm in height (37). Briefly, tumor hyperthermia involved a 20-min exposure to 810 nm of light emitted from an $AlArO_4$ diode laser at a dose rate of 220 mW/cm^2. This procedure resulted in an intratumor temperature at a 1-mm depth of 44.5°C-45°C as measured with a 27-gauge needle thermister. PDT procedures included an i.v. injection of either PH or NPe6 at 5 mg/kg. Nonthermal PDT laser irradiation of tumors was initiated either 4 h (for NPe6) or 24 h (for PH) after photosensitizer administration. An argon-pumped dye laser emitted red light at 630 nm for PH-mediated PDT and 664 nm of light for NPe6-mediated PDT. A light dose rate of 75 mW/cm^2 was used for all *in vivo* PDT treatments. Total PDT light doses were 100 J/cm^2 for PH and 200 J/cm^2 for NPe6.

Reporter Gene Assays. Inducible expression of the *lacZ* gene product, β-gal, was evaluated in cells and tissue by photometric monitoring of the enzymatic cleavage of o-nitrophenyl-B-D-pyranogalactose (38). Briefly, treated cells were lysed in commercial Reporter Lysis Buffer (Promega, Madison, WI), scraped off the plastic dishes, and transferred to microcentrifuge tubes. The suspension was centrifuged, and 150 μl of supernatant were incubated for 3 h at 37°C with an equal volume of assay buffer containing o-nitrophenyl-B-D-pyranogalactose. Absorbance at 420 nm was determined for each sample, and β-gal activity (milliunits of β-gal per mg of protein) was calculated from a standard curve. For analysis of tumor tissue, samples were first homogenized with a Polytron in Reporter Lysis Buffer (40). β-gal activity was then determined as described above. *CAT* activity was determined by monitoring the transfer of the acetyl group from acetyl-CoA to ^{14}C-chloramphenicol using TLC (39). Briefly, treated cells were incubated with 1 ml of TEN solution [40 mM Tris (pH 7.5), 1 mM EDTA (pH 8.0), 150 mM NaCl], scraped off dishes, and concentrated by centrifugation. Cell pellets were lysed by freeze/thawing, and protein concentration was determined using a Bio-Rad protein assay. Cellular protein extracts were combined with acetyl-CoA solution and ^{14}C-chloramphenicol (40–60 mCi/mmol, ICN, Costa Mesa, CA) and incubated for 30 min at 37°C. Acetylated chloramphenicol was extracted in ethyl acetate and run on a silica gel TLC plate. CAT activity was determined by calculating the percent conversion to the acetylated forms of chloramphenicol.

Western Blot Analysis. Cells were collected in SDS lysing buffer at various times after treatment and evaluated for protein expression as described previously (16). Briefly, protein samples were size-separated on 10% polyacrylamide gels and transferred overnight to nitrocellulose membranes. Filters were blocked with 5% nonfat milk and then incubated with a mouse antihuman p53 monoclonal antibody (clone DO-1, Lab Vision Corp., Fremont, CA) or a mouse antiactin monoclonal antibody (clone C-4, ICN, Aurora, OH). Filters were then incubated with an antimouse peroxidase conjugate (Sigma, St. Louis, MO), and the resulting complex was visualized by enhanced chemiluminescence autoradiography.

Mobility Shift Assays. Tumor bearing mice with 6–8-mm diameter RIF tumors or RIF cells grown in culture were treated with either hyperthermia or PDT as described above. Binding of RIF-derived cellular protein to a mouse HSE was then analyzed with minor modifications of a previous procedure (18). Tumor samples were minced on ice and resuspended in extraction solution [20 mM HEPES (pH 7.9), 0.35 M NaCl, 20% glycerol, 1 mM $MgCl_2$, 1% Nonidet, 1 mM DTT, 0.5 mM EDTA, 1 mM phenylmethylsulfonyl fluoride, 10 μg/ml leupeptin, and 1 μg/ml aprotinin). Samples were centrifuged, and supernatants were collected. A double-stranded 30-base oligonucleotide corresponding to the mouse HSE was 5′ end-labeled with ^{32}P using a T4 polynucleotide kinase. Tumor-derived protein (10 μg) was then added to a mixture containing 2 μg of poly(dI-dC) and 10,000 cpm of ^{32}P-labeled HSE in 5 × binding buffer (18). For competitive analysis, 100-fold excess of nonradioactive HSE was added to duplicate reactions. Resulting DNA-protein complexes were resolved by electrophoresis on a 4% polyacrylamide gel. In supershift experiments involving the addition of antibodies to protein extracts before gel shift analysis, 0.2 μg of a monoclonal antibody against HSF-1 or HSF-2 (Chemicon International, Inc., Temecula, CA) were added to the reaction mixture for 20 min at room temperature immediately before the addition of the radiolabeled HSE probe or cold competitor. After adding the probe, the reaction incubation was continued for 20 min at 37°C (41).

ELISA Analysis of TNF-α Secretion. A commercial TNF-α ELISA kit (Predicta, Genzyme Diagnostics, Cambridge, MA) was used for quantitative evaluation of TNF-α expression and secretion. Cells (10^5) were seeded into 24-well plates, incubated overnight, and treated with either PDT or hyperther-

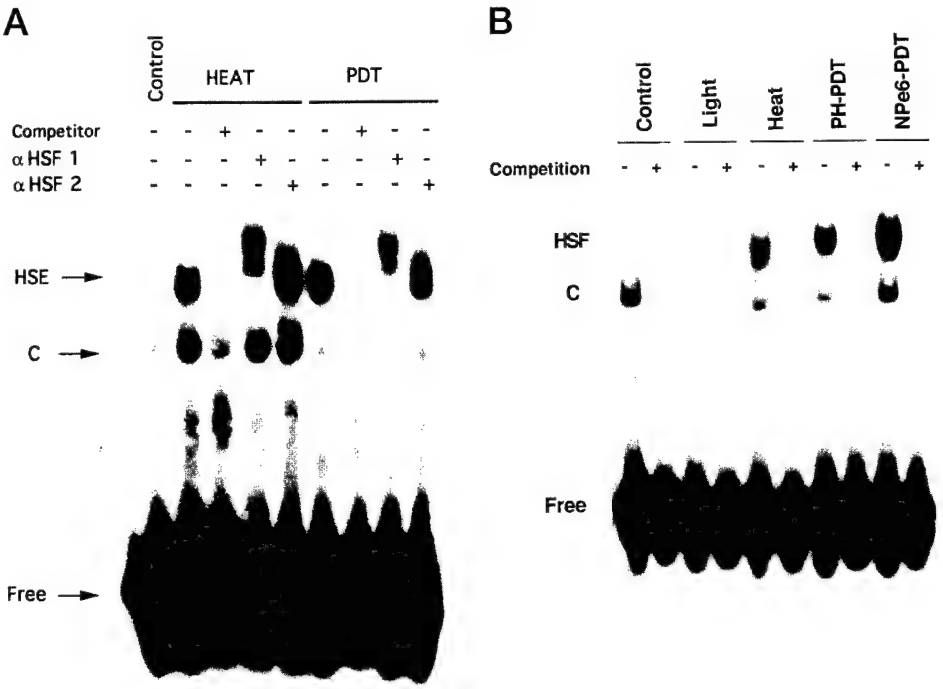

Fig. 1. Selective and inducible HSF DNA-binding activity occurs in RIF cells and tumors treated with hyperthermia or PDT. *A*, cells treated with hyperthermia or PDT exhibit specific HSF-1 binding to HSE. Whole cell extracts were collected 2 h after exposure to heat (45°C for 20 min) or 1 h after NPe6-mediated PDT (3400 J/m^2). Protein extracts were incubated with either HSF-1 or HSF-2 antiserum for 20 min. Reaction mixtures were then incubated with a ^{32}P-labeled 30-bp mouse HSE fragment for 20 min and subjected to EMSA. Lanes marked *Competitor* were incubated with a 100-fold excess of nonradioactive HSE oligonucleotide; *C* indicates constitutive HSE binding activity; and *Free* indicates nonreactive mixtures. *B*, EMSA showing specific HSE binding activity of protein extracts from RIF tumors treated with either hyperthermia (45°C for 20 min), NPe6-mediated PDT (100 J/cm^2), or PH-mediated PDT (100 J/cm^2). Nontreated tumors and tumors exposed to only light served as controls. Mice were sacrificed 2 h after treatment, and tumor tissue was immediately collected and processed.

mia as described above. Culture media was collected 24 h after treatment and analyzed for TNF-α according to the manufacturer's instructions.

TNF-α Bioassay Analysis. The biological activity of secreted TNF-α was evaluated by measuring cytotoxicity in TNF-α sensitive WEHI-13VAR cells (33). Cells were seeded in 96-well plates at a density of 2×10^4 cells/well and incubated overnight. PDT and hyperthermia treatments were performed on SKOV-3 parental and TNF-S2 clones as described above, and media from these cells was collected 22 h after treatment when secreted TNF-α levels were found to be highest. The TNF-α-containing media was added to the WEHI-13VAR cells along with 0.5 μg/ml actinomycin. Twenty four h later, the WEHI-13 VAR cells were evaluated for cytotoxicity using a 3-(4,5-dimethylthiazol-2-yl)-2,5-diphenyltetrazolium bromide assay from Chemicon Inc. (Temecula, CA).

RESULTS

Specific HSF Binding to HSE Is Observed Following *in Vitro* and *in Vivo* PDT. Activation of HSF involves the trimerization of monomeric HSF moieties followed by nuclear translocation and binding to an evolutionary conserved HSE (22). We reported previously that *in vitro* PDT can activate HSF in mammalian cells, but at that time, we did not identify the actual species of HSF (18). In the present study, we used murine RIF tumor cells and an electrophorectic gel mobility shift assay combined with HSF-1- and HSF-2-specific antiserum to determine which transcription factor(s) were activated by PDT. Fig. 1*A* shows that after PDT (using a 16-h cellular incubation

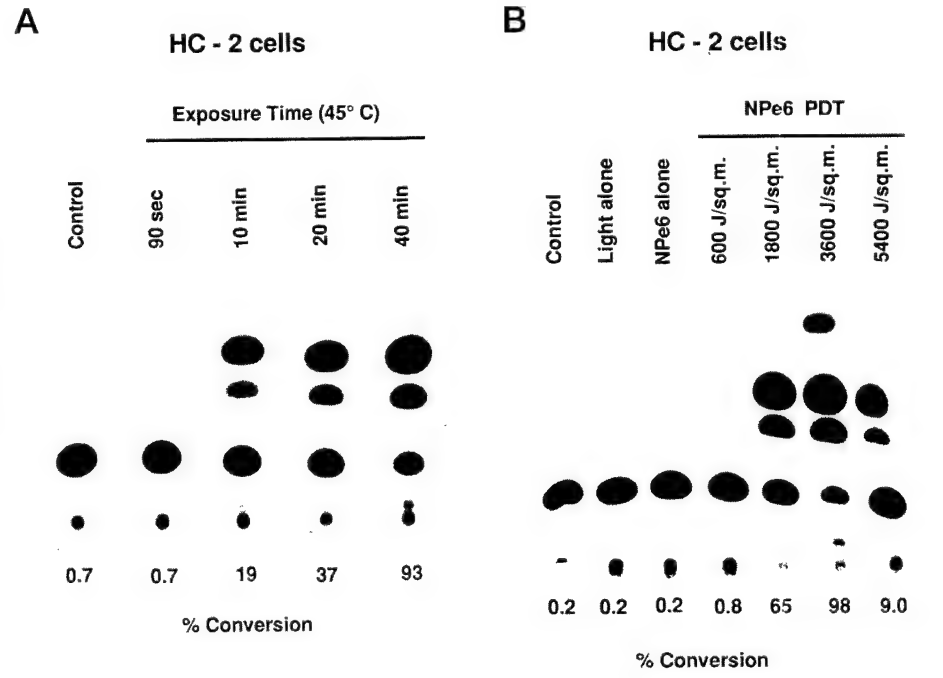

Fig. 2. Heat and PDT induce selective expression of CAT in RIF HC-2 cells stably transfected with the hsp promoter-controlled p2500-CAT plasmid. CAT activity in transfected HC-2 cells treated with increasing doses of (*A*) heat (45°C for times ranging from 1.5 to 40 min) or (*B*) NPe6-mediated PDT (25 μg/ml NPe6 for 16 h; 600-5400 J/m^2). Light alone and photosensitizer alone conditions did not induce CAT expression. Protein samples were collected 24 h after treatment. Conversion of chloramphenicol to acetylated chloramphenicol was calculated by counting radioactivity from resulting TLC plates.

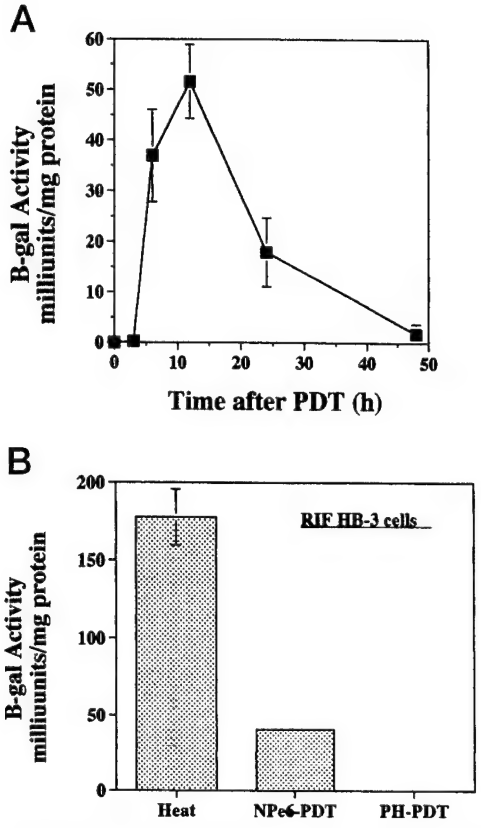

Fig. 3. Temporal- and photosensitizer-specific expression of the β-gal reporter gene occurs in RIF HB-3 cells stably transfected with the hsp promoter-controlled p173OR plasmid. *A*, kinetics of β-gal expression in RIF HB-3 cells treated with NPe6-PDT (16-h drug incubation; 3000 J/m^2). Minimal enzyme activity was detected 3 h after treatment. Peak β-gal activity was observed 6 and 12 h after NPe6-mediated PDT. β-gal expression was not detected after light alone or photosensitizer alone conditions. Each data point represents the mean of at least three separate experiments ± SE. *B*, differential expression of β-gal is observed in HB-3 cells exposed to isoeffective doses (inducing 15–25% survival) of heat, NPe6 PDT, or PH PDT. Treated cells were assayed for β-gal 6 h after treatment. Levels are the mean ± SE from four to five separate experiments.

with NPe6), a supershift in the EMSA occurs in the presence of HSF-1 antibody but not in the presence of HSF-2. Treatment of RIF cells with PH and NPe6-mediated PDT (1 h photosensitizer incubation) also induced a positive but weaker supershift with HSF-1 (data not shown). Heat was used as a positive control and induced selective activation of HSF-1, which agrees with previous studies (21). Positive EMSA and supershift assays were not obtained after isoeffective *in vitro* PDT when a 16-h PH incubation was examined (data not shown). The ability of PDT to induce selective HSF binding to HSE was next examined under *in vivo* treatment conditions. Fig. 1*B* shows a representative EMSA for cellular protein extracted from RIF tumors growing in C3H mice. Protein from control tumors did not elicit selective HSE binding. However, protein extracted from tumors treated with either PH- or NPe6-mediated PDT produced extensive HSE binding, which could be competed away with cold HSE. Diode laser-generated tumor hyperthermia served as a positive control. These results indicate that PDT can induce both *in vitro* and *in vivo* HSF binding, which would be essential for PDT to transcriptionally activate heterologous genes under the control of an hsp promoter.

PDT and Hyperthermia Induce Selective and Dose-dependent Expression of CAT Under the Control of a 2.5-kb hsp Promoter Fragment. Stable integration of reporter gene expression vectors containing an inducible hsp70 promoter was achieved in RIF cells. Sensitivity of parental RIF and transfected HC-2 and HB-3 cells to either PDT or hyperthermia was similar (data not shown). This indicates that transfection procedures and integration of heterologous DNA into mammalian cells does not modulate photosensitivity or thermal sensitivity. Fig. 2*A* shows that HC-2 cells exposed to 45°C expressed a dose-dependent increase in CAT activity. A similar pattern of induced CAT expression was documented in HC-2 cells exposed to increasing doses of NPe6-mediated PDT as shown in Fig. 2*B*. Inducible expression occurred when a 16-h NPe6 incubation was used. CAT expression was not initiated by either light alone or photosensitizer alone, indicating that the induction was the sole result of PDT-mediated oxidative stress. CAT expression initially increased with increasing PDT doses and then decreased as a greater percentage of cells were killed by the treatment. A reduction in CAT expression at increasingly lethal hyperthermia doses was also observed (data not shown). These results provide the first demonstration that PDT-mediated oxidative stress can activate a transgene under the control of an hsp promoter.

PDT-mediated Expression of hsp Promoter-inducible Reporter Genes Is Transient As Well as Photosensitizer- and Incubation-specific. High level expression of β-gal was observed in RIF HB-3 cells treated with either hyperthermia or NPe6-mediated PDT. Fig. 3*A* shows the kinetics of β-gal expression in HB-3 cells incubated for 16 h with NPe6 and then exposed to a 3000-J/m^2 light dose. β-gal activity was detected within 6 h of PDT treatment and continued to increase for at least 12 h before declining to background levels by 48 h after PDT. Similar kinetics of β-gal expression were observed following an isoeffective hyperthermia treatment (data not shown). Interestingly, the ability of PDT to induce β-gal or CAT expression in transfected RIF cells cultured *in vitro* was strongly dependent on the specific photosensitizer and incubation conditions being evaluated. Fig. 3*B* shows β-gal expression in HB-3 cells at 6 h after exposure to either heat or PDT. Maximal reporter gene expression was observed after hyperthermia. Significant β-gal expression was also observed in cells treated with NPe6 PDT (using a 16-h photosensitizer incubation protocol). A 16-h PH incubation before *in vitro* PDT resulted in minimally detectable β-gal expression. Likewise, β-gal expression was not detected in transfected RIF cells incubated for 1 h with either NPe6 or PH before light exposure (data not shown). Interestingly, different results were obtained when the transfected RIF cells were grown as solid tumors in C3H mice and treated with PDT (as described below).

***In Vivo* PDT Induces hsp Promoter-directed Reporter Gene Expression.** The stable integration of reporter gene constructs in RIF cells provided an opportunity to evaluate the ability of the hsp promoter to function under *in vivo* oxidative stress treatment parameters.

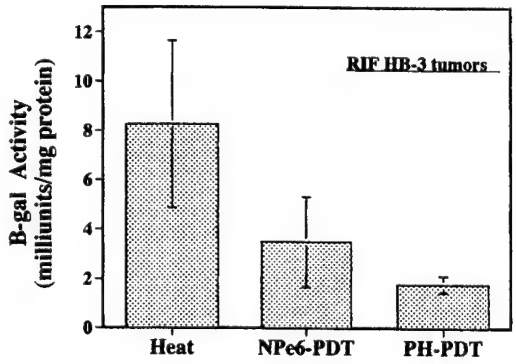

Fig. 4. NPe6- and PH-mediated PDT and laser-generated hyperthermia induce hsp promoter-directed β-gal expression in RIF HB-3 tumors growing in C3H/HeJ mice. Tumor samples were collected 16 h after PDT and heat treatments (as described in "Materials and Methods"). β-gal measurements represent the mean ± SE from five individual tumors. β-gal activity was not detected in nontreated tumors or in tumors treated with light or photosensitizer alone (data not shown).

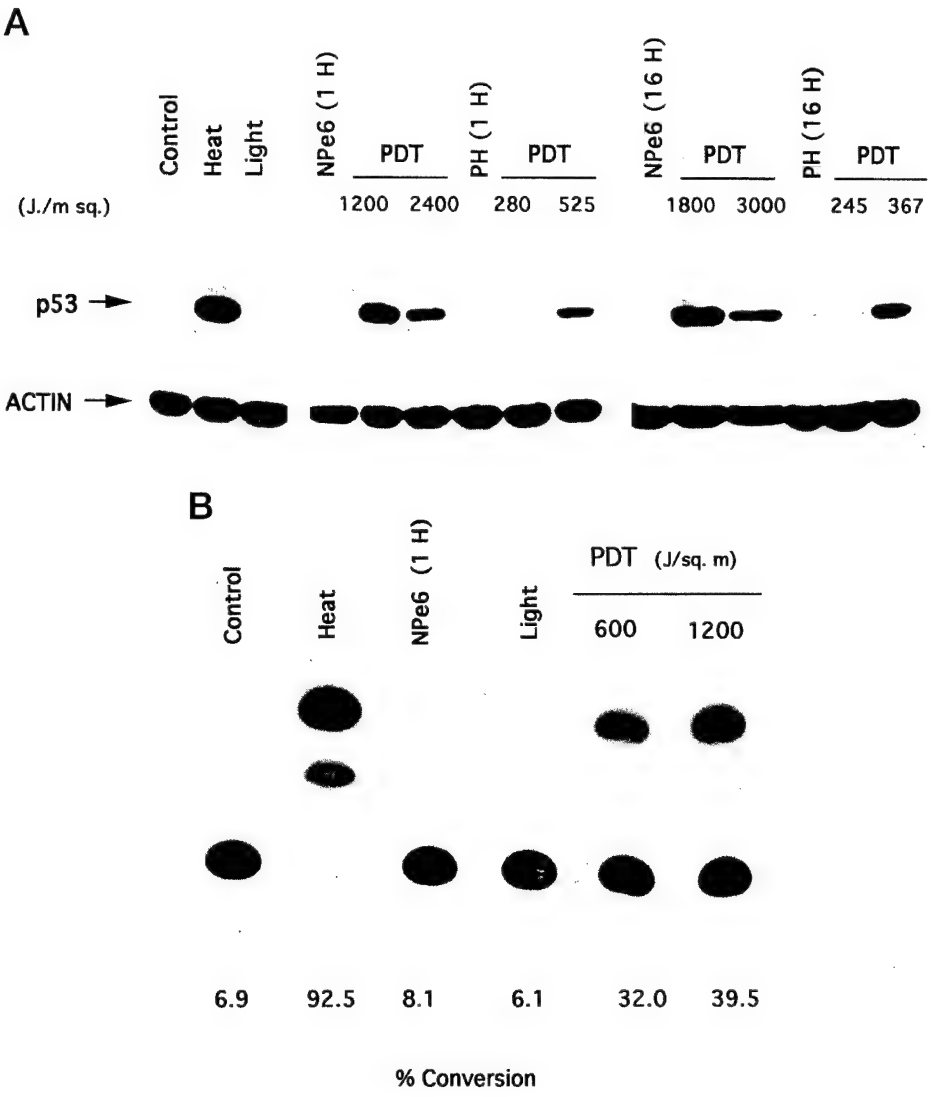

Fig. 5. PDT and heat induce selective expression of a functional human p53 protein in *p53* null SKOV-3 cells stably transfected with the hsp promoter-controlled pHSP.3hp53 plasmid. *A*, Western immunoblots are shown for the parental SKOV-3 cells (control) and p53-S4 cells exposed to heat (45°C for 20 min) or various PDT treatments involving short (1 h) or extended (16 h) NPe6 and PH incubations prior to light. p53 expression was analyzed 6 h after treatment. The p53 blots were reprobed for actin protein levels as an indicator of sample loading. *B*, p53 induced by heat or PDT functions as a transcription factor. p53-dependent CAT expression is observed in p53-S4 cells transiently transfected with the p53-HBS reporter plasmid and exposed to either heat or NPe6-mediated PDT. CAT expression occurs when functional p53 binds to the p53-specific HBS motif of a minimal thymidine kinase promoter. Protein samples were collected 24 h after heat or PDT. Nontreated controls as well as light alone and photosensitizer alone conditions exhibited background CAT expression. Conversion of chloramphenicol to acetylated chloramphenicol was calculated by counting radioactivity from resulting TLC plates.

s.c. injection of parental RIF cells as well as HC-2 and HB-3 cells into the hind flank of C3H mice resulted in the reproducible formation of solid tumors amenable to laser hyperthermia or PDT treatment. Fig. 4 shows β-gal expression levels in tumors treated with either heat or PDT. Laser-induced hyperthermia produced a significant expression of β-gal, which was in agreement with *in vitro* data. *In vivo* PDT also functioned as an efficient molecular switch for inducible expression of β-gal in exposed tumor tissue. Both NPe6 and PH were equally capable of eliciting PDT-induced β-gal expression, although only NPe6 was capable of eliciting a significant *in vitro* response in RIF cells.

PDT Induces Functional p53 Expression in Transfected SKOV-3 Cells. Heat and PDT-inducible expression of *p53* was evaluated in *p53* null SKOV-3 cells stably transfected with pHSP.3p53 (p53-S4 cells). p53 protein expression was observed within 6 h of heat or PDT treatment and was maximal at 24 h (data not shown). The p53 expression decreased with extended times and dissipated by 72 h. Fig. 5*A* shows p53 protein expression assayed 6 h after cells were treated with either heat, PH-mediated PDT, or NPe6-mediated PDT. We conclude that PDT-mediated oxidative stress was responsible for inducing p53 expression because neither photosensitizer alone nor light alone induced any p53. Promoter leakiness was not observed in p53-S4 cells because p53 expression was not detected under control conditions. The functionality of induced expression of p53 was determine using a transactivation reporter gene assay (38, 41). Fig. 5*B* shows *p53*-mediated CAT expression in p53-S4 cells treated with either heat or PDT. CAT expression was observed 24 h after both heat and NPe6-mediated PDT in transfected cells, indicating that expressed p53, documented by Western analysis in Fig. 5*A*, also functioned efficiently as a transcription factor. Comparable results were also observed for cells exposed to PDT using both 1-h and 16-h PH incubations (data not shown).

Biologically Active TNF-α Is Secreted from SKOV-3 TNF-S4 Cells Following PDT and Hyperthermia. The use of TNF-α in gene expression studies requires that the expressed cytokine can also be secreted from transfected cells. Fig. 6, *A* and *B* show that inducible secretion of biologically active TNF-α was achieved in TNF-S2 cells exposed to hyperthermia or PDT. The figures show levels of either heat or NPe6 PDT-induced TNF-α detected in the media of cultured TNF-S2 cells 24 h after treatment. The figures also show concomitant biological activity of the secreted cytokine. TNF-α was not detected in the culture media of parental SKOV-3 cells under any treatment conditions. However, a measurable and reproducible level of secreted TNF-α (23 pg/ml) was routinely obtained in transfected TNF-S2 cells under basal conditions. This indicates that hsp promoter leakiness occurred in our transfected human TNF-S2 cells. Fig. 6*A* shows that

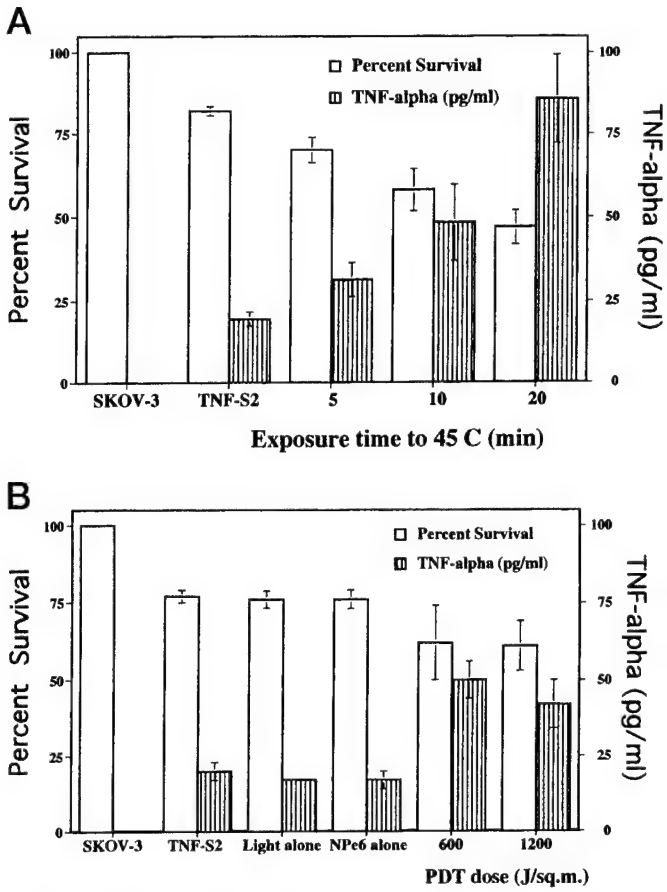

Fig. 6. PDT and hyperthermia induce expression and secretion of biologically active TNF-α in SKOV-3 cells stably transfected with the hsp promoter-controlled pHSP.3hTNF plasmid. Levels of TNF-α secreted into the culture media and concomitant sensitivity of WEHI-13 VAR cells exposed to this media are shown for TNF-S2 cells treated with either heat (*A*) or NPe6-mediated PDT (*B*). Treatment conditions included: heat (45°C for 5, 10, or 20 min) or PDT (1 h of NPe6 incubation followed by exposure to 600 or 1200 J/m^2 of 664-nm light). Supernatants were collected 22 h after treatment and either assayed for TNF-α using an ELISA kit or added to the culture media of WEHI-13VAR cells in the presence of 0.5 μg/ml actinomycin. Cell survival was determined using a 3-(4,5-dimethylthiazol-2-yl)-2,5-diphenyltetrazolium bromide assay 24 h after adding the TNF-α containing media. Each point represents the mean ± SE from three separate experiments. Nontreated TNF-S2 cells as well as cells exposed to photosensitizer alone or light alone exhibit a detectable level of biologically active TNF-α indicative of promoter leakiness and constitutive background expression.

increasing heat exposure times resulted in an elevation in secreted TNF-α levels. Biological activity of the secreted TNF-α was determined using WEHI-13VAR cells. These cells provide a sensitive, reliable, and stable bioassay system for measuring TNF-α activity (33). Increased cell sensitivity was observed after incubation with media containing elevated TNF-α concentrations. Fig. 6*B* shows TNF-α secretion and concomitant biological activity for TNF-S2 cells exposed to NPe6-mediated PDT using a 1 h photosensitizer incubation protocol. Comparable induction of TNF-α was obtained using a 16-h NPe6 incubation PDT protocol as well as following both 1- and 16-h Photofrin incubation PDT protocols (data not shown). TNF-S2 cells exhibited basal expression of TNF-α, but exposure to photosensitizer alone or light alone did not activate the hsp promoter because TNF-α expression levels were comparable to levels for nontreated TNF-S2 cells.

DISCUSSION

A primary goal of our study was to determine whether PDT could function as a molecular switch for controlling the expression of heterologous genes. Clinically directed gene therapy uses expression constructs to replace/modify defective genes or to introduce genes encoding cytotoxic proteins or immunomodulators (42). However, the translation of gene therapy objectives into actual clinical practice requires overcoming a number of obstacles. These challenges include developing reproducible procedures for the efficient and safe delivery of DNA expression vectors to cells and tissues (43). For our study, we chose to focus on evaluating an inducible promoter approach for PDT-controlled activation of gene expression. A variety of inducible expression strategies are presently being examined in the context of localized gene therapy. Constructs responsive to ionizing radiation (using the egr-1 promoter), hyperthermia (using the hsp-70 promoter), and hypoxia (using the grp-78 promoter or a hypoxia responsive element) are being tested for selective expression of therapeutic genes (28, 44–46). We hypothesized that the hsp promoter could be exploited for coupling the oxidative effects of PDT to an inducible procedure for expressing heterologous genes. Our results confirmed that PDT initiates HSF-1 binding to HSE in RIF cells incubated with NPe6. This is a necessary first step in using the hsp promoter with PDT for inducible transgene expression. We are unclear as to why differential binding was observed after PDT using NPe6 *versus* PH, but it may involve different subcellular targets (18). Interestingly, HSF binding to HSE and reporter gene expression occurred with both PH- and NPe6-mediated PDT when RIF cells were grown as solid tumors in mouse. *In vivo* PDT treatment elicits a pronounced inflammatory response involving the release of vasoactive and inflammatory mediators as well as the accumulation of host cells (4, 10). In this regard, prostaglandins activate HSF in mammalian cells and result in a thermotolerant state (47). Therefore, secondary physiological responses in PDT-treated tumor tissue may play a role in hsp promoter-controlled expression.

A variable PDT-induced gene expression profile was observed for porphyrin and chlorin photosensitizers in RIF cells. Similar differences were not observed in SKOV cells. The variable results detected in mouse *versus* human cells suggest that care must be taken in extrapolating preclinical studies to clinical PDT. These observations also agree with reports indicating that generalizations of PDT-induced biochemical and molecular pathways should not be made because responses vary depending on the specific photosensitizers and/or treatment parameters (2, 11). The effectiveness of the PDT-mediated molecular switch did not always follow HSF-HSE binding patterns. In RIF cells, PDT using a 16-h NPe6 incubation resulted in selective binding of HSF-1 to HSE. This treatment protocol also produced selective CAT and B-gal expression. Conversely, PH-mediated PDT did not elicit reporter gene expression in RIF cells but could induce HSF-HSE binding. Because both PDT procedures are associated with singlet oxygen-mediated oxidative stress, we conclude that distinct subcellular targets or molecular pathways may contribute to the differential results (48, 49). Additionally, a conserved 76-amino acid protein HSF binding protein has been identified in mammalian cells (50). This protein negatively effects HSF-1 DNA binding activity, and overexpression of this protein represses the transactivation activity of HSF-1. Likewise, overexpression of bcl-2 suppresses transcriptional activation of hsp70 (51). Various photosensitizers may have different effects on the expression of these molecules, but this still needs to be verified.

We selected two therapeutically relevant human genes, *p53* and *TNF-α*, for initial analysis of our PDT-responsive molecular switch. These genes exhibit different biological functions and expression properties. *p53* encodes a tumor suppressor protein and functions as a transcription factor (52). This protein is mutated or deleted in numerous solid cancers, and overexpression of wild-type *p53* can enhance the therapeutic response of some malignancies to chemotherapy and

ionizing radiation (53). The significance of *p53* expression on PDT sensitivity has recently been examined, and responses appear to vary with cell type (38, 54). *p53* exerts its activity as a transcription factor within the same cells in which the protein is expressed. Our results confirmed that all examined PDT exposure parameters were able to selectively induce the transient expression of biologically active p53 in p53-S4 cells. Parental SKOV cells are p53 null, and therefore, we can conclude that p53 expression in the transfected S4 cells was a direct consequence of PDT. Background expression or promoter leakiness was not observed in p53-S4 cells. Likewise, we were unable to detect *p53* expression when cells were exposed to photosensitizer or light alone.

In contrast to *p53*, TNF-α must first be secreted from producer cells before eliciting biological activity on cells with TNF-specific receptors (55). This cytokine is measurable in culture media with an ELISA assay, and the biological activity of TNF-α in this media can be monitored using a WEHI cell sensitivity assay (33). Systemically administered TNF-α enhances the cytotoxic effectiveness of therapeutic agents, including ionizing radiation and PDT (56, 57). However, toxicity associated with systemic TNF-α administration precludes its use as a therapeutic adjuvant. Inducible expression of *TNF-α* within target tissue or cells provides for local concentrations of the cytokine with minimal systemic effects. We documented that PDT exposure parameters can induce transient expression of biologically active TNF-α in TNF-S2 cells. Photofrin-mediated PDT produces a dose-dependent increase in TNF-α expression in peritoneal macrophages in treated mice (58). TNF-α is also detected in urine of patients undergoing local PDT for bladder cancer (59). However, we did not detect TNF-α in nontransfected SKOV tumor cells treated with PDT or hyperthermia. Our results indicate that the hsp promoter vigorously drives transgene expression. Secreted cytokine levels induced by PDT or heat in TNF-S2 cells were comparable or higher than TNF-α levels previously reported for constitutive expression systems driven by a CMV enhancer and B-actin promoter (60).

Background or basal expression of genes ligated to the hsp promoter was variable. Expression constructs transfected in RIF cells included a 2.5-kb fragment of the hsp promoter, whereas a 0.3-kb fragment of the hsp promoter was used with human SKOV-3 cells. Neither CAT nor β-gal expression was detected in RIF HC-2 and HB-3 cells under control conditions. Likewise, we did not observe any background leakiness of p53 expression in p53-S4 cells. However, promoter leakiness was observed in TNF-S2 cells with a constant basal expression and secretion of TNF-α. Therefore, hsp promoter size does not appear to be a primary determinant modulating transgene leakiness. However, vector insertion site could be involved in the differences we observed in basal expression. There are also three binding sites within the hsp promoter for the SP1 transcription factor, which may contribute to basal expression under various conditions (61). In addition, the hsp promoter contains a variety of regulatory elements, including AP-2, SRE, and c-myc binding sites (61). These elements can effect basal hsp promoter activity and can vary as a function of cell type and culture conditions.

In summary, PDT continues to show promise in the clinical treatment of solid malignancies. Nevertheless, methods to enhance the local tumoricidal responsiveness of PDT are still important because tumor recurrences are observed. We demonstrate for the first time that PDT-mediated oxidative stress can effectively induce selective expression of heterologous genes placed under the control of an hsp promoter. These results extend previous findings showing that PDT functions at the level of transcription to activate stress proteins (18). Our investigation provides initial proof of principle results indicating that PDT-responsive expression vectors should be examined in subsequent preclinical studies combining PDT and gene therapy.

REFERENCES

1. Fisher, A. M. R., Murphree, A. L., and Gomer, C. J. Clinical, and preclinical photodynamic therapy. Lasers Surg. Med., *17:* 2–31, 1995.
2. Dougherty, T. J., Gomer, C. J., Henderson, B. W., Jori, G., Kessel, D., Korbelik, M., Moan, J., and Peng, Q. Photodynamic therapy. J. Natl. Cancer Inst., *90:* 889–905, 1998.
3. Reynolds, T. Photodynamic therapy expands its horizons. J. Natl. Cancer Inst., *89:* 112–114, 1997.
4. Henderson, B. W., and Dougherty, T. J. How does photodynamic therapy work? Photochem. Photobiol., *55:* 145–157, 1992.
5. Gomer, C. J. Preclinical examination of first and second generation photosensitizers used in photodynamic therapy. Photochem. Photobiol., *54:* 1093–1107, 1991.
6. Tabor, S. W., Fingar, V. H., Coots, C. T., and Wieman, T. J. Photodynamic therapy using mono-l-aspartyl chlorin e6 (Npe6) for the treatment of cutaneous disease: a Phase I clinical study. Clin. Cancer Res., *11:* 2741–2746, 1998.
7. Kessel, D. Pharmacokinetics of n-aspartyl chlorin e6 in cancer patients. J. Photochem. Photobiol., *39:* 81–83, 1997.
8. McMahon, K. S., Wieman, T. J., Moore, P. H., and Fingar, V. H. Effects of photodynamic therapy using mono-l-aspartyl chlorin e6 on vessel constriction, vessel leakage and tumor response. Cancer Res., *54:* 5374–5379, 1994.
9. Ferrario, A., Kessel, D., and Gomer, C. J. Metabolic properties & photosensitizing responsiveness of mono-l-aspartyl chlorin e6 in a mouse tumor model. Cancer Res., *52:* 2890–2893, 1992.
10. Pass, H. I. Photodynamic therapy in oncology: mechanisms and clinical use. J. Natl. Cancer Inst., *85:* 443–456, 1993.
11. Kessel, D., Deng, L. Y., and Chang, C. K. The role of subcellular localization in initiation of apoptosis by photodynamic therapy. Photochem. Photobiol., *65:* 422–426, 1997.
12. Oleinick, N. L., and Evans, H. E. The photobiology of photodynamic therapy: cellular targets and mechanisms. Radiat. Res., *150:* S146–S156, 1998.
13. Luna, M. C., Wong, S., and Gomer, C. J. Photodynamic therapy mediated induction of early response genes. Cancer Res., *53:* 1374–1380, 1994.
14. Gollnick, S. O., Liu, X., Owczarczak, B., Musser, D., and Henderson, B. W. Altered expression of interleukin 6 and interleukin 10 as a result of photodynamic therapy *in vivo*. Cancer Res., *57:* 3904–3909, 1997.
15. Tao, J-S., Sanghera, J. S., Pelech, S. L., Wong, G., and Levy, J. G. Stimulation of stress-activated protein kinase and p38 HOG1 kinase in murine keratinocytes following photodynamic therapy with benzoporphyrin derivative. J. Biol. Chem., *271:* 27107–27115, 1996.
16. Gomer, C. J., Luna, M., Ferrario, A., and Rucker, N. Increased transcription and translation of heme oxygenase in Chinese hamster fibroblasts following photodynamic stress or Photofrin II incubation. Photochem. Photobiol., *53:* 275–279, 1991.
17. Gomer, C. J., Ferrario, A., Rucker, N., Wong, S., and Lee, A. Glucose regulated protein induction and cellular resistance to oxidative stress mediated by porphyrin photosensitization. Cancer Res., *51:* 6574–6579, 1991.
18. Gomer, C., Ryter, S., Ferrario, A., Rucker, N., Wong, S., and Fisher, A. Photodynamic therapy mediated oxidative stress can induce heat shock proteins. Cancer Res., *56:* 2355–2360, 1996.
19. Curry, P. M., and Levy, J. Stress protein expression in murine tumor cells following photodynamic therapy with benzoporphyrin derivative. Photochem. Photobiol., *58:* 374–379, 1993.
20. Lindquist, S., and Craig, E. A. The heat shock proteins. Ann. Rev. Genet., *22:* 631–677, 1988.
21. Cotto, J. J., and Morimoto, R. I. Stress induced activation of the heat shock response: cell and molecular biology of heat shock factors. Biochem Soc. Symp., *64:* 105–118, 1999.
22. Morimoto, R. I. Cells in stress: transcriptional activation of heat shock genes. Science (Washington DC), *259:* 1409–1410, 1993.
23. Dreano, M., Brochot, J., Myers, A., Cheng-Meyer, C., Rungger, D., Voellmy, R., and Bromley, P. High-level, heat-regulated synthesis of proteins in eukaryotic cells. Gene, *49:* 1–8, 1986.
24. Dreano, M., Fouillet, X., Brochot, J., Vallet, J-M., Michel, M-L., Rungger, D., and Bromley, P. Heat-regulated expression of the hepatitis B virus surface antigen in the human Wish cell line. Virus Res., *8:* 43–59, 1987.
25. Schweinfest, C. W., Jorcyk, C. L., Fujiwara, S., and Papas, T. S. A heat-shock-inducible eukaryotic expression vector. Gene, *71:* 207–210, 1988.
26. Pass, H. I., Mew, D. J. Y., Carbone, M., Matthews, W. A., Donington, J. S., Baserga, R., Walker, C. I., Resnicoff, M., and Steinberg, S. M. Inhibition of hamster mesothelioma tumorigenesis by an antisense expression plasmid to the insulin like growth factor-1 receptor. Cancer Res., *56:* 4044–4048, 1996.
27. Madio, D. P., van Gelderen, P., DesPres, D., Olson, A. W., de Zwart, J. A., Fawcett, T. W., Holbrook, N. J., Mandel, M., and Moonen, C. T. On the feasibility of MRI-guided focused ultrasound for local induction of gene expression. J. Magn. Reson. Imaging, *8:* 101–104, 1998.
28. Blackburn, R. V., Galoforo, S. S., Corry, P. M., and Lee, Y. J. Adenoviral-mediated transfer of a heat-inducible double suicide gene into prostate carcinoma cells. Cancer Res., *58:* 1358–1362, 1998.
29. Luna, M., and Gomer, C. J. Isolation and initial characterization of mouse tumor cells resistant to porphyrin mediated photodynamic therapy. Cancer Res., *51:* 4243–4249, 1991.
30. Gallardo, D., Drazan, K. E., and McBride, W. H. Adenovirus-based transfer of wild-type p53 gene increases ovarian tumor radiosensitivity. Cancer Res., *56:* 4891–4893, 1996.
31. Yaginuma, Y., and Westphal, H. Abnormal structure and expression of the p53 gene in human ovarian carcinoma cell lines. Cancer Res., *52:* 4196–4199, 1992.

32. Nio, Y., Zighelboim, J., Berek, J. S., and Bonavida, B. Sensitivity of fresh and cultured ovarian tumor cells to tumor necrosis factor, interferon-α, and OK-432. Cancer Immunol. Immunother., *27:* 246–254, 1988.
33. Khabar, K. S. A., Siddiqui, S., and Armstrong, J. A. WEHI-13VAR: a stable and sensitive variant of WEHI 164 clone 13 fibrosarcoma for tumor necrosis factor bioassay. Immunol. Lett., *46:* 107–110, 1995.
34. T'ang, A., and Fung, Y. K. T. Conserved homologous structural motifs between pRB and p53 that determine their conformation and functions. Challenges Mod. Med., *10:* 73–82, 1995.
35. Chumakov, A. M., Miller, C. W., Chen, D. L., and Koeffler, H. P. Analysis of p53 transactivation through high affinity binding sites. Oncogene, *8:* 3005–3011, 1993.
36. Gomer, C. J., Rucker, N., and Wong, S. Porphyrin photosensitivity in cell lines expressing a heat resistant phenotype. Cancer Res., *50:* 5365–5368, 1990.
37. Gomer, C. J., and Ferrario, A. Tissue distribution and photosensitizing properties of mono-l-aspartyl chlorin e6 (NPe6) in a mouse tumor model. Cancer Res., *50:* 3985–3990, 1990.
38. Lake, B. D. An improved method for the detection of β-galactosidase activity and its application to gangliosidosis and mucopolysaccharidosis. Histochem. J., *6:* 218–221, 1974.
39. Fisher, A. M. R., Ferrario, A., Rucker, N., Zhang, S., and Gomer, C. J. Photodynamic therapy sensitivity is not altered in human tumor cells after abrogation of p53 function. Cancer Res., *59:* 331–335, 1999.
40. Goring, D. R., Rossant, J., Clapoff, S., Breitman, M. L., and Tsui, L. C. *In situ* detection of β-galactosidase in lenes of transgenic mice with a γ-crytallin-lac-z gene. Science (Washington DC), *252:* 456–458, 1987.
41. Sarge, K. D., Murphy, S. P., and Morimoto, R. I. Activation of heat shock gene transcription by heat shock factor 1 involves oligomerization, acquisition of DNA-binding activity, and nuclear localization and can occur in the absence of stress. Mol. Cell Biol., *13:* 1392–1407, 1993.
42. Anderson, W. Gene therapy for cancer. Hum. Gene Ther., *5:* 1–2, 1994.
43. Verma, I. M., and Somia, N. Gene therapy—promises, problems and prospects. Nature (Lond.), *389:* 239–242, 1997.
44. Hallahan, D. E., Mauceri, H. J., Seung, L. P., Dunphy, E. J., Wayne, J. D., Hanna, N. N., Toledano, A., Hellman, S., Kufe, D. W., and Weichselbaum, R. R. Spatial and temporal control of gene therapy using ionizing radiation. Nat. Med., *1:* 786–791, 1995.
45. Gazit, G., Hung, G., Chen, X., Anderson, W. F., and Lee, A. S. Use of the glucose starvation-inducible glucose regulated protein 78 promoter in suicide gene therapy of murine fibrosarcoma. Cancer Res., *59:* 3100–3106, 1999.
46. Dachs, G. U., Patterson, A. V., Firth, J. D., Ratcliffe, P. J., Townsend, K. M., Stratford, I. J., and Harris, A. L. Targeting gene expression to hypoxic tumor cells. Nat. Med., *3:* 515–520, 1997.
47. Sistonen, A. C., Santoro, L., and Morimoto, R. I. Antiproliferative prostaglandins activate heat shock transcription factor. Proc. Natl. Acad. Sci. USA, *89:* 6227–6231, 1992.
48. Roberts, W. G., Liaw, L-H., and Berns, M. W. *In vitro* Photosensitization. An electron microscopy study of cellular destruction with mono-L-aspartyl chlorin e6 and Photofrin. Laser Surg. Med., *9:* 102–108, 1989.
49. Kessel, D. Sites of photosensitization by derivatives of hematoporphyrin. Photochem. Photobiol., *44:* 489–494, 1986.
50. Satyal, S. H., Chen, D., Fox, S. G., Kramer, J. M., and Morimoto, R. I. Negative regulation of the heat shock transcriptional response by HSBP1. Genes Dev., *12:* 1962–1974, 1998.
51. Lee, Y. J., and Corry, P. M. Metabolic oxidative stress induced HSP70 gene expression is mediated through SAPK pathway. Role of Bcl-2 and c-Jun NH2-terminal kinase. J. Biol. Chem., *273:* 29857–29863, 1998.
52. Harris, C. C., and Hollstein, M. Clinical implications of the p53 tumor suppressor gene. N. Engl. J. Med., *329:* 1318–1327, 1993.
53. Lowe, S. W., Bodis, S., McClatchey, A., Reminton, L., Ruley, H. E., Fisher, D. E., Housman, D. E., and Jacks, T. p53 status and the efficacy of cancer therapy in-vivo. Science (Washington DC), *266:* 807–810, 1994.
54. Fisher, A. Danenberg, K., Banerjee, D., Bertino, J., Danenberg, P., and Gomer, C. Increased photosensitivity in HL60 cells expressing wild type p53. Photochem. Photobiol., *66:* 88–93, 1997.
55. Old, L. J. Tumor necrosis factor (TNF). Science (Washington DC), *230:* 630–632, 1985.
56. Sersa, G., Willingham, V., and Milas, L. Anti-tumor effects of tumor necrosis factor alone or combined with radiotherapy. Int. J. Cancer, *42:* 129–134, 1988.
57. Bellnier, D. A. Potentiation of photodynamic therapy in mice with recombinant human tumor necrosis factor-α. J. Photochem. Photobiol., *8:* 203–210, 1991.
58. Evans, S., Matthews, W., Perry, R., Fraker, D., Norton, J., and Pass, H. Effects of photodynamic therapy on tumor necrosis factor production by murine macrophages. J. Natl. Cancer Inst., *82:* 34–38, 1990.
59. Nseyo, U. O., Whalen, R. K., Duncan, M. R., and Berman, B. Urinary cytokines following photodynamic therapy for bladder cancer. A preliminary report. Urology, *36:* 167–171, 1990.
60. Mizuguchi, H., Nakagawa, T., Toyosawa, S., Nakanishi, M., Imazu, S., Nakanishi, T., Tsutsumi, Y., Nakagawa, S., Hayakawa, T., Ijuhin, N., and Mayumi, T. Tumor necrosis factor α-mediated tumor regression by the *in vivo* transfer of genes into the artery that leads to tumors. Cancer Res., *58:* 5725–5730, 1998.
61. Lin, H., Head, M., Han, L., Jim, M., and Goodman, R. Myc-mediated transactivation of hsp70 expression following exposure to magnetic fields. J. Cell. Biochem., *69:* 181–188, 1998.

[CANCER RESEARCH 60, 4066–4069, August 1, 2000]

Advances in Brief

Antiangiogenic Treatment Enhances Photodynamic Therapy Responsiveness in a Mouse Mammary Carcinoma[1]

Angela Ferrario, Karl F. von Tiehl, Natalie Rucker, Margaret A. Schwarz, Parkash S. Gill, and Charles J. Gomer[2]

Clayton Center for Ocular Oncology, Childrens Hospital Los Angeles, Los Angeles, California 90027 [A. F., K. F. v. T., N. R., C. J. G.], and Departments of Pediatrics [C. J. G., M. A. S.], Radiation Oncology [C. J. G.], Medicine [P. S. G.], Pathology [P. S. G.], and Surgery [M. A. S.], Keck School of Medicine, University of Southern California, Los Angeles, California 90033

Abstract

Photodynamic therapy (PDT) is a promising cancer treatment that induces localized tumor destruction via the photochemical generation of cytotoxic singlet oxygen. PDT-mediated oxidative stress elicits direct tumor cell damage as well as microvascular injury within exposed tumors. Reduction in vascular perfusion associated with PDT-mediated microvascular injury produces tumor tissue hypoxia. Using a transplantable BA mouse mammary carcinoma, we show that Photofrin-mediated PDT induced expression of the hypoxia-inducible factor-1α (HIF-1α) subunit of the heterodimeric HIF-1 transcription factor and also increased protein levels of the HIF-1 target gene, vascular endothelial growth factor (VEGF), within treated tumors. HIF-1α and VEGF expression were also observed following tumor clamping, which was used as a positive control for inducing tissue hypoxia. PDT treatment of BA tumor cells grown in culture resulted in a small increase in VEGF expression above basal levels, indicating that PDT-mediated hypoxia and oxidative stress could both be involved in the overexpression of VEGF. Tumor-bearing mice treated with combined antiangiogenic therapy (IM862 or EMAP-II) and PDT had improved tumoricidal responses compared with individual treatments. We also demonstrated that PDT-induced VEGF expression in tumors decreased when either IM862 or EMAP-II was included in the PDT treatment protocol. Our results indicate that combination procedures using antiangiogenic treatments can improve the therapeutic effectiveness of PDT.

Introduction

PDT[3] involves treating solid malignancies with tissue-penetrating laser light following the systemic administration of a tumor localizing photosensitizer (1). Properties of photosensitizer localization in tumor tissue and photochemical generation of reactive oxygen species are combined with precise delivery of laser-generated light to produce a treatment offering local tumoricidal activity (2, 3). The porphyrin photosensitizer PH recently received Food and Drug Administration approval for PDT treatment of esophageal and endobronchial carcinomas (1). PDT is also undergoing clinical evaluation for the treatment of bladder, head and neck, brain, intrathoracic, and skin malignancies (1). PDT targets include tumor cells, tumor microvasculature, inflammatory cells, and immune host cells (1–3). Vascular effects induced by PH-mediated PDT include perfusion changes, vessel constriction, macromolecular vessel leakage, leukocyte adhesion, and thrombus formation (1, 4). These effects appear to be linked to platelet activation and release of thromboxane (5). Microvasculature damage is readily observed histologically following PDT and leads to a significant decrease in blood flow as well as severe and persistent tumor tissue hypoxia (6, 7). Rapid and substantial reductions in tissue oxygenation can also occur during illumination by direct utilization of oxygen during the photochemical generation of reactive oxygen species (7, 8).

Tissue hypoxia induces a plethora of molecular and physiological responses, including an adaptive response associated with gene activation (9). A primary step in hypoxia-mediated gene activation is the formation of the HIF-1 transcription factor complex (9, 10). HIF-1 is a heterodimeric complex of two helix-loop-helix proteins, HIF-1β (ARNT) and HIF-1α (11). ARNT is constitutively expressed, whereas HIF-1α is rapidly degraded under normoxic conditions. Hypoxia induces the stabilization of the HIF-1α subunit, which in turn allows for the formation of the transcriptionally active protein complex (11, 12). A number of HIF-1-responsive genes have been identified, including VEGF, erythropoietin, and glucose transporter-1 (11). VEGF, also called vascular permeability factor, is an endothelial cell-specific mitogen involved in the induction and maintenance of the neovasculature in solid tumors (11, 13). VEGF expression increases in tumor tissue under hypoxia as a result of both transcriptional activation and increased stabilization (11, 14).

In the current study, we examined whether PDT-induced microvascular damage and the resulting hypoxia could serve as activators of molecular events leading to the increased expression of VEGF within treated tumor tissue. We also determined whether antiangiogenic compounds, which counter the actions of VEGF, could improve PDT tumor responsiveness. Our results document that PH-mediated PDT induces expression of HIF-1α and the transcription factor's target gene, *VEGF*, in a transplanted mouse mammary carcinoma. We also document enhanced tumoricidal activity when PDT is combined with antiangiogenic therapy.

Materials and Methods

Drugs and Reagents. The photosensitizer Photofrin porfimer sodium was a gift from QLT PhotoTherapeutics, Inc. (Vancouver, British Columbia, Canada) and was dissolved in 5% dextrose in water to make a 2.5 mg/ml stock solution. Recombinant EMAP-II was prepared as described previously (15). A working solution at 10 μg/ml was prepared in PBS containing 0.1% BSA. IM862 was obtained from Cytran Inc. (Kirkland, WA) and was dissolved in saline to make a 5 mg/ml working solution (16). $CoCl_2$ was obtained from Sigma Chemical Co. (St. Louis, MO), and a 10 mM stock solution was prepared in water.

Received 4/19/00; accepted 6/14/00.

The costs of publication of this article were defrayed in part by the payment of page charges. This article must therefore be hereby marked *advertisement* in accordance with 18 U.S.C. Section 1734 solely to indicate this fact.

[1] This investigation was performed in conjunction with the Clayton Foundation for Research and was supported in part by USPHS Grants CA-31230, HL-60061, and HL 03981 from the NIH; Office of Naval Research Grant N000014-91-J-4047 from the Department of Defense; United States Army Medical Research Grant BC981102 from the Department of Defense; the Neil Bogart Memorial Fund of the T. J. Martell Foundation for Leukemia, Cancer and AIDS Research; and the Las Madrinas Endowment for Experimental Therapeutics in Ophthalmology.

[2] To whom requests for reprints should be addressed, at Childrens Hospital Los Angeles, Mail Stop 67, 4650 Sunset Boulevard, Los Angeles, CA 90027. Phone: (323) 669-2335; Fax: (323) 669-0742; E-mail: cgomer@hsc.usc.edu.

[3] The abbreviations used are: PDT, photodynamic therapy; PH, Photofrin porfimer sodium; HIF-1, hypoxia-inducible transcription factor; ARNT, aryl hydrocarbon nuclear receptor-translocator; VEGF, vascular endothelial growth factor; EMAP-II, endothelial-monocyte activating polypeptide.

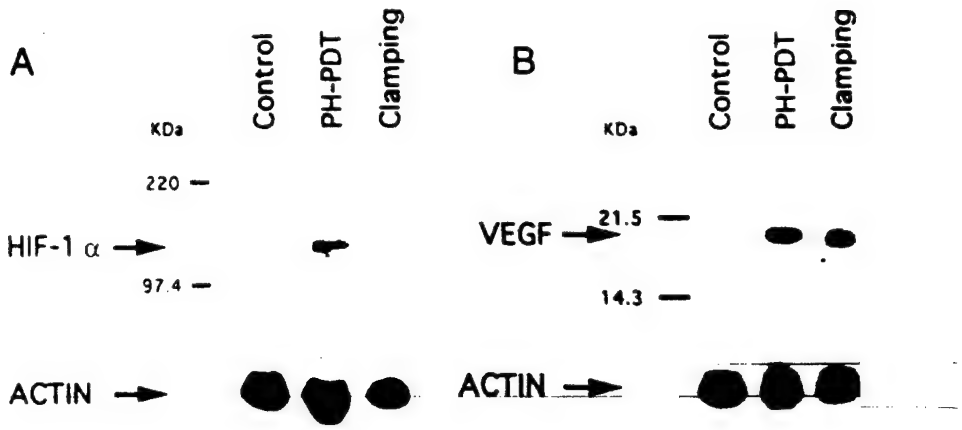

Fig. 1. PDT treatment of BA mammary carcinoma tumors growing in C3H mice induced expression of the transcription factor subunit HIF-1α and VEGF. *A*, tumors were collected immediately after treatment and evaluated for HIF-1α expression by Western immunoblot analysis. HIF-1α was not detectable in control tumors measuring 6–7 mm in diameter. Both PDT (5 mg/kg PH; 200 J/cm^2) and tumor clamping (45 min) induced HIF-1α expression *B*, separate tumors were collected 24 h after PDT or clamping (45 min) and assayed for VEGF expression by Western immunoblot analysis. Expression of actin was used to monitor protein loading.

Cells and *in Vivo* Tumor Model. BA mouse mammary carcinoma cells (originally obtained from the NIH tumor bank) were used in all *in vitro* and *in vivo* experiments (17). Cells were grown as a monolayer in RPMI 1640 supplemented with 10% FCS and antibiotics. The plating efficiency for the BA cells was 40–60%. s.c. BA mammary carcinomas were generated by trocar injection of 1-mm^3 pieces of tumor to the hind right flank of 8- to 12-week-old female C3H/HeJ mice (17).

***In Vitro* and *in Vivo* Treatment Protocols.** *In vitro* photosensitization protocols involved seeding cells into plastic Petri dishes and incubating overnight in complete growth medium to allow for cell attachment. PDT treatments included incubating cells in the dark at 37°C for 16 h with PH (25 μg/ml) in medium containing 5% FCS. Cells were then incubated for an additional 30 min in growth medium containing 10% FCS, rinsed in medium without serum, and exposed to red light (570–650 nm) generated by a parallel series of red Mylar-filtered 30 W fluorescent bulbs and delivered at a dose rate of 0.35 mW/cm^2. In specified experiments, cells were incubated with $CoCl_2$ (100 μM) in growth medium containing 5% FCS for 16 h. Treated cells were then re-fed with complete growth medium and incubated in the dark at 37°C until collected for analysis of VEGF secretion into the culture media. *In vivo* PDT tumor treatments were performed as reported previously on tumors measuring 6–7 mm in diameter (17). Briefly, PDT procedures included an i.v. injection of PH (5 mg/kg) followed 24 h later with non-thermal laser tumor irradiation using an argon-pumped dye laser emitting red light at 630 nm. A light dose rate of 75 mW/cm^2 and a total light dose of 200 J/cm^2 were used for all *in vivo* PDT treatments. After treatment, tumors were measured three times per week. Cures were defined as being disease free for at least 40 days after PDT (17). Antiangiogenic treatment was performed using either EMAP-II or IM862. Each compound was administered as daily i.p. injections for 10 consecutive days starting 1 h prior to PDT light treatment. Individual IM862 doses were 25 mg/kg, and individual EMAP-II doses were 50 μg/kg. Tumor tissue hypoxia was induced in selected experiments by clamping lesions for 45 min.

Western Blot Analysis. Tumors were collected at various times after treatment, homogenized with a Polytron in 1× reporter lysis buffer (Promega, Madison, WI), and evaluated for protein expression as described previously (18). Briefly, protein samples (30 μg) were size-separated on 10% (for HIF-1α) or 12.5% (for VEGF) discontinuous polyacrylamide gels and transferred overnight to nitrocellulose membranes. Filters were blocked for 1 h with 5% nonfat milk and then incubated for 2 h with either a mouse monoclonal anti-HIF-1α antibody (clone 54; Transduction Laboratories, Lexington, KY), a rabbit polyclonal anti-VEGF antibody (no. sc-507; Santa Cruz Biotechnology, Santa Cruz, CA), or a mouse monoclonal antiactin antibody (clone C-4; ICN, Aurora, OH). Filters were then incubated with either an antimouse or antirabbit peroxidase conjugate (Sigma), and the resulting complexes were visualized by enhanced chemiluminescence autoradiography (Amersham Life Science, Chicago, IL).

ELISA Assays. A Quantikine M mouse VEGF ELISA kit (R&D Systems, Minneapolis, MN) was used to quantify VEGF levels in cell culture media as well as in tumor extracts from control and treated mice. Results were normalized to protein concentrations from tumor tissue or cell lysates.

Statistics. Statistical analysis was performed using a two-tailed Student's *t* test to analyze VEGF levels and the χ^2 test for evaluation of tumor cure rates.

Results and Discussion

PDT continues to show promise in the treatment of a variety of malignant and nonmalignant disorders (1, 19). The use of PDT for advanced esophageal tumors offers prolonged tumor responses compared with standard Nd-YAG laser ablation treatments. Extended tumor responses are also observed in advanced non-small cell lung cancer patients treated with PDT compared with Nd-YAG laser ablation. Likewise, PDT applications continue to be encouraging for early stage lung cancer, brain cancers, head and neck cancers, and for nononcological disorders such as age-related macular degeneration (1, 19). Nevertheless, recurrences are observed after PDT, and methods to improve the therapeutic efficacy of this procedure are needed. Multiple physiological, biophysical, and/or pharmacological variables may account for recurrences after PDT (2, 3). Nonuniform distribution of photosensitizers within tumor tissue, inadequate light distribution, photosensitizer photobleaching, and treatment-induced oxy-

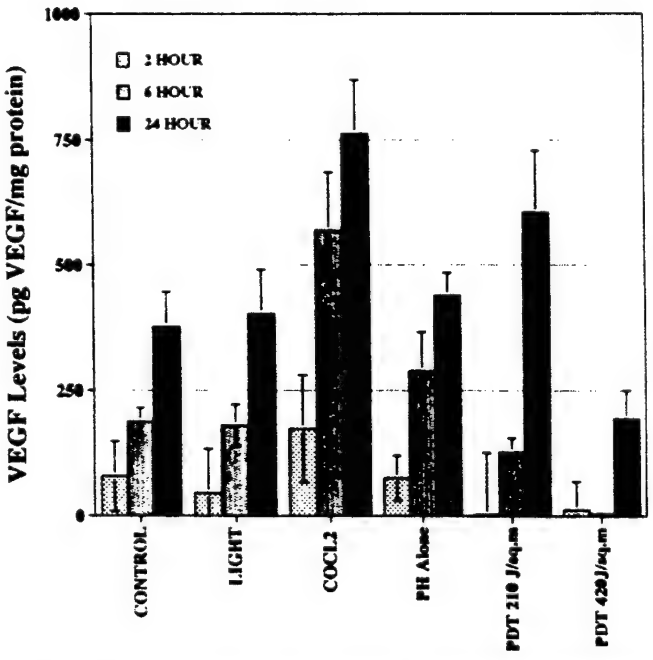

Fig. 2. VEGF levels in culture media from control BA mammary carcinoma cells and from cells exposed to light alone, $CoCl_2$, PH alone, or PDT. Culture medium was collected 2, 6, or 24 h after treatment, and VEGF concentrations were determined by ELISA. Each group represents the mean (*bars*, SE) of five individual experiments. A statistically significant difference in VEGF levels was observed only between $CoCl_2$ and control samples ($P < 0.05$).

gen deprivation may all contribute to suboptimal PDT responses. In the current study, we examined molecular events associated with PDT-induced hypoxia with an emphasis on determining whether PDT effectiveness could be enhanced with antiangiogenic therapy.

Several laboratories have shown that PDT produces microvascular damage within treated tumors and that PDT leads to tumor tissue hypoxia (4–8). Hypoxia mediates adaptive gene expression through the HIF transcription factor (9). An initial step in hypoxia-mediated gene activation is the formation of the HIF-1 heterodimeric transcription factor complex (10). One subunit, HIF-1β (ARNT), is constitutively expressed, whereas the second subunit, HIF-1α, is rapidly degraded under normoxic conditions by the ubiquitin-proteasome system (9, 10, 12). Because hypoxia induces increased expression and stabilization of the HIF-1α subunit as well as activates the HIF-1 transcription complex, it seemed likely that PDT-induced microvascular damage and resulting tumor tissue hypoxia could also stabilize HIF-1α and initiate HIF-1-mediated transcription. Fig. 1*A* uses Western analysis to show that PDT treatment of BA mammary carcinoma tumors growing in C3H mice induced expression of HIF-1α. This response was rapid, being observed within the first 5 min after PDT. Tumor clamping was used as a positive control and resulted in comparable HIF-1α expression. The HIF-1 complex functions via binding to a hypoxia response element found in the promoter region of the *VEGF* gene as well as in the 3′ flanking region of the *erythropoietin* gene (11). Expression of VEGF in areas around histologically documented tumor necrosis originally led to suggestions that hypoxia is a major regulator of tumor angiogenesis (13, 14). VEGF is a dimeric glycoprotein with strong mitogenic activity restricted primarily to endothelial cells (14). Fig. 1*B* documents VEGF expression after *in vivo* PDT. Western analysis was performed under reducing conditions on tumor lysates collected 24 h after PDT. PDT and tumor clamping both induced significant increases in VEGF expression within treated lesions. VEGF-induced angiogenesis plays an important role in tumor growth. Inhibition of VEGF activity with neutralizing antibodies inhibits the growth of primary and metastatic tumors, and attenuation of VEGF expression decreases tumor growth and vascularity (20). Our results suggest that PDT may be functioning as a mediator of tumor angiogenesis and tumor recurrence by enhancing expression of VEGF within the treated tumor mass (14).

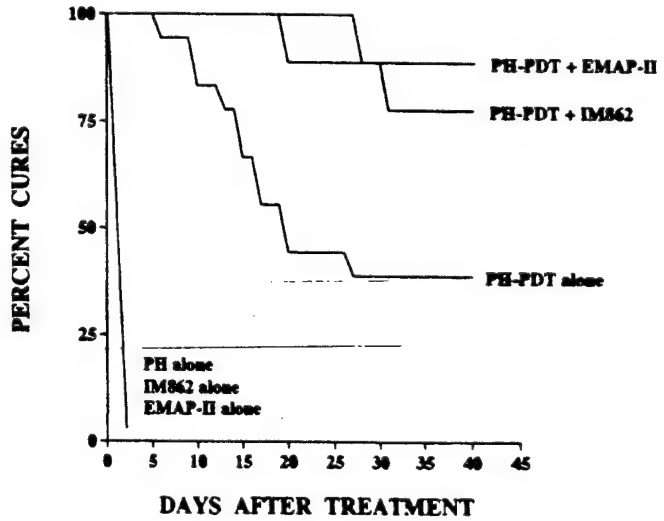

Fig. 3. Antiangiogenic treatments enhance the tumoricidal action of PDT. C3H mice transplanted with BA mammary carcinomas received daily injections for 10 days of either IM-862 (25 mg/kg per dose; $n = 9$) or EMAP-II (50 μg/kg per dose, $n = 9$) commencing 1 h prior to a single PDT treatment (5 mg/kg PH; 200 J/cm^2). Mice were monitored for tumor recurrences three times per week for 40 days. Control conditions included individual antiangiogenic treatments alone ($n = 9$) and PDT treatment alone ($n = 18$). There was a statistically significant difference in the percentage of cures between PDT alone *versus* PDT + EMAP-II or PDT + IM862 ($P < 0.05$).

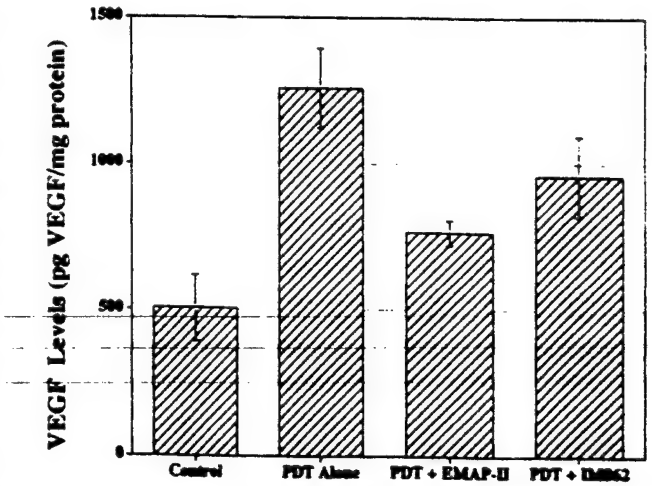

Fig. 4. The antiangiogenic compounds IM862 and EMAP-II can decrease VEGF levels in PDT-treated tumors. Tumor-bearing mice received no treatment (*Control*), PDT alone, or PDT plus two injections of either EMAP-II or IM862 (1 h prior to PDT and 23 h after PDT). Tumor samples were collected 24 h after PDT and assayed for VEGF expression using a commercial ELISA assay kit. Each group represents the mean (*bars*, SE) of six individual tumor samples. There was a statistically significant difference in VEGF levels between PDT alone and PDT plus EMAP-II ($P < 0.01$).

We next examined whether *in vitro* PDT of BA mammary carcinoma cells could also induce expression of VEGF. Fig. 2 shows VEGF levels collected from culture media at various time intervals for control and treatment conditions. Exposure to $CoCl_2$ served as a statistically significant positive control because exposure to this divalent metal induces cellular VEGF expression (11). A 210 J/m^2 PDT dose resulted in a modestly increase in VEGF levels when measured 24 h after treatment. The PDT doses (210 and 420 J/m^2) and $CoCl_2$ treatment produced clonogenic survival levels ranging from 33% to 96%. The *in vitro* PDT conditions would be expected to involve singlet oxygen-mediated oxidative stress but not induced hypoxia. These results suggest that the increase in VEGF expression observed in tumors after *in vivo* PDT may be associated with treatment-induced hypoxia and to a lesser extent with treatment-induced oxidative stress. Exposure of various mouse and human tumor cells to ionizing radiation and exposure of rat endothelial cells to hydrogen peroxide can up-regulate VEGF expression (20, 21). Additional studies will be required to determine similarities and differences in VEGF induction for various types of oxidative stress.

A growing number of reports have indicated that antiangiogenic agents can enhance the tumoricidal effectiveness of chemotherapy and radiation treatments (20, 22, 23). We next examined whether antiangiogenic treatments, using either EMAP-II or IM862, could enhance the tumoricidal action of PDT. EMAP-II is a single chain polypeptide that inhibits tumor growth and has antiangiogenic activity (15). EMAP-II induces apoptosis in growing capillary endothelial cells in both a time- and dose-dependent manner. EMAP-II also prevents vessel ingrowth in experimental angiogenesis models and in primary tumors. Interestingly, EMAP-II does not induce toxicity in normal organs. IM862 is a dipeptide of L-glutamyl-L-tryptophan that was initially isolated from the thymus (16). Preclinical studies have shown that the dipeptide inhibits angiogenesis in chorioallantoic membrane assays and inhibits VEGF production in monocytic lineage cells.[4] IM862 also inhibits tumor growth in xenograft models but has no direct cytotoxic effect on tumor cells. IM862 mediates these effects by

[4] R. Masood and P. Gill, unpublished data.

inhibiting production of VEGF and by activating natural killer cells. Intranasal administration of IM862 exhibits antitumor activity in patients with AIDS-associated Kaposi's sarcoma (16). IM862 also appears to be safe and well tolerated when delivered over prolonged time periods. A PDT procedure that produced a moderate cure rate alone was used to measure positive or negative changes in tumor response when a single PDT treatment was combined with daily injections of EMAP-II or IM862 for 10 days (17). Fig. 3 shows that antiangiogenic treatment statistically enhanced ($P < 0.05$) the tumoricidal action of PDT as measured by tumor cures. Specifically, the 200 J/cm^2 PDT dose alone produced a 39% cure rate, whereas PDT plus EMAP-II or IM862 produced tumor cures of 89 and 78%, respectively. The antiangiogenic treatments alone did not produce any tumor cures or tumor regression and only slightly modified tumor growth parameters.

Finally, we examined whether the antiangiogenic derivatives used in this study modulated PDT-induced VEGF levels in treated tumors. The *in vivo* PDT dose delivered to tumors (200 J/cm^2) induced rapid and severe tissue necrosis. Therefore, tumor samples were only collected 24 h after PDT. This timeframe allowed for two antiangiogenic drug doses (1 h prior to light treatment and 1 h prior to sacrifice). Fig. 4 shows a decrease in VEGF levels, measured by ELISA, in tumors treated with PDT combined with EMAP-II or IM862 compared with tumors treated with PDT alone. These results were obtained after only two doses of either EMAP-II or IM862. Nevertheless, a statistically significant decrease ($P < 0.01$) in PDT-induced VEGF levels was observed when EMAP-II was included in the treatment protocol. It is likely the 10 daily doses of EMAP-II or IM862 used in the PDT tumor treatment experiments would further attenuate VEGF levels.

In summary, we demonstrate that antiangiogenic treatments can potentiate PDT responsiveness. This result may involve attenuating the angiogenic actions of VEGF, which was observed to increase in PDT-treated tumors. Optimization of antiangiogenic parameters as well as an examination of various methods to block angiogenesis are being performed at present. The minimal systemic toxicity associated with antiangiogenic therapy suggests that these procedures should be compatible with clinical PDT and may provide an efficient strategy for selectively enhancing PDT tumor responsiveness. It will also be of clinical interest to determine whether antiangiogenic treatments can enhance PDT procedures for age-related macular degeneration because this pathology is marked by neovascularization (19).

Acknowledgments

We thank QLT PhotoTherapeutics, Inc. (Vancouver, British Columbia, Canada) for the generous gift of Photofrin, and Cytran Inc. (Kirkland, WA) for the generous gift of IM862.

References

1. Dougherty, T. J., Gomer, C. J., Henderson, B. W., Jori, G., Kessel, D., Korbelik, M., Moan, J., and Peng, Q. Photodynamic therapy. J. Natl. Cancer Inst., *90:* 889–905, 1998.
2. Henderson, B. W., and Dougherty, T. J. How does photodynamic therapy work? Photochem. Photobiol., *55:* 145–157, 1992.
3. Oleinick, N. L., and Evans, H. E. The photobiology of photodynamic therapy: cellular targets and mechanisms. Radiat. Res., *150:* S146–S156, 1998.
4. Fingar, V. H., Wieman, T. J., Wiehle, S. A., and Cerrito, P. B. The role of microvascular damage in photodynamic therapy: the effect of treatment on vessel constriction, permeability, and leukocyte adhesion. Cancer Res., *52:* 4914–4921, 1992.
5. Fingar, V. H., Wieman, T. J., and Haydon, P. S. The effects of thrombocytopenia on vessel stasis and micromolecular leakage after photodynamic therapy using Photofrin. Photochem. Photobiol., *66:* 513–517, 1997.
6. van Geel, I. P. J., Oppelaar, H., Rijken, P. F. J. W., Bernsen, H. J. J. A., Hagemeier, N. E. M., van der Kogel, A. L., Hodgkiss, R. J., and Stewart, F. A. Vascular perfusion and hypoxic areas in RIF-1 tumours after photodynamic therapy. Br. J. Cancer, *73:* 288–293, 1996.
7. Sitnik, T. M., Hampton, J. A., and Henderson, B. W. Reduction of tumor oxygenation during and after photodynamic therapy in-vivo: effects of fluence rate. Br. J. Cancer, *77:* 1386–1394, 1998.
8. Foster, T. H., Murant, R. S., Byrant, R. G., Knox, R. S., Gibson, S. L., and Hilf, R. Oxygen consumption and diffusion effects in photodynamic therapy. Radiat. Res., *126:* 296–303, 1991.
9. Ratcliffe, P. J., O'Rourke, J. F., Maxwell, P. H., and Pugh, C. W. Oxygen sensing, hypoxia-inducible factor-1 and the regulation of mammalian gene expression. J. Exp. Biol., *201:* 1153–1162, 1998.
10. Wang, G. L., and Semenza, G. L. General involvement of hypoxia-inducible factor in transcriptional response to hypoxia. Proc. Natl. Acad. Sci. USA, *90:* 4303–4308, 1993.
11. Forsythe, J. A., Jiang, B-H., Iyer, N. V., Agani, F., Leung, S. W., Koos, R. D., and Semenza, G. L. Activation of vascular endothelial growth factor gene transcription by hypoxia-inducible factor 1. Mol. Cell Biol., *16:* 4604–4613, 1996.
12. Huang, L. E., Gu, J., Schau, M., and Bunn, H. F. Regulation of hypoxia-inducible factor 1a is mediated by an oxygen dependent degradation domain via the ubiquitin proteasome pathway. Proc. Natl. Acad. Sci. USA, *95:* 7987–7992, 1998.
13. Senger, D. R., Peruzzi, C. A., Feder, J., and Dvorak, H. F. A highly conserved vascular permeability factor secreted by a variety of human and rodent tumor cell lines. Cancer Res., *46:* 5629–5632, 1986.
14. Shweiki, D., Itin, A., Soffer, D., and Keshet, E. Vascular endothelial growth factor induced by hypoxia may mediate hypoxia-initiated angiogenesis. Nature (Lond.), *359:* 843–845, 1992.
15. Schwarz, M. A., Kandel, J., Brett, J., Li, J., Hayward, J., Schwarz, R. E., Chappey, O., Wautier, J-L., Chabot, J., Gerfo, P. L., and Stern, D. Endothelial-monocyte activating polypeptide II, a novel antitumor cytokine that suppresses primary and metastatic tumor growth and induces apoptosis in growing endothelial cells. J. Exp. Med., *190:* 341–353, 1999.
16. Tulpule, A., Scadden, D. T., Espina, B. M., Cabriales, S., Howard, W., Shea, K., and Gill, P. S. Results of a randomized study of IM862 nasal solution in the treatment of AIDS-related Kaposi's sarcoma. J. Clin. Oncol., *18:* 716–723, 2000.
17. Ferrario, A., Kessel, D., and Gomer, C. J. Metabolic properties and photosensitizing responsiveness of mono-L-aspartyl chlorin e_6 in a mouse tumor model. Cancer Res., *52:* 2890–2893, 1992.
18. Fisher, A. M. R., Ferrario, A., Rucker, N., Zhang, S., and Gomer, C. J. Photodynamic therapy sensitivity is not altered in human tumor cells after abrogation of p53 function. Cancer Res., *59:* 331–335, 1999.
19. Miller, J. W., Schmidt-Erfurth, U., Sickenberg, M., Pournaras, C. J., Laqua, H., Barbazetto, I., Zografos, L., Piguet, B., Donati, G., Lane, A. M., Birngruber, R., van den Berg, H., Strong, A., Manjuris, U., Gray, T., Fsadni, M., Bressler, N. M., and Gragoudas, E. S., Photodynamic therapy with verteporfin for choroidal neovascularization caused by age-related macular degeneration: results of a single treatment in a phase 1 and 2 study. Arch. Ophthalmol., *117:* 1161–1173, 1999.
20. Gorski, D. H., Beckett, M. A., Jaskowiak, N. T., Calvin, D. P., Mauceri, H. J., Salloum, R. M., Seetharam, S., Koons, A., Hari, D. M., Kufe, D. W., and Weichselbaum, R. R. Blockade of the vascular endothelial growth factor stress response increases the antitumor effects of ionizing radiation. Cancer Res., *59:* 3374–3378, 1999.
21. Chua, C. C., Hamdy, R. C., and Chua, B. H. Upregulation of vascular endothelial growth factor by H_2O2 in rat heart endothelial cells. Free Radic. Biol. Med., *25:* 891–897, 1998.
22. Teicher, B. A., Sotomayor, E. A., and Huang, Z. D. Antiangiogenic agents potentiate cytotoxic cancer therapies against primary and metastatic disease. Cancer Res., *52:* 6702–6704, 1992.
23. Mauceri, H. J., Hanna, N. N., Beckett, M. A., Gorski, D. H., Staba, M. J., Stellato, K. A., Bigelow, K., Heimann, R., Gately, S., Dhanabal, M., Soff, G. A., Sukhatme, V. P., Kufe, D. W., and Weichselbaum, R. R. Combined effects of angiostatin and ionizing radiation in antitumor therapy. Nature (Lond.), *394:* 287–291, 1998.

Journal of Porphyrins and Phthalocyanines
J. Porphyrins Phthalocyanines 2001; **5**: 143–146

Constitutive overexpression of HSP-70 in thermal resistant tumor cells does not alter sensitivity to porphyrin-, chlorin-, or purpurin-mediated PDT

NATALIE RUCKER[1], ANGELA FERRARIO[1] and CHARLES J. GOMER[1,2]*

[1]*Clayton Center for Ocular Oncology, Children's Hospital Los Angeles, Los Angeles, CA 90027, USA*
[2]*Departments of Pediatrics, Radiation Oncology, and Molecular Pharmacology & Toxicology, University of Southern California, Los Angeles, CA 90027, USA*

Received 9 May 2000
Accepted 15 June 2000

ABSTRACT: Cellular expression of the 70 kDa heat shock protein (HSP-70) is observed following hyperthermia and is correlated with transient resistance to subsequent heating. Photodynamic therapy (PDT) mediated oxidative stress can also induce transcriptional and translational expression of a variety of genes including HSP-70. However, PDT-mediated HSP-70 expression can vary as a function of photosensitizer type and incubation conditions. In the current study we used three clinically relevant photosensitizers, a porphyrin (Photofrin), a purpurin (SnET2), and a chlorin (NPe6), to examine PDT-mediated HSP-70 expression profiles and photosensitivity characteristics in parental radiation-induced fibrosarcoma cells (RIF-1) and in thermal resistant RIF-1 clones. We observed that *in vitro* PDT treatments using either SnET2 or NPe6 induced HSP-70 expression but that comparable PDT treatments using Photofrin did not result in increased HSP-70 levels. We also observed that PDT sensitivity in parental and heat-resistant cell clones were similar for each photosensitizer while thermal sensitivity was significantly reduced in the RIF clones which constitutively overexpressed HSP-70. These results indicate that definable differences can exist in the molecular pathways induced by PDT for different photosensitizers. Our results also demonstrate that constitutive overexpression of HSP-70 does not modulate PDT photosensitivity regardless of whether PDT treatments induce HSP-70 expression. We conclude that HSP-70 expression does not play a significant role in cellular PDT photosensitivity. Copyright © 2001 John Wiley & Sons, Ltd.

KEYWORDS: photodynamic therapy; heat shock protein; oxidative stress; photosensitivity; photosensitizer

INTRODUCTION

Photodynamic therapy (PDT) is a promising treatment modality for a variety of solid tumors [1, 2]. PDT involves treating solid malignancies with tissue penetrating visible light following the administration of a tumor-localizing photosensitizer [3]. Properties of photosensitizer localization in tumor tissue and photochemical generation of reactive oxygen species are combined with precise delivery of laser-generated light to produce a procedure offering effective local tumoricidal activity [4]. The porphyrin photosensitizer, Photofrin (PH), recently received FDA approval for PDT treatment of esophageal and endobronchial carcinomas [2]. PH-mediated PDT is also undergoing clinical evaluation for the treatment of bladder, head and neck, brain, intrathoracic, and skin malignancies [1, 2]. At the same time, a growing number of second-generation photosensitizers are also undergoing clinical evaluation [2, 4, 5]. These new compounds exhibit properties comparable or superior to PH, including: chemical purity, increased photon absorption at longer wavelengths, improved tumor tissue retention, rapid clearance from surrounding normal tissues, high quantum yields for the generation of reactive oxygen species, and minimal dark toxicity [3–5].

Biochemical analysis indicates a variety of subcellular PDT targets, including the mitochondria, plasma membrane, and lysosomes [4]. PDT can induce damage to tumor cells, tumor microvasculature, inflammatory cells, and immune host cells [6, 7]. Apoptotic and necrotic pathways are both involved in PDT-mediated cell death [4]. An assortment of early response genes, genes associated with signal transduction pathways and cytokine expression, as well as stress response genes are activated by PDT [2, 8–11]. Stress proteins identified as HSPs are expressed following PDT and this response is at the level of transcription [12]. HSPs are highly conserved throughout evolution and function as molecular chaperones of nascent proteins [13]. HSPs are also involved in protecting cells from stress by binding to denatured proteins and assisting in proper refolding [13]. There is a large body of evidence indicating that HSPs modulate cellular responses to heat and are involved in the development of thermotolerance [14–16].

We previously examined Photofrin (PH)-mediated photosensitivity using parental RIF and RIF-TR clones constitutively overexpressing HSP-70 and did not observed cross resistance following hyperthermia and PH-mediated PDT

*Correspondence to: C. J. Gomer, Children's Hospital Los Angeles, Mail Stop 67 4650 Sunset Boulevard, Los Angeles, CA 90027, USA. E-mail: cgomer@hsc.usc.edu

[8]. However, unlike hyperthermia, PH-mediated PDT does not induce HSP-70 expression in RIF cells grown in culture [11]. In the current study, we have examined photosensitivity in parental and RIF-TR cells using photosensitizers which can induce HSP-70 expression. These experiments were designed to further examine the biological relevance of HSP-70 as a potential modulator of PDT sensitivity.

EXPERIMENTAL

Photosensitizers

All photosensitizers are in clinical trials [2]. Photofrin(R) (porfimer sodium) (PH) was a gift from QLT Phototherapeutics (Vancouver, British Columbia, Canada); NPe6 was a gift from Porphyrin Products (Logan, UT); and SnET2 was a gift from PDT Systems, (Miravant Medical Technologies, Santa Barbara, CA).

Cells and Cell Culture Conditions

Parental mouse radiation-induced fibrosarcoma cells (RIF-1) and three thermal resistant RIF-1 clones (TR-4, TR-5, and TR-10) were used in all experiments [16]. Cells were grown in RPMI 1640 culture media supplemented with 15% FCS and antibiotics.

In vitro PDT and Hyperthermia Treatments

Prior to treatments, appropriate numbers of cells were plated into 60 mm or 100 mm plastic Petri dishes (for PDT exposures) or into T-25 or T-75 plastic flasks (for hyperthermia exposures). For PDT, cells were incubated in the dark at 37 °C for 16 h with one of the three photosensitizers (25 $\mu g\ ml^{-1}$ for Photofrin and NPe6 or 0.75 $\mu g\ ml^{-1}$ for SnET2) in RPMI 1640 containing 5% FCS. The cells were then rinsed for 30 min in growth media containing 15% FCS and exposed to graded doses of light. Cells incubated with PH were exposed to broad spectrum (570 nm to 650 nm) red light (0.35 mW cm^{-2}) generated by a parallel series of 30 W fluorescent bulbs. NPe6-treated cells were exposed to 664 nm light (2 mW cm^{-2}) generated by an argon ion laser-pumped dye laser and SnET2-treated cells were exposed to 660 nm light (2 mW/ cm^{-2}) generated by the same laser. After light treatments, cells were re-fed with complete growth media and incubated at 37 °C. Cytotoxicity was determined 8 days after treatment by clonogenic assay. Hyperthermia involved exposing cells to 45 °C in a temperature-controlled water bath. *In vitro* hyperthermia involved exposing cells to warmed media and placement in a temperature-controlled water bath for designated time intervals.

Photosensitizer Uptake Analysis

Cellular photosensitizer levels were determined by absorption spectroscopy as previously described. Briefly, photosensitizers were extracted from cells by sonication in 0.1 N NaOH. Drug concentrations were then determined from calibration curves using absorption measurements ratios of: 390 nm and 470 nm for PH, 437 nm and 480 nm for SnET2, and 400 nm and 440 nm for NPe6. Photosensitizer concentrations were expressed as µg per mg cellular protein.

Western Analysis

Treated cells were incubated at 37 °C for 6 h and then collected by trypsinization for analysis of protein expression as described previously [11]. Briefly, cell pellets were lysed in 2 × sample buffer (Tris base 0.125 M, pH 6.8, 4% SDS, 10% glycerol, 0.02% bromophenol blue, 4% β-mercaptoethanol) at a concentration of 2×10^7 cells per ml. Protein concentrations were determined using a Biorad protein assay. Samples containing 60 µg of protein were size separated by electrophoresis on a 10% polyacrylamide gel at room temperature. Proteins were then transferred overnight to nitrocellulose paper. Filters were blocked for 2 h with 10% nonfat milk and then incubated for 2 h with a mouse monoclonal antibody specific for inducible HSP-72 (SPA-810, StressGen Biotechnologies Corp., Victoria, British Columbia, Canada). Filters were then incubated with an anti-mouse peroxidase conjugate (Sigma, St. Louis, MO) and the resulting complexes visualized with an alkaline phosphatase linked avidin/biotin detection system (Vectastain, Vector Laboratories, Burlingame, CA).

RESULTS AND DISCUSSION

Thermal Resistant RIF Clones Constitutively Overexpress HSP-70 and Exhibit Reduced Sensitivity to Hyperthermia

Figure 1 shows Western immunoblots of HSP-70 expression in parental RIF cells and TR clones under control and heat-treated conditions. Constitutive overexpression of HSP-70 is observed in the TR clones and this agrees with previous reports. Heat shock proteins represent a highly conserved family of constitutively expressed and stress inducible proteins ranging in size from approximately 20 kDa to 110 kDa [13]. These proteins can function as molecular chaperones and assist in the folding and/or translocation of nascent proteins [13]. They can also bind to denatured proteins and are associated with the development of thermal tolerance or transient resistance to hyperthermia [13]. Interestingly, hyperthermia increased HSP-70 levels in both the parental RIF cells and TR clones. Overexpression of HSP-70 has been correlated with enhanced resistance to hyperthermia [14]. Figure 2 shows survival curves for RIF-1 and TR clones exposed to hyperthermia. Cells were exposed to 45 °C for varying time intervals and then analyzed for survival using a clonogenic assay. The decreased heat

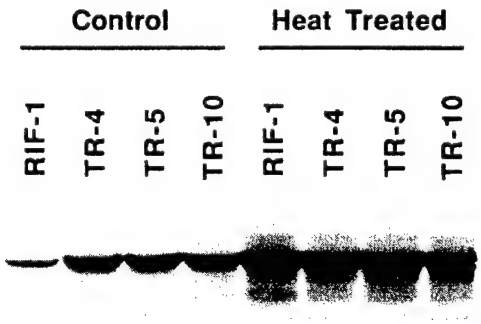

Fig. 1. Western immunoblot analysis of HSP-70 expression in parental RIF and RIF-TR clones. Non-treated cells served as controls and heat-treated cells were exposed to 45 °C for 20 min and then collected 6 h after treatment.

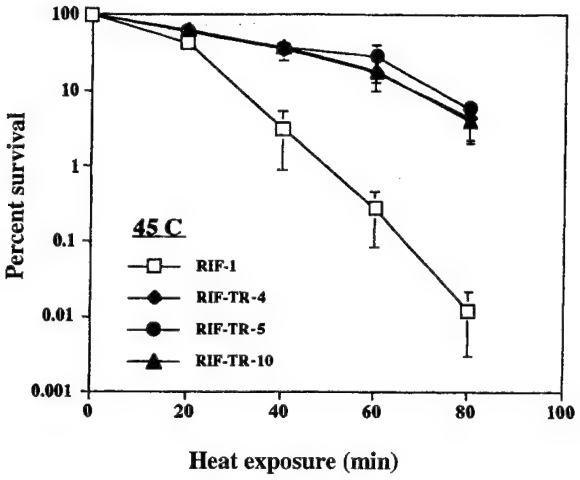

Fig. 2. Survival curves for parental RIF cells (□), TR-4 (◆), TR-5 (●), and TR-10 (▲) clones exposed to increasing time intervals at 45°C. Points represent the mean ± SD of five separate experiments.

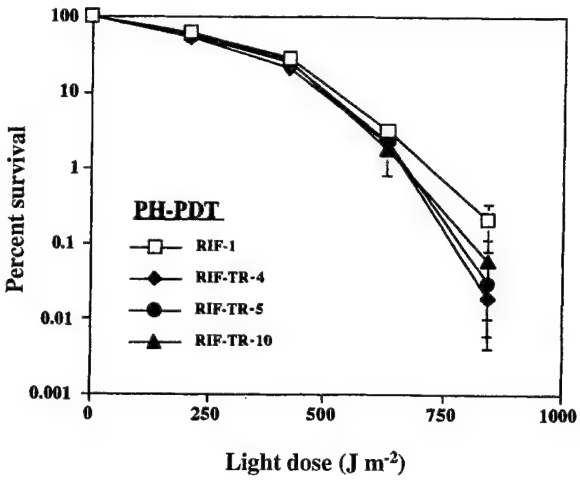

Fig. 4. Survival curves for parental RIF cells (□), TR-4 (◆), TR-5 (●), and TR-10 (▲) clones exposed to increasing doses of PH-mediated PDT. Points represent the mean ± SE of five separate experiments.

sensitivity for the TR clones also agrees with previous reports [16].

Chlorin-and Purpurin-Mediated PDT Induces Expression of HSP-70

Figure 3 shows Western immunoblot analysis of HSP-70 expression in parental RIF and TR clones following PDT using either NPe6, SnET2, or PH as photosensitizers. PDT treatments were effective at inducing HSP-70 expression when NPe6 and SnET2 were used as photosensitizers. However, PH-mediated PDT did not induce expression of HSP-70. Interestingly, SnET2 incubation in the absence of light, also induced increased HSP-70 expression in parental RIF cells. All photosensitizers are involved in the Type II photochemical generation of singlet oxygen [2, 3] and therefore these results indicate that random singlet oxygen exposure to cells is not sufficient by itself to activate the heat-shock response. As we previously suggested, differences in subcellular targets (mitochondria for PH and lysosomal for Npe6 and SnET2) may play a role in the variations in HSP-70 expression observed following cellular PDT [11]. All three photosensitizers can elicit HSP-70 expression following *in vivo* PDT and therefore additional studies are required to differentiate whether *in vitro* PDT experiments actually mimic *in vivo* procedures [11].

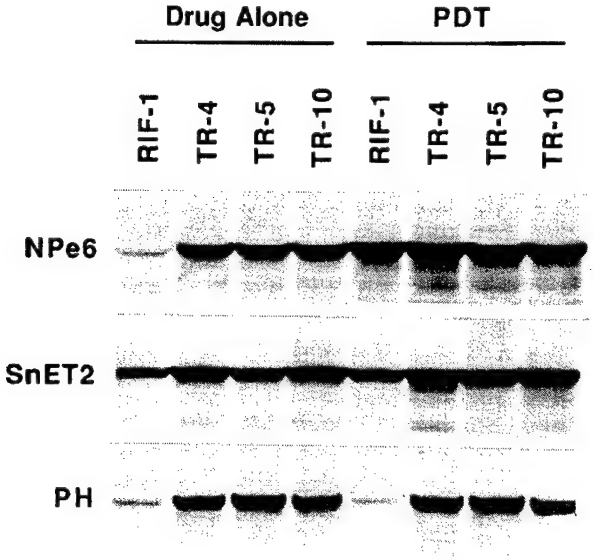

Fig. 3. Western immunoblot analysis of HSP-70 expression in parental RIF cells and RIF-TR clones. Cells were either exposed to photosensitizer alone without light (drug alone) or to photosensitizer plus light (PDT) at light doses of 315 J m^{-2} for PH, 3600 J m^{-2} for NPe6, and 1600 J m^{-2} for SnET2. Protein samples were collected 6 h after light treatment.

PDT Photosensitivity is not Altered in HSP-70 Expressing TR Cells

We reported previously that RIF TR clones exhibit comparable photosensitivity as parental RIF cells when exposed to PH-mediated PDT [8]. However, PH-mediated PDT does not induce increased HSP-70 expression in RIF

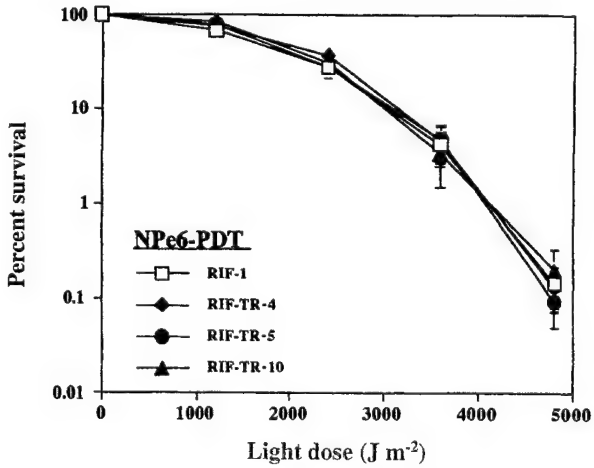

Fig. 5. Survival curves for parental RIF cells (□), TR-4 (◆), TR-5 (●), and TR-10 (▲) clones exposed to increasing doses of NPe6-mediated PDT. Points represent the mean ± SE of five separate experiments.

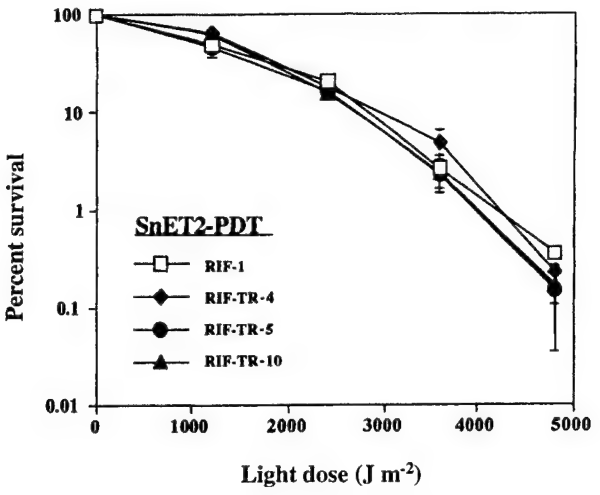

Fig. 6. Survival curves for parental RIF cells (□), TR-4 (◆), TR-5 (●), and TR-10 (▲) clones exposed to increasing doses of SnET2-mediated PDT. Points represent the mean ± SE of five separate experiments.

cells and therefore one might expect that PH-mediated PDT would not exhibit cross-resistance [11]. Interesting, NPe6- and SnET2-mediated PDT can induce HSP-70 expression (as described above) and therefore we examined whether PDT using these photosensitizers resulted in differential photosensitivity in TR cells that consitutively overexpress HSP-70. Figures 4–6 show that comparable levels of cell photosensitivity were obtained for all cell lines exposed to NPe6-, SnET2-, or PH-mediated PDT. Likewise, individual photosensitizer uptake levels in the parental and TR clones were also comparable (data not shown). Therefore, regardless of whether PDT induced HSP-70 expression, we did not observe modulated photosensitivity in RIF-TR cells compared to parental RIF cells. This implies that *in vitro* targets and/or cell death pathways are different for hyperthermia and PDT treatments.

Acknowledgements

This investigation was performed in conjunction with the Clayton Foundation for Research, and was supported in part by USPHS grant RO1-CA-31230 from the National Institutes of Health, Office of Naval Research grant N000014-91-J-4047 from the Department of Defense, US Army Medical Research grant BC981102 from the Department of Defense, the Neil Bogart Memorial Fund of the T.J. Martell Foundation for Leukemia, Cancer and AIDS Research, and the Las Madrinas Endowment for Experimental Therapeutics in Ophthalmology.

REFERENCES

1. Fisher AMR, Murphree A, Gomer CJ. *Laser Surg. Med.* 1995; **17**: 2.
2. Dougherty TJ, Gomer CJ, Henderson BW, Jori G, Kessel D, Korbelik M, Moan J, Peng Q. *J. Natl. Cancer Inst.* 1998; **9**: 889.
3. Henderson BW, Dougherty TJ. *Photochem. Photobiol.* 1992; **55**: 145.
4. Oleinick NL, Evans HE. *Radiat. Res.* 1998; **150**: S146.
5. Pandey RK, Constantine S, Tsuchida T, Zheng G, Medforth CJ, Aoudia M, Kozyrev AN, Rodgers MA, Kato H, Smith KM, Dougherty TJ. *J. Med. Chem.* 1997; **40**: 2770.
6. Fingar VH, Wieman TJ, Wiehle SA, Cerrito PB. *Cancer Res.* 1992; **52**: 4914.
7. Fingar VH, Wieman TJ, Haydon PS. *Photochem. Photobiol.* 1997; **66**: 513.
8. Gomer CJ, Rucker N, Wong S. *Cancer Res.* 1990; **50**: 5365.
9. Gomer CJ, Ferrario A, Rucker N, Wong S, Lee A. *Cancer Res.* 1991; **51**: 6574.
10. Luna MC, Wong S, Gomer CJ. *Cancer Res.* 1994; **53**: 1374.
11. Gomer CJ, Ryter SW, Ferrario A, Rucker N, Wong S, Fisher AMR. *Cancer Res.* 1996; **56**: 2355.
12. Luna M, Ferrario A, Wong S, Fisher AMR, Rucker N, Gomer CJ. *Cancer Res.* 2000; **60**: 1637.
13. Li GC, Mivechi NF, Weitzel G. *Int. J. Hyperthermia* 1995; **11**: 459.
14. Angelidis CE, Lazaridis I, Pagoulato GN. *Eur. J. Biochem.* 1991; **199**: 35.
15. Park Y-MK, Mivechi NF, Auger EA, Hahn GM. *Int. J. Radiat. Oncol. Biol. Phys.* 1994; **28**: 179.
16. Hahn GM, van Kersen I. *Cancer Res.* 1988; **48**: 1803.

[CANCER RESEARCH 61, 6185–6193, August 15, 2001]

Loss of p53 Function Confers High-Level Multidrug Resistance in Neuroblastoma Cell Lines[1]

Nino Keshelava, Juan J. Zuo, Ping Chen, Sitara N. Waidyaratne, Marian C. Luna, Charles J. Gomer, Timothy J. Triche, and C. Patrick Reynolds[2]

Division of Hematology-Oncology, Children's Hospital Los Angeles, Los Angeles, California 90027 [N. K., J. J. Z., P. C., S. N. W., M. C. L., C. J. G., T. J. T., C. P. R.], and Departments of Pediatrics [N. K., J. J. Z., P. C., M. C. L., C. J. G., C. P. R.] and Pathology [S. N. W., T. J. T.], University of Southern California School of Medicine, Los Angeles, California 90033

ABSTRACT

Neuroblastomas can acquire a sustained high-level drug resistance during chemotherapy and especially myeloablative chemoradiotherapy. p53 mutations are rare in primary neuroblastomas, but a loss of p53 function could play a role in multidrug resistance. We determined p53 function by measuring induction of p21 and/or MDM2 proteins in response to melphalan (L-PAM) in seven L-PAM-sensitive and 11 L-PAM-resistant neuroblastoma cell lines. p53 was functional in seven/seven drug-sensitive but in only 4/11 drug-resistant cell lines ($P = 0.01$). In four of the seven cell lines lacking p53 function, mutations of p53 were detected by the microarray GeneChip p53 Assay and automated sequencing, whereas six cell lines with functional p53 had no evidence of p53 mutations. All of the cell lines with wild-type (wt) p53 showed a strong transactivation of the *p53-HBS/CAT* reporter gene, whereas the four cell lines with mutant p53 failed to transactivate p53 HBS/CAT. Overexpression of MDM2 protein (relative to p53 functional lines) was seen in two p53-nonfunctional cell lines with wt p53; one showed genomic amplification of MDM2. Nonfunctional and mutated p53 was detected in a resistant cell line, whereas a sensitive cell line derived from the same patient before treatment had functional and wt p53. Loss of p53 function was selectively achieved by transduction of human papillomavirus 16 E6 (which degrades p53) into two drug-sensitive neuroblastoma cell lines with intact p53, causing high-level drug resistance to L-PAM, carboplatin, and etoposide. These data obtained with neuroblastoma cell lines suggest that the high-level drug resistance observed in some recurrent neuroblastomas is attributable to p53 mutations and/or a loss of p53 function acquired during chemotherapy. If confirmed in patient tumor samples, these data support development of p53-independent therapies for consolidation and/or salvage of recurrent neuroblastomas.

INTRODUCTION

Neuroblastoma is a malignant childhood neoplasm of the sympathetic nervous system. Intensive chemoradiotherapy supported with autologous bone marrow transplantation has improved survival for high-risk neuroblastoma, especially if followed by 13-*cis*-retinoic acid (1). However, most high-risk neuroblastoma patients develop recurrent disease that is refractory to additional therapy (2). We have shown that during therapy neuroblastomas acquire a sustained high-level drug resistance, which correlates with the clinical therapy of the patient and the intensity of the therapy received (3).

p53 is a transcriptional regulatory protein (reviewed in Refs. 4 and 5), of which the target genes include: $p21^{WAF1/CIP1/SID1}$, *MDM2*, *Bax*, and *Gadd45*. Products of these genes are critical for cell cycle regulation, apoptosis, and DNA repair. In response to genotoxic stress, wt p53 exerts antiproliferative effects such as induction of cell cycle arrest and apoptosis. Inactivation of p53 results in genomic instability (6), and tumors either fail to arrest in G_1 or exhibit diminished apoptosis (7) and can be resistant to chemotherapeutic agents (8–10). p53 mutations and/or deletions have been linked to drug resistance in acute lymphoblastic leukemia (11); melanoma (12); osteosarcoma (13); and breast (14), ovarian (15), and testicular (16) cancers.

Mutations of p53 are commonly found in many human cancers (17) but are seen in only 2% of neuroblastoma tumors examined (18–23), with most p53 mutations observed in tumors coming from patients with progressive disease (18–20). As an alternative to mutations, cytoplasmic sequestration and defective translocation of p53 have been suggested as mechanisms of nonmutational inactivation (24), but several studies have shown that p53 function is intact in neuroblastoma cell lines (25–27).

Like neuroblastomas, mutations of p53 are infrequent in testicular cancers (28). However, a study of testicular cancers showed that for those tumors that either were resistant to initial chemotherapy or recurred with drug-resistant disease after therapy, p53 mutations were identified within exons 6–9 in 50% of tumor samples with teratomatous histology (16). On the basis of these observations we sought to determine whether drug resistance in neuroblastoma cell lines was associated with a lack of p53 function and/or p53 mutations.

We have examined p53 function by measuring p53 transcriptional activity in response to alkylating agent-mediated induction of p21 and MDM2 in a panel of neuroblastoma cell lines with a spectrum of resistance (acquired during therapy in patients) to L-PAM,[3] CBDCA, and ETOP, all commonly used drugs in neuroblastoma therapy. We examined the cell lines for p53 mutations by the GeneChip p53 Assay (29) and confirmed mutations by automated dideoxy DNA sequencing (29). In addition, we studied p53 function using a p53 transactivation assay (30). Finally, we abrogated p53 function by transducing drug-sensitive neuroblastoma cell lines with HPV16 E6, which targets cellular p53 for rapid degradation and renders cells expressing HPV16 E6 devoid of p53 function (31). We then determined sensitivities of HPV16 E6-transduced clones to L-PAM, CBDCA, and ETOP.

Here we show in a panel of neuroblastoma cell lines that a loss of p53 function is correlated with high-level drug resistance, that selective abrogation of p53 function can confer high-level drug resistance, and that loss of p53 function in neuroblastoma can be attributable to both mutational and nonmutational mechanisms.

MATERIALS AND METHODS

Cell Lines. We used a panel of 18 neuroblastoma cell lines (3, 32–34) obtained from patients at various points of disease: 3 at DX before any therapy (SK-N-BE(1), SMS-SAN, and CHLA-122), 2 at progressive disease during dual-agent induction therapy (SMS-LHN and SMS-KCNR), 6 at progressive

Received 2/15/01; accepted 6/8/01.

The costs of publication of this article were defrayed in part by the payment of page charges. This article must therefore be hereby marked *advertisement* in accordance with 18 U.S.C. Section 1734 solely to indicate this fact.

[1] Supported in part by the Neil Bogart Memorial Laboratories of the T. J. Martell Foundation for Leukemia, Cancer, and AIDS Research, and by National Cancer Institute Grants CA82830, CA60104, and CA31230.

[2] To whom requests for reprints should be addressed, at Division of Hematology-Oncology, MS# 57, Children's Hospital Los Angeles, 4650 Sunset Boulevard, Los Angeles, CA 90027. Phone: (323) 669-5646; Fax: (323) 664-9226 or 9455; E-mail: preynolds@chla.usc.edu.

[3] The abbreviations used are: L-PAM, melphalan; wt, wild-type; CBDCA, carboplatin; ETOP, etoposide; HPV, human papillomavirus; DX, diagnosis; FBS, fetal bovine serum; HBS, high-affinity binding site; CAT, chloramphenicol acetyl transferase; LC_{90}, drug concentration that was cytotoxic for 90% of the cell population; GSH, glutathione; HRP, horseradish peroxidase; ECL, enhanced chemiluminescence.

disease during intensive multiagent chemotherapy (SK-N-BE(2), SK-N-RA, LA-N-6, CHLA-119, CHLA-171, and CHLA-225), and 7 derived at relapse after bone marrow transplantation (CHLA-8, CHLA-51, CHLA-79, CHLA-90, CHLA-134, CHLA-136, and CHLA-172).

A neuroblastoma origin for CHLA-122, CHLA-119, and CHLA-172 cell lines was confirmed by reverse transcription-PCR detection of tyrosine hydroxylase (TH) RNA expression, which is a specific marker for neuroblastoma (3, 35). CHLA-225 showed no TH expression but did show a pattern for binding of the neuroblastoma-associated monoclonal antibody HSAN1.2 and the anti-HLA class I antibody W6–32 characteristic of neuroblastoma (3, 34). Other cell lines in the panel were described previously (3, 32–34).

SMS-SAN, SMS-LHN, and SK-N-RA were cultured in complete medium made from RPMI 1640 (Irvine Scientific, Santa Ana, CA) supplemented with 10% heat inactivated FBS (Gemini Bio-Products, Inc., Calabasas, CA). SMS-KCNR, SK-N-BE(1) SK-N-BE(2), LA-N-6, CHLA-122, CHLA-171, CHLA-225, CHLA-119, CHLA-51, CHLA-8, CHLA-79, CHLA-90, CHLA-134, CHLA-136, and CHLA-172 were cultured in complete medium made from Iscove's modified Dulbecco's medium (Bio Whittaker, Walkersville, MD) supplemented with ~3 mM L-glutamine (Gemini Bioproducts, Inc., Calabasas, CA), 5 μg/ml each of insulin and transferrin, 5 ng/ml of selenous acid (ITS Culture Supplement; Collaborative Biomedical Products, Bedford, MA), and 20% heat inactivated FBS. All of the cell lines used in the study were under passage 30, *Mycoplasma* free, and were cultured at 37°C in a humidified incubator containing 95% air + 5% CO_2 atmosphere without antibiotics. Because cell lines were not selected for resistance to drugs *in vitro*, drug-resistance represents selection that occurred in patients during therapy and correlates with those drugs used during therapy (3, 32).

Retroviral Infection. PA317 packaging cells transfected with the control retrovirus vector, pLXSN, or with the vector pLXSN16E6 (31) containing the HPV type 16 E6 gene, were obtained from American Type Culture Collection. Supernatant was harvested from the packaging cells and filtered through a 0.45-μM filter. SMS-SAN and SMS-LHN cells were then plated in retrovirus stock (three parts) with Polybrene (final concentration 0.5 μg/ml) and in complete medium composed of RPMI 1640 supplemented with 10% FBS (five parts). After a 5-h incubation, 5 ml of complete medium was added, and after overnight incubation cells were resuspended in fresh complete medium. Forty-eight h later cells were seeded into six-well plates in complete medium containing 250 μg/ml of G418. Individual clones were then picked and expanded in G418 containing medium. The integration of HPV16 E6 into G418-resistant clones was confirmed by Western blotting.

Drugs and Reagents. Antibodies p53 (DO-1) mouse monoclonal, p21 (C-19) rabbit polyclonal, MDM2 (SMP14) mouse monoclonal, and HRP-labeled secondary antimouse and antirabbit antibodies were purchased from Santa Cruz Biotechnology, Inc., Santa Cruz, CA. ECL Western blotting detection reagents were purchased from Amersham Pharmacia Biotech (Piscataway, NJ). ETOP was obtained from Bristol-Myers Squibb Co., Princeton, NJ; the NIH, Bethesda, MD provided L-PAM and CBDCA. Fluorescein diacetate was purchased from Eastman Kodak Company, Rochester, NY. Eosin Y and Polybrene (hexadimethrine bromide) were ordered from Sigma Chemical Co., St. Louis, MO.

Protein Expression. Proteins were extracted in radioimmunoprecipitation assay buffer (50 mM NaCl, 50 mM Tris, 1% Triton X-100, 1% sodium deoxycholate, and 0.1% SDS) and 40 μg (p53 and MDM2 expression) or 60 μg (p21 expression) of total protein was loaded per lane. Proteins were fractionated on 12–14% Tris-Glycine pre-cast gels (Novex, San Diego, CA), transferred to nitrocellulose membrane (Protran, Keene, NH), and probed with primary antibodies and then HRP-labeled secondary antibodies. Proteins were visualized using ECL Western blotting detection reagents.

GeneChip Probe Array. The GeneChip p53 Assay (Ref. 29; Affymetrix Inc., Santa Clara, CA) was used to detect mutated p53 sequences on exons 2–11 of 11 cell lines as described in the manufacturer's instructions. Briefly, 500 ng of genomic DNA, isolated using DNAzol Reagent (Life Technologies, Inc., Grand Island, NY), and the normal reference DNA were amplified with the PCR using the GeneChip p53 primer set and Taq DNA polymerase enzyme. The coding regions of the *p53* gene were amplified as 10 separate amplicons in a single reaction. Each PCR reaction contained genomic DNA, 5 μl of the p53 primer set (Affymetrix), 10 units of AmpliTaq Gold (Perkin-Elmer), PCR buffer II (Perkin-Elmer), 2.5 mM $MgCl_2$, and 0.2 mM each deoxynucleotide triphosphate in a final volume of 100 μl. PCR was carried out under the following conditions: heated at 95°C for 10 min; then 35 cycles of 95°C for 30 s, 60°C for 30 s, and 72°C for 45 s; followed by a final extension of 10 min at 72°C. Amplified cell line and reference DNA (45 μl) were fragmented with 0.25 units of fragmentation reagent (Affymetrix) at 25°C for 18 min in 2.5 units of calf intestine alkaline phosphatase, 0.4 mM EDTA, and 0.5 mM Tris-acetate (pH 8.2) followed by heat inactivation at 95°C for 10 min.

The DNA amplicons were labeled at 3′ ends with a fluoresceinated dideoxynucleotide using the terminal transferase enzyme. The fluorescently labeled DNA fragments were hybridized in a reaction containing 6 × saline-sodium phosphate-EDTA, 0.05% Triton X-100, 1 mg of acetylated BSA, and 2 nM control oligonucleotide F1 (Affymetrix) to the probes on the probe array for 30 min at 45°C, after which the probe array was washed [4 times with wash buffer (3 × SSPE, 0.005% Triton X-100)] and scanned with the GeneChip Scanner 50 with a laser that excites the fluorescent label. Thus, the amount of emitted light was proportional to DNA fragments on the probe array.

Data were analyzed using the GeneChip software. The software calculated the mean intensity of each probe cell. The hybridization intensities of the sample sequence were compared with those of a reference sequence, intensity patterns diverging from the reference were identified, and sites containing mutant bases were displayed. A score was assigned for each site containing a mutation or deletion. The higher the score for a given position, the greater the likelihood that site contained a mutant base. Scores exceeding 13 identified mutations (29).

Automated p53 Sequencing. Exons 5–8 of 11 neuroblastoma cell lines and exon 10 of one cell line were sequenced by the fluorescent dideoxy terminator method of cycle sequencing (29) on an ABI 377XL (96-well format) automated DNA sequencer at Laragen, Inc. (Los Angeles, CA). The primers were synthesized at Only DNA (Midland, TX) according to sequence information provided by Affymetrix GeneChip Assay in the manufacturer's booklet.

p53 Transactivation Assay. p53 status was also studied by transactivation assay (30). Cells were transiently transfected by calcium phosphate-DNA precipitation with a p53-HBS reporter plasmid containing two copies of a 20-bp motif encoding a p53-HBS ligated immediately upstream from a minimal thymidine kinase promoter linked to CAT. CAT expression occurs only when transcriptionally functional p53 binds to the HBS motif within the promoter. Cells were collected 48 h after transfection and assayed for CAT activity, determined the percentage conversion to the acetylated forms of [^{14}C]chloramphenicol measured by autoradiography of TLC. β-Galactosidase enzymatic activity (β-Galactosidase Enzyme Assay System with Reporter Lysis Buffer; Promega, Madison, WI) was used to standardize the efficiency of transfection.

Southern Blot Analysis. Aliquots of genomic DNA (20 μg) were digested with *Eco*RI, separated on 0.7% agarose gel and then transferred onto Hybond-N+ membranes (Amersham Pharmacia Biotech, Amersham, England). The blot was hybridized with a MDM2 cDNA probe labeled with [α-^{32}P]dCTP and filmed. MDM2 cDNA was cloned in the laboratory of Dr. B. Vogelstein (36). To confirm equal loading of DNA the blot was hybridized to β-actin (Clontech Laboratories, Inc., Palo Alto, CA). Human blood mononuclear cells were used as a reference for normal MDM2 copy number. Densitometric analysis of hybridization signals was performed using the Un-Scan-It Gel (Silk Scientific, Inc., Orem, Utah) software.

Cytotoxicity Assay. The cytotoxicity of L-PAM, ETOP, and CBDCA for neuroblastoma cell lines was determined using the DIMSCAN assay system, which has a 4 log dynamic range (3, 32, 34). The drug concentration ranges used were: L-PAM, 0–10 μg/ml; CBDCA, 0–5 μg/ml; and ETOP, 0–5 μg/ml. Each condition was tested in 12 replicates. Cells (1,000–15,000) were seeded in each well. After incubation of cell lines with L-PAM for 3 days, CBDCA for 7 days, and ETOP for 4 days, 10 μg/ml fluorescein diacetate was added to each well, plates were incubated for 30 min at 37°C, and finally 0.5% eosin Y was added. The total fluorescence was then measured using digital image microscopy, and results were expressed as surviving fractions of treated cells compared with control cells. LC_{90} values were calculated using the software "Dose-Effect Analysis with Microcomputers" (37). Cell lines with an L-PAM LC_{90} value >3.7 μg/ml [3.7 = 3 × the mean of LC_{90} values from the three cell lines (Table 1) established at DX before treatment] were considered drug resistant.

Statistical Analysis. Logarithmically transformed data of fractional cytotoxicity for SAN/E6, SAN/LXSN, LHN/E6, and LHN/LXSN clones were used

Table 1 *LC_{90} values of neuroblastoma and HPV 16E6 transfected clones of SMS-SAN and SMS-LHN cell lines*

	Phase of therapy	LC_{90} values (μg/ml)[a]			
		cell lines	L-PAM[b]	CBDCA[c]	ETOP[d]
Sensitive cell lines:	DX[e]	SK-N-BE(1)	0.8	0.2	0.2
	DX	SMS-SAN	1.3	0.7	0.1
	DX	CHLA-122	1.6	0.1	0.1
	PD-Ind_c[f]	SMS-LHN	2.1	1.3	2.1
	PD-Ind_c	SMS-KCNR	1.0	1.2	<0.1
	PD-BMT[g]	CHLA-8	0.3	2.3	<0.1
	PD-BMT	CHLA-51	2.2	2.6	<0.1
Resistant cell lines:	PD-Ind_i[h]	SK-N-BE(2)	24.0	2.1	1.1
	PD-Ind_i	SK-N-RA	37.5	>10.0	181.5
	PD-Ind_i	LA-N-6	15.4	8.6	27.3
	PD-Ind_i	CHLA-119	7.4	6.6	20.5
	PD-Ind_i	CHLA-171	68.9	11.6	443.6
	PD-Ind_i	CHLA-225	8.4	2.4	0.5
	PD-BMT	CHLA-79	5.0	3.2	12.6
	PD-BMT	CHLA-90	375.0	13.8	51.3
	PD-BMT	CHLA-134	37.1	26.3	256.0
	PD-BMT	CHLA-136	17.0	2.6	56.7
	PD-BMT	CHLA-172	101.4	43.4	31.2
Transduced clones:		SAN-LXSN[i]	1.8	1.3	0.7
		SAN/EG D4[j]	8.3	19.6	29.1
		SAN/E6 B3[j]	10.8	31.7	110.4
		LHN/LXSN[i]	4.7	6.4	3.7
		LHN/E6 2–6[j]	13.1	52.5	7.6
		LHN/E6 5-B5[j]	32.1	693.5	166.2

[a] Drug concentration that was cytotoxic for 90% of treated cells.
[b] Melphalan (Reference drug level for resistance defined as 3 × mean of LC_{90} values of cell lines established at diagnosis = 3.7 μg/ml).
[c] Carboplatin (Reference drug level for resistance = 1 μg/ml).
[d] Etoposide (Reference drug level for resistance = 0.4 μg/ml).
[e] Cell lines established from the patients before treatment.
[f] Cell lines established from patients at the time of disease progression after dual-agent induction chemotherapy.
[g] Cell lines established from patients at the time of disease progression after marrow ablative chemoradiotherapy followed by bone marrow transplantation.
[h] Cell lines established from patients at the time of disease progression after intensive multiagent chemotherapy.
[i] Empty vector controls of SMS-SAN and SMS-LHN cell lines.
[j] HPV 16 E6 clones of SMS-SAN and SMS-LHN cell lines.

for ANOVA analysis. SAN/E6 clones were compared with SAN/LXSN controls, and LHN/E6 clones were compared with LHN/LXSN controls. Linear contrasts were used to compare for difference in fractional cytotoxicity at each dose level between transfected clones. Statistical significance was designed as $P < 0.05$. To perform statistical analysis SAS software was used (SAS Institute, Inc., Cary, NC).

Fisher's exact test was performed to determine the correlation between drug resistance and p53 loss of function. Statistical significance was designed as $P < 0.05$.

RESULTS

Cell Line Panel. The cell lines used in this study and their drug sensitivity profile to L-PAM, CBDCA, and ETOP are shown in Table 1. The concentration of drug lethal for 90% of treated cells (LC_{90}) was calculated from dose-response curves for each drug tested using the DIMSCAN assay, which provides a 4 log dynamic range (3). Dose-response curves for three representative cell lines treated with L-PAM, CBDCA, and ETOP are shown in Fig. 1. Cell lines with an L-PAM LC_{90} value >3.7 μg/ml (3 × mean of cell lines established at DX before treatment) were considered resistant. We studied seven sensitive and 11 resistant cell lines. All 11 L-PAM-resistant cell lines showed cross-resistance to CBDCA (reference drug concentration = 1 μg/ml) and ETOP (reference drug concentration = 0.4 μg/ml).

Expression of p53, p21, and MDM2 in Neuroblastoma Cell Lines. Expression was measured by immunoblotting the basal expression and induction of p53, p21, and MDM2 (the latter two as indices of p53 function) 16 h after challenge by 6 μg/ml L-PAM, (Fig. 2*a*). Normally, wt p53 expression is either undetectable or very low but increases briefly on exposure to DNA-damaging agents. In contrast, stabilization of p53 in the absence of genotoxic stress is a hallmark of mutation and can be detected by immunoblotting (38). We found that p53 steady-state expression was low and inducible (≥2.5-fold), in seven/seven drug-sensitive cell lines: SK-N-BE(1), SMS-SAN, CHLA-122, SMS-LHN, SMS-KCNR, CHLA-8, and CHLA-51, and in 3/11 drug-resistant cell lines: LA-N-6, CHLA-79, and CHLA-136. A failure to induce p53 (≤2.5-fold) was observed in 8/11 drug-resistant cell lines: SK-N-BE(2), SK-N-RA, CHLA-119, CHLA-225, CHLA-171, CHLA-90, CHLA-134, and CHLA-172.

Cell lines that failed to induce p21 and/or MDM2 ≥1.5-fold (median p21 and MDM2 inductions) were defined as p53 nonfunctional. All seven drug-sensitive cell lines [SK-N-BE(1), SMS-SAN, CHLA-122, SMS-LHN, SMS-KCNR, CHLA-8, and CHLA-51] and 4/11 drug-resistant cell lines (LA-N-6, CHLA-79, CHLA-136, and SK-N-RA) demonstrated p21 and/or MDM2 induction after L-PAM challenge. Seven of the 11 drug-resistant-cell lines [SK-N-BE(2), CHLA-119, CHLA-171, CHLA-225, CHLA-90, CHLA-134, and CHLA-172] lacked functional p53 (Fig. 2, *b* and *c*). Thus, there was a significant correlation between drug resistance and p53 loss of function ($P = 0.01$).

Analysis of p53 Mutations. (Table 2). The Affymetrix GeneChip p53 Assay was used to analyze exons 2–11 for p53 mutations. Then, automated fluorescence dideoxynucleotide sequencing was used to confirm the Affymetrix GeneChip findings by analyzing exons 5–8 (where the most mutations were found). Sequencing of exon 10 was also carried out by automated sequencing for CHLA-119 to confirm a mutation detected by the GeneChip p53 Assay.

Wt p53 was found in six cell lines with functional p53 [SK-N-BE(1), SMS-LHN, LA-N-6, SK-N-RA, CHLA-79, and CHLA-136],

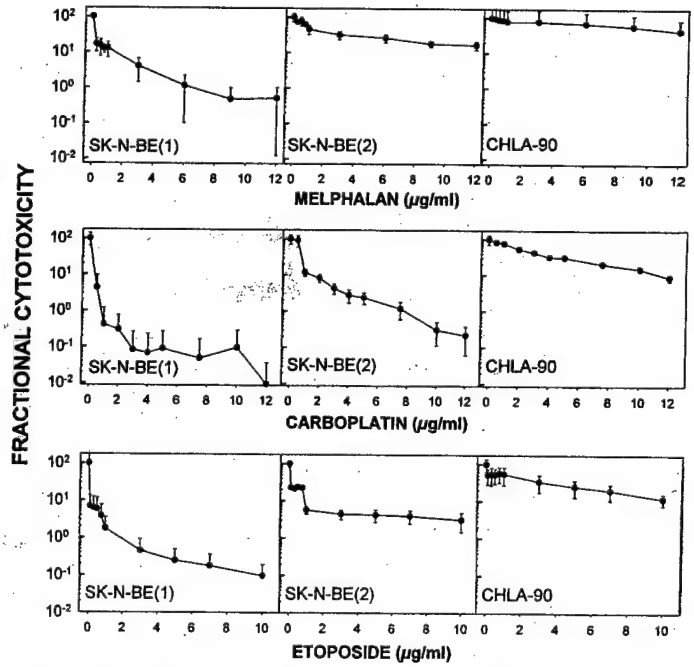

Fig. 1. Representative dose-response curves obtained by DIMSCAN assay. SK-N-BE(1) was established at DX before treatment. SK-N-BE(2) was established at the time of relapse after conventional induction chemotherapy and CHLA-90 at relapse after myeloablative chemoradiotherapy followed by bone marrow transplantation. Cell lines were treated with melphalan, carboplatin, and etoposide. Dose-response curves show the decreased drug sensitivity in cell lines established after induction chemotherapy and myeloablative chemoradiotherapy compared with cell lines established before treatment.

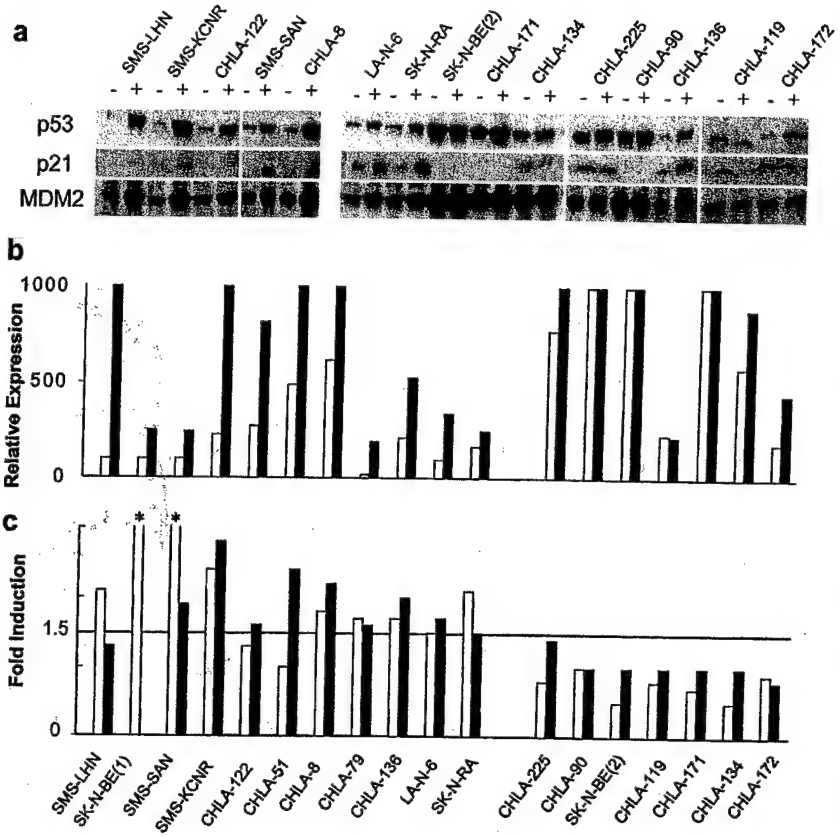

Fig. 2. *a*, Western blot analysis of p53, p21, and MDM2 expressions. −, protein steady state expressions; +, protein expression after 6 μg/ml L-PAM exposure for 16 h. *b*, quantitative analysis of p53 Western blots. Steady state (□) and induced levels (■) by 6 μg/ml L-PAM exposure (16 h) are shown. *c*, quantitative analysis for p21 (□) and MDM2 (■) induction by 6 μg/ml L-PAM (16 h) as assessed by Western blotting. *, off-scale values of SK-N-BE(1) and SMS-SAN for p21 induction were 23 and 40, respectively. *Horizontal line*, median induction value of 1.5 for p21 and MDM2, which was used as a cutoff for significant induction.

and in three of the seven cell lines with nonfunctional p53 (CHLA-225, CHLA-171, and CHLA-134). Mutations of p53 were found by both automated sequencing and the GeneChip Assay in four of the seven cell lines lacking functional p53 [SK-N-BE(2), CHLA-119, CHLA172, and CHLA-90].

p53 Transactivation Assay. (Fig. 3). We tested eight cell lines with functional p53 (SMS-LHN, CHLA-122, CHLA-51, CHLA-8, SK-N-RA, LA-N-6, CHLA-79, and CHLA-136) and all seven of the cell lines with nonfunctional p53 [CHLA-225, CHLA-134, CHLA-171, SK-N-BE(2), CHLA-90, CHLA-119, and CHLA-172] for their ability to transactivate a p53-HBS reporter gene construct. We could not carry out this assay for all of the cell lines because of an inability to transfect to some of the lines. CAT activity was detected (and, by inference, p53 transactivation) in all of the cell lines with wt p53, but in two cell lines (SMS-LHN and LA-N-6) CAT activity was lower than the other cell lines. The four cell lines with mutated p53 [SK-N-BE(2), CHLA-90, CHLA-119, and CHLA172] showed no transactivation of the p53-HBS reporter gene construct.

Table 2 *Sequence analysis of p53 in neuroblastoma cell lines*

Cell lines	Exon	Codon	Nucleotide change	Amino acid change	Induction of p21 and/or MDM2[a]	MDM2	
						Protein[b]	DNA[c]
Representative drug-sensitive cell lines							
SK-N-BE(1)			wt[d]		+	+	−
SMS-LHN			wt[d]		+	+	−
Drug-resistant cell lines							
LA-N-6			wt[e]		+	+	−
SK-N-RA			wt[e]		+	+	−
CHLA-79			wt[f]		+	+	−
CHLA-136			wt[e]		+	+	−
CHLA-171			wt[e]		−	↑↑	−
CHLA-225			wt[e]		−	↑	−
CHLA-134			wt[e]		−	↑	+
SK-N-BE(2)	5	135	TGC → TTC[e]	Cys → Phe	−	↑↑	nt
CHLA-119[g]	10	342	CGA → CTA[e]	Arg → Leu	−	↑	nt
CHLA-90	8	286	GAA → AAA[e]	Glu → Lys	−	↑↑	nt
CHLA-172	6	216	GTG → TTG[e]	Val → Leu	−	↑	nt

[a] Induction of p21 and/or MDM2 were used as indices of p53 function: +, induction of p21 and/or MDM2 by L-PAM challenge, −, failure to induce p21 or MDM2 by L-PAM challenge.

[b] Basal MDM2 protein expression by immunoblotting: +, protein is expressed; ↑, 1.1 to 1.4 times higher than median basal expression of MDM2; ↑↑, 1.7 to 2 times higher than median basal expression of MDM2.

[c] Genomic amplification of MDM2: +, amplified MDM2; −, nonamplified MDM2; nt, not tested.

[d] Studied using the GeneChip p53 Assay.

[e] Identical results were obtained by GeneChip p53 Assay and automated sequencing.

[f] Studied using the automated sequencing.

[g] In addition to the above mutation in CHLA-119, a polymorphism at codon 213 (a silent alteration of CGA to CGG) was also detected.

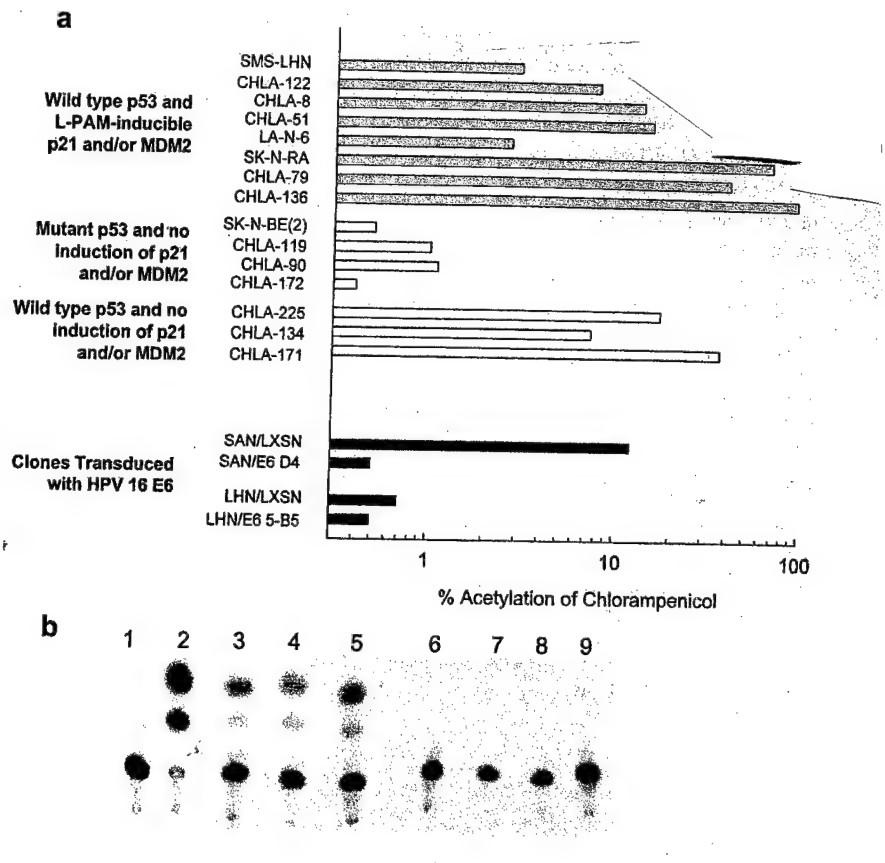

Fig. 3. p53 transactivation assay. *a*, *bars*, conversion values (%) of acetylated forms of chloramphenicol from total chloramphenicol. Cell lines with functional p53 (inducible p21 and/or MDM2) ▨, cell lines with nonfunctional p53 □, and transfected clones ■. *b*, results of CAT assay for three representative cell lines with functional p53 and four cell lines with mutated p53. SKOV-3 human ovarian carcinoma cell line (p53 null) was used as a negative control (*Lane 1*), and SKOV-3 cell line transfected with wt p53-HSP promoter was used as a positive control (*Lane 2*). *Lane 3*, CHLA-225; *Lane 4*, CHLA-134; *Lane 5*, CHLA171; *Lane 6*, SK-N-BE(2); *Lane 7*, CHLA-90; *Lane 8*, CHLA-172; and *Lane 9*, CHLA-119. CAT activation was visualized by TLC as acetylated form of ^{14}C-labeled chloramphenicol.

MDM2 Gene Amplification. A high baseline expression of MDM2 protein was seen in four of the seven cell lines lacking p53 function (Fig. 2) including two of the three p53 nonfunctional cell lines with wt p53 (CHLA-134 and CHLA-171). Genomic DNA from 11 cell lines and from normal human lymphocytes was analyzed for MDM2 amplification using Southern blot analysis. Genomic amplification of MDM2 was detected in only one cell line (CHLA-134), which showed a signal 6–14 × greater than the other samples analyzed (Fig. 4).

Paired Cell Lines. Within the panel studied, there were pairs of cell lines derived from two patients: one cell line at DX before treatment and then another after disease progression. SK-N-BE(1) was established at DX and then SK-N-BE(2) was established from the same patient at disease progression during nonmyeloablative (induction) chemotherapy. Similarly, CHLA-122 was established at DX and then from the same patient, CHLA-136 was established at time of relapse after myeloablative therapy supported with bone marrow transplantation. LC_{90} values of SK-N-BE(2) were 30 × greater for L-PAM, 13 × for CBDCA, and 7 × for ETOP relative to SK-N-BE(1); Table 1. SK-N-BE(1) had functional (Fig. 2, *b* and *c*) and wt p53 (Table 2), whereas SK-N-BE(2) showed a lack of functional p53 by p21/MDM2 induction (Fig. 2, *a–c*) and by p53 transactivation assay (Fig. 3), and showed mutation of p53 (Table 2). CHLA-136 showed drug resistance relative to CHLA-122, and LC_{90} values of CHLA-136 were 10.6 × greater for L-PAM, 26 × for CBDCA and 567 × for ETOP compared with CHLA-122 (Table 1). However, drug-resistance acquired by CHLA-136 was not associated with a loss of p53 function (Figs. 2 and 3) or p53 mutation (Table 2).

Selective Abrogation of p53 Function with HPV16 E6 Confers Multidrug Resistance. (Table 1; Fig. 5). To abrogate p53 activity in drug-sensitive, p53-functional neuroblastoma cell lines, we transduced the papillomavirus gene HPV16 E6 (which encodes a protein that promotes degradation of p53 and renders cells p53 nonfunctional; Ref. 31) into two drug-sensitive neuroblastoma cell lines. SMS-SAN (*MYCN* gene amplified) and SMS-LHN (*MYCN* nonamplified) were transduced with HPV16 E6 or with the pLXSN retrovirus empty vector as a control, and G418-resistant clones were selected from each. We then compared the sensitivity to L-PAM, CBDCA, and ETOP of HPV16 E6-transduced clones to the parental cell lines and pLXSN (empty vector) transduced controls. Reduced p53 activity was confirmed by the lack of p53 induction in L-PAM-challenged samples using Western blotting (data not shown) and the p53 transactivation assay (Fig. 3). Transduction of HPV16 E6 conferred high-level multidrug resistance to both SMS-SAN and SMS-LHN. LC_{90} values of SAN/E6 clones were 4.5–6 × higher for L-PAM, 15.4–25 × for CBDCA, and 41.6–157.7 × for ETOP relative to SAN/LXSN controls. Similarly, LC_{90} values of LHN/E6 clones were 3–7 × higher for L-PAM, 8–109 × for CBDCA, and 2–45.3 × for ETOP relative to LHN/LXSN cells.

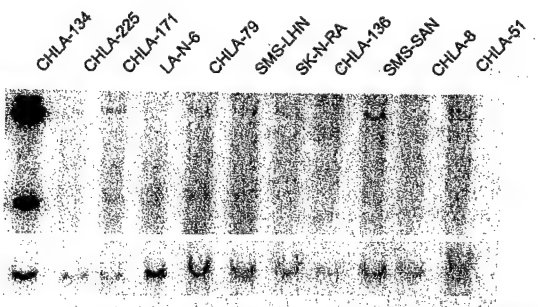

Fig. 4. Southern blot analysis of MDM2 gene amplification. *Eco*RI digested DNA samples were hybridized with an MDM2 cDNA probe (*top*) and as a control with β-actin probe (*bottom*).

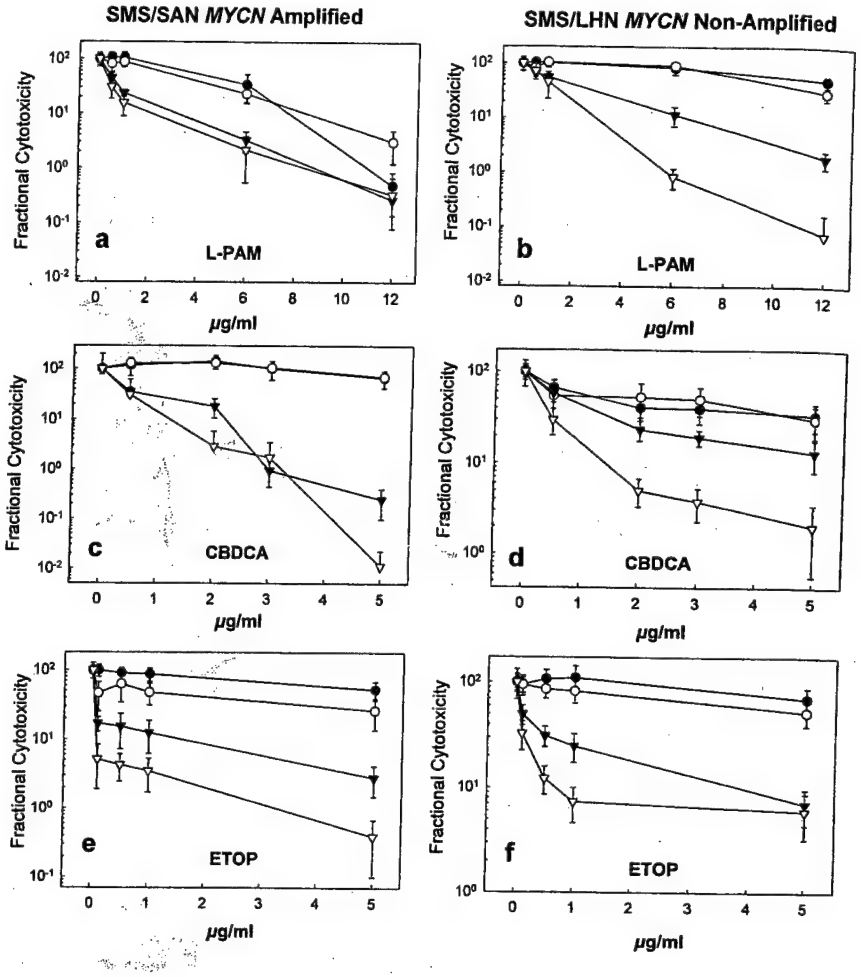

Fig. 5. Dose-response curves of neuroblastoma cell lines and their transfected clones. *a* and *b*, dose-response curves to L-PAM. *c* and *d*, dose-response curves to CBDCA. *e* and *f*, dose-response curves to ETOP. *a*, *c*, and *e*, cytotoxicity assays of SMS-SAN parental cell line (▽), SAN/E6 clones (○ and ●), and SAN/LXSN empty vector clone (▼) to L-PAM, CBDCA, and ETOP. *b*, *d*, and *f*, cytotoxicity assays of SMS-LHN parental cell line (▽), LHN/E6 clones (○ and ●), and LHN/LXSN empty vector clone (▼) to L-PAM, CBDCA, and ETOP. *P*s were calculated based on contrasts from ANOVA (see "Materials and Methods"). Generally, HPV16 E6 transfected clones were more resistant ($P \leq 0.002$) to all drugs than LXSN controls, and fractional cytotoxicity for the two transfected clones were not different ($P > 0.05$) for most drug concentrations.

DISCUSSION

Although most neuroblastomas show a good response to initial chemotherapy, tumors from many patients with high-risk disease (stage IV diagnosed after 1 year of age and/or tumor with *MYCN* amplification) acquire drug resistance during the therapy (1, 2). Neuroblastomas established as cell lines and maintained without drug exposure *in vitro* manifest drug resistance that was acquired in patients and correlates with the intensity of chemotherapy employed *in vivo*, suggesting that selection occurs for tumor cells resistant to those drugs used during therapy (3, 32). Identification of the molecular events conferring drug resistance in neuroblastoma may allow developing therapies to overcome the particular form of drug resistance manifested by this tumor and could provide markers to identify patients likely to develop progressive disease when treated with currently available chemotherapeutic agents.

As p53 mutations are infrequent in primary neuroblastomas (18–23), it has been suggested that functionally inactive p53 is attributable to cytoplasmic localization of p53 (24). Goldman *et al.* (25) reported that although p53 showed mainly cytoplasmic localization in neuroblastoma cell lines, p53 levels increased mainly in the nucleus after γ irradiation and showed that transcriptional activity of p53 was intact. Other studies have confirmed the presence of functional p53 in neuroblastoma cell lines in response to γ irradiation (39), UV light (26), and cisplatin (27).

It is well known that p53 mediates responses to cytotoxic agents (8, 40) and that mutant p53 is correlated with resistance to DNA-damaging agents (11, 14, 16, 41). Here we have shown that for 18 neuroblastoma cell lines, p53 loss of function correlated with drug resistance ($P = 0.01$). Using Western blot analysis for p53 target genes, we found that p53 was functional, as determined by transcriptionally intact p53 (induction of p21 and/or MDM2 after 16 h of 6 μg/ml L-PAM) in seven/seven drug-sensitive cell lines. Moreover, the low steady-state expression and inducible p53 observed in these cell lines also suggested the presence of functional p53.

We found that p53 was nonfunctional in 7 of 11 drug-resistant cell lines [SK-N-BE(2), CHLA-119, CHLA-225, CHLA-171, CHLA-90, CHLA-134, and CHLA-172] as demonstrated by a failure to induce downstream genes (p21 and MDM2) by L-PAM. High steady state p53 expression, a hallmark of p53 mutation (38), was found only in cell lines with nonfunctional p53 [SK-N-BE(2), CHLA-225, CHLA-171, CHLA-90, and CHLA-134].

Sequence analysis for p53 of all seven cell lines with loss of p53 function was performed by both the Affymetrix GeneChip p53 Assay and automated sequencing using the fluorescent dideoxy terminator method. First, we analyzed exons 2–11 by the GeneChip p53 Assay and then exons 5–8 (DNA-binding region) using automated DNA sequencing. As the Affymetrix GeneChip Assay provides far greater sensitivity for detection of p53 mutations than does automated DNA sequencing (29), we sequenced only exons 5–8 (where most of mutations were located) by automated sequencing to confirm the findings of the Affymetrix GeneChip Assay; to confirm a mutation identified by the GeneChip Assay, exon 10 was also sequenced in CHLA-119. We found mutations in the DNA-binding domain in SK-N-BE(2), CHLA-90, and CHLA-172 (CHLA-119 harbors a polymorphism in this region), all of which were drug-resistant cell lines with nonfunctional p53 that were derived from heavily treated pa-

tients. These mutations have been identified previously in various tumors.[4] In addition to mutations in the DNA binding region, we identified a mutation in exon 10 in CHLA-119, which can also render p53 nonfunctional (42). Mutations of p53 were not found in CHLA-225, CHLA-171, and CHLA-134 using either the GeneChip p53 Assay or automated p53 sequencing. As expected, two representative drug-sensitive/p53-functional cell lines [SK-N-BE(1) and SMS-LHN] showed no p53 mutations by the GeneChip p53 Assay.

Only 4/11 drug-resistant cell lines (LA-N-6, SK-N-RA, CHLA-79, and CHLA-136) had functional p53 (as demonstrated by induction of p21 and/or MDM2 in response to L-PAM), and all 4 cell lines had wt p53 by both automated p53 sequencing and GeneChip p53 Assay. It is possible that genetic alterations in apoptotic events downstream of p53, *e.g.*, Bax (7) or caspase-8 (43), could account for drug resistance seen in these cell lines. Data from tumors other than neuroblastoma have shown that decreased L-PAM uptake (44) or increased GSH biosynthesis (45), together with increased export of GSH-alkylator complex (46), are also associated with drug resistance. One or more of these may account for the drug resistance observed in neuroblastoma cell lines with intact p53 function. However, our data suggest that the most frequent event conferring high-level, multidrug resistance in neuroblastomas is a loss of p53 function.

MDM2 is a transcriptional target of p53, which regulates p53 expression in a negative regulatory feedback fashion. The role of MDM2 has been implicated in the pathogenesis of cancer via inhibition of p53 tumor suppressor function, and MDM2 overexpression attributable to *MDM2* gene amplification or increased translation can inactivate p53 (47, 48). There were three cell lines (CHLA-225, CHLA-171, and CHLA-134) in our panel that displayed increased accumulation and stabilization of p53 and failed to induce p21 and MDM2 proteins after L-PAM challenge (Fig. 2). All three had wt p53, and unlike the cells with mutant p53, these three cell lines showed intact p53 transactivation using the *p53-HBS/CAT* reporter gene (Fig. 3). Two of these cell lines (CHLA-171 and CHLA-134) showed overexpression of MDM2 protein by Western blotting, and we found genomic amplification of MDM2 in one of these cell lines (CHLA-134) by Southern blotting. Thus, MDM2 protein overexpression is likely one mechanism by which p53 function is compromised in some neuroblastomas.

The level of expression of unstimulated MDM2 protein was high in two neuroblastoma cell lines with mutated p53 [SK-N-BE(2) and CHLA-90; Fig. 2]. It has been shown that MDM2 can be stabilized by mutant p53 and proposed that it occurs because of inhibition of MDM2 ubiquitination after forming a complex with mutant p53 (49).

To demonstrate that a loss of p53 function mediates multidrug resistance in neuroblastoma we transduced two sensitive neuroblastoma cell lines carrying functional p53 with the HPV type 16 gene (HPV16 E6). HPV16 E6 protein and cellular E6-associated protein form a complex and function as a ubiquitin ligase for p53 for increased degradation, thus disrupting the p53-mediated response (31). HPV16 E6-transformed cells have been used to examine the effect of p53 loss on genomic stability, apoptosis, and sensitivity to chemotherapeutic agents or ionizing radiation (50–52). As *MYCN* amplification has been linked to tumor progression and poor outcome in neuroblastomas (53), we used *MYCN* amplified (SMS-SAN) and *MYCN* nonamplified (SMS-LHN) cell lines for these experiments. The LC_{90} values of two separate HPV16 E6 clones of both cell lines were increased relative to the pLXSN empty vector controls: 3–7 times for L-PAM; 8–109 times for CBDCA; and 2–158 times for ETOP. Decreased sensitivity of pLXSN empty vector clones compared with parental cells was observed in both cell lines, suggesting that selection for resistance to G418 can mediate modest cross resistance to chemotherapeutic drugs.

We showed that p53 is functional in all of the tested neuroblastoma cell lines established before chemotherapy [SK-N-BE(1), SMS-SAN, and CHLA-122] and that loss of p53 function appears to be one of the major mechanisms responsible for high-level multidrug resistance in neuroblastoma. In one pair of cell lines derived from the same patient before treatment [SK-N-BE(1)] and then after disease progression on induction chemotherapy [SK-N-BE(2)], we demonstrated acquisition of a drug-resistant phenotype (3, 32), which we and others (54–56) showed was associated with acquisition of a p53 mutation on codon 135 and the loss of p53 function. This is consistent with previous observations that neuroblastomas lacking p53 mutations at DX showed mutations of p53 in tumors obtained at relapse after chemotherapy (19, 20). These observations, combined with the high frequency of p53 mutations and loss of p53 function in chemotherapy-resistant cell lines relative to those established at DX, suggests that selection for neuroblastoma cells with p53 mutations and/or loss of p53 function (in some cases attributable to overexpression of MDM2) occurs during therapy, leading to multidrug resistance. As all of the drug-sensitive neuroblastoma cell lines had functional p53 and lacked p53 mutations, it is unlikely that loss of p53 function was acquired as a result of growth *in vitro*.

Our data suggest that the relationship of p53 mutations and/or functionality to drug resistance should be investigated in tumor samples from patients with neuroblastoma. One possible approach to studying clinical samples is the Affymetrix GeneChip p53 Assay. The GeneChip p53 Assay (recently developed by Affymetrix Inc.) is an oligonucleotide microarray approach that provides an accurate, sensitive, and specific method for detection of p53 mutations (29, 57, 58). Our results confirm that the GeneChip Assay reliably detects p53 mutations. However, as loss of p53 function in some cell lines occurred without p53 mutations, methods for detecting p53 functionality in clinical specimens may also be required to complement detection of mutations. We are currently analyzing p53 mutations in tumor samples obtained from patients in which the tumor persisted or progressed after chemotherapy. Confirmation with patient tumors that inactivation of p53 correlates with a poor response to chemotherapy in neuroblastoma would additionally support a focus on p53-independent therapies (*e.g.*, ceramide modulators; Refs. 27, 59), L-PAM in combination with the GSH depletor buthionine sulfoximine (34, 60), immunotherapy (61), or antimicrotubule agents (62, 63) for neuroblastomas recurring after chemotherapy.

ACKNOWLEDGMENTS

We thank Dr. June Biedler for providing the SK-N-BE(1) and SK-N-BE(2) cell lines, Dr. Susan Groshen and Denice Wei for their help in statistical analysis, and Dr. Carl Miller for providing the MDM2 probe.

REFERENCES

1. Matthay, K. K., Villablanca, J. G., Seeger, R. C., Stram, D. O., Harris, R. E., Ramsay, N. K., Swift, P., Shimada, H., Black, C. T., Brodeur, G. M., Gerbing, R. B., and Reynolds, C. P. Treatment of high-risk neuroblastoma with intensive chemotherapy, radiotherapy, autologous bone marrow transplantation, and 13-*cis*-retinoic acid. Children's Cancer Group. N. Engl. J. Med., *341:* 1165–1173, 1999.
2. Seeger, R. C., and Reynolds, C. P. Treatment of high-risk solid tumors of childhood with intensive therapy and autologous bone marrow transplantation. Pediatr. Clin. N. Am., *38:* 393–424, 1991.
3. Keshelava, N., Seeger, R. C., Groshen, S., and Reynolds, C. P. Drug resistance patterns of human neuroblastoma cell lines derived from patients at different phases of therapy. Cancer Res., *58:* 5396–5405, 1998.

[4] See the p53 website: http://perso.curie.fr/Thierry.Soussi/.

4. Ko, L. J., and Prives, C. p53: puzzle and paradigm. Genes Dev., *10:* 1054–1072, 1996.
5. May, P., and May, E. Twenty years of p53 research: structural and functional aspects of the p53 protein (published erratum appears in Oncogene, *19:* 1734, 2000). Oncogene, *18:* 7621–7636, 1999.
6. Malkin, D. p53 and the Li-Fraumeni syndrome. Biochim. Biophys. Acta, *1198:* 197–213, 1994.
7. McCurrach, M. E., Connor, T. M., Knudson, C. M., Korsmeyer, S. J., and Lowe, S. W. bax-deficiency promotes drug resistance and oncogenic transformation by attenuating p53-dependent apoptosis. Proc. Natl. Acad. Sci. USA, *94:* 2345–2349, 1997.
8. Lowe, S. W., Bodis, S., McClatchey, A., Remington, L., Ruley, H. E., Fisher, D. E., Housman, D. E., and Jacks, T. p53 status and the efficacy of cancer therapy *in vivo*. Science (Wash. DC), *266:* 807–810, 1994.
9. Perego, P., Giarola, M., Righetti, S. C., Supino, R., Caserini, C., Delia, D., Pierotti, M. A., Miyashita, T., Reed, J. C., and Zunino, F. Association between cisplatin resistance and mutation of *p53* gene and reduced bax expression in ovarian carcinoma cell systems. Cancer Res., *56:* 556–562, 1996.
10. Pievesan, B., Pennell, N., and Bernstein, N. L. Human lymphoblastoid cell lines expressing mutant p53 exhibit decreased sensitivity to cisplatin-induced cytotoxicity. Oncogene, *17:* 2339–2350, 1998.
11. Lam, V., McPherson, J. P., Salmena, L., Lees, J., Chu, W., Sexsmith, E., Hedley, D. W., Freedman, M. H., Reed, J. C., Malkin, D., and Goldenberg, G. J. *p53* gene status and chemosensitivity of childhood acute lymphoblastic leukemia cells to Adriamycin. Leuk. Res., *23:* 871–880, 1999.
12. Li, G., Tang, L., Zhou, X., Tron, V., and Ho, V. Chemotherapy-induced apoptosis in melanoma cells is p53 dependent. Melanoma Res., *8:* 17–23, 1998.
13. Asada, N., Tsuchiya, H., and Tomita, K. *De novo* deletions of *p53* gene and wild-type p53 correlate with acquired cisplatin-resistance in human osteosarcoma OST cell line. Anticancer Res., *19:* 5131–5137, 1999.
14. Berns, E. M., Foekens, J. A., Vossen, R., Look, M. P., Devilee, P., Henzen-Logmans, S. C., van Staveren, I. L., van Putten, W. L., Inganas, M., Meijer-van Gelder, M. E., Cornelissse, C., Claassen, C. J., Portengen, H., Bakker, B., and Klijn, J. G. Complete sequencing of TP53 predicts poor response to systemic therapy of advanced breast cancer. Cancer Res., *60:* 2155–2162, 2000.
15. Righetti, S. C., Perego, P., Corna, E., Pierotti, M. A., and Zunino, F. Emergence of p53 mutant cisplatin-resistant ovarian carcinoma cells following drug exposure: spontaneously mutant selection. Cell Growth Differ., *10:* 473–478, 1999.
16. Houldsworth, J., Xiao, H., Murty, V. V., Chen, W., Ray, B., Reuter, V. E., Bosl, G. J., and Chaganti, R. S. Human male germ cell tumor resistance to cisplatin is linked to *TP53* gene mutation. Oncogene, *16:* 2345–2349, 1998.
17. Harris, C. C. The Walter Hubert lecture–molecular epidemiology of human cancer: insights from the mutational analysis of the *p53* tumour-suppressor gene. Br. J. Cancer, *73:* 261–269, 1996.
18. Hosoi, G., Hara, J., Okamura, T., Osugi, Y., Ishihara, S., Fukuzawa, M., Okada, A., Okada, S., and Tawa, A. Low frequency of the *p53* gene mutations in neuroblastoma. Cancer (Phila.), *73:* 3087–3093, 1994.
19. Imamura, J., Bartram, C. R., Berthold, F., Harms, D., Nakamura, H., and Koeffler, H. P. Mutation of the *p53* gene in neuroblastoma and its relationship with *N*-myc amplification. Cancer Res., *53:* 4053–4058, 1993.
20. Maahani, R., Cristofani, L. M., Odone, F. V., and Bendit, I. Concomitant p53 mutation and MYCN amplification in neuroblastoma. Med. Pediatr. Oncol., *29:* 206–207, 1997.
21. Vogan, K., Bernstein, M., Leclerc, J. M., Brisson, L., Brossard, J., Brodeur, G. M., Pelletier, J., and Gros, P. Absence of *p53* gene mutations in primary neuroblastomas. Cancer Res., *53:* 5269–5273, 1993.
22. Castresana, J. S., Bello, M. J., Rey, J. A., Nebreda, P., Queizan, A., Garcia-Miguel, P., and Pestana, A. No TP53 mutations in neuroblastomas detected by PCR-SSCP analysis. Genes Chromosomes Cancer, *10:* 136–138, 1994.
23. Komuro, H., Hayashi, Y., Kawamura, M., Hayashi, K., Kaneko, Y., Kamoshita, S., Hanada, R., Yamamoto, K., Hongo, T., and Yamada, M. Mutations of the *p53* gene are involved in Ewing's sarcomas but not in neuroblastomas. Cancer Res., *53:* 5284–5288, 1993.
24. Ostermeyer, A. G., Runko, E., Winkfield, B., Ahn, B., and Moll, U. M. Cytoplasmically sequestered wild-type p53 protein in neuroblastoma is relocated to the nucleus by a C-terminal peptide. Proc. Natl. Acad. Sci. USA, *93:* 15190–15194, 1996.
25. Goldman, S. C., Chen, C. Y., Lansing, T. J., Gilmer, T. M., and Kastan, M. B. The p53 signal transduction pathway is intact in human neuroblastoma despite cytoplasmic localization. Am. J. Pathol., *148:* 1381–1385, 1996.
26. McKenzie, P. P., Guichard, S. M., Middlemas, D. S., Ashmun, R. A., Danks, M. K., and Harris, L. C. Wild-type p53 can induce p21 and apoptosis in neuroblastoma cells but the DNA damage-induced G1 checkpoint function is attenuated. Clin. Cancer Res., *5:* 4199–4207, 1999.
27. Maurer, B. J., Metcalfe, L. S., Seeger, R. C., Cabot, M. C., and Reynolds, C. P. Increase of ceramide and induction of mixed apoptosis/necrosis by *N*-(4-hydroxyphenyl)-retinamide in neuroblastoma cell lines. J. Natl. Cancer Inst., *91:* 1138–1146, 1999.
28. Heimdal, K., Lothe, R. A., Lystad, S., Holm, R., Fossa, S. D., and Borresen, A. L. No germline TP53 mutations detected in familial and bilateral testicular cancer. Genes Chromosomes Cancer, *6:* 92–97, 1993.
29. Ahrendt, S. A., Halachmi, S., Chow, J. T., Wu, L., Halachmi, N., Yang, S. C., Wehage, S., Jen, J., and Sidransky, D. Rapid p53 sequence analysis in primary lung cancer using an oligonucleotide probe array. Proc. Natl. Acad. Sci. USA, *96:* 7382–7387, 1999.
30. Chumakov, A. M., Miller, C. W., Chen, D. L., and Koeffler, H. P. Analysis of p53 transactivation through high-affinity binding sites. Oncogene, *8:* 3005–3011, 1993.
31. Scheffner, M., Huibregtse, J. M., Vierstra, R. D., and Howley, P. M. The HPV-16 E6 and E6-AP complex functions as a ubiquitin-protein ligase in the ubiquitination of p53. Cell, *75:* 495–505, 1993.
32. Keshelava, N., Groshen, S., and Reynolds, C. P. Cross-resistance of topoisomerase I and II inhibitors in neuroblastoma cell lines. Cancer Chemother. Pharmacol., *45:* 1–8, 2000.
33. Reynolds, C. P., Tomayko, M. M., Donner, L., Helson, L., Seeger, R. C., Triche, T. J., and Brodeur, G. M. Biological classification of cell lines derived from human extra-cranial neural tumors. Prog. Clin. Biol. Res., *271:* 291–306, 1988.
34. Anderson, C. P., Seeger, R. C., Satake, N., Meek, W. E., Keshelava, N., Bailey, H. H., Monforte-Munoz, H. L., and Reynolds, C. P. Buthionine sulfoximine and myeloablative concentrations of melphalan overcome resistance in melphalan-resistant neuroblastoma cell line. J. Pediatr. Hematol. Oncol., in press, 2001.
35. Wang, Y., Einhorn, P., Triche, T. J., Seeger, R. C., and Reynolds, C. P. Expression of protein gene product 9.5 and tyrosine hydroxylase in childhood small round cell tumors. Clin. Cancer Res., *6:* 551–558, 2000.
36. Oliner, J. D., Kinzler, K. W., Meltzer, P. S., George, D. L., and Vogelstein, B. Amplification of a gene encoding a p53-associated protein in human sarcomas. Nature (Lond.), *358:* 80–83, 1992.
37. Chou, J., and Chou, T. C. Multiple drug-effect analysis (program B). *In:* J. Chou and T. C. Chou (eds.), Dose-effect Analysis with Microcomputers, pp. 19–64. New York: Memorial Sloan-Kettering Cancer Center, 1987.
38. Blagosklonny, M. V. Loss of function and p53 protein stabilization. Oncogene, *15:* 1889–1893, 1997.
39. Jasty, R., Lu, J., Irwin, T., Suchard, S., Clarke, M. F., and Castle, V. P. Role of p53 in the regulation of irradiation-induced apoptosis in neuroblastoma cells. Mol. Genet. Metab., *65:* 155–164, 1998.
40. Lowe, S. W., Ruley, H. E., Jacks, T., and Housman, D. E. p53-dependent apoptosis modulates the cytotoxicity of anticancer agents. Cell, *74:* 957–967, 1993.
41. Lee, J. M., and Bernstein, A. p53 mutations increase resistance to ionizing radiation. Proc. Natl. Acad. Sci. USA, *90:* 5742–5746, 1993.
42. Rollenhagen, C., and Chene, P. Characterization of p53 mutants identified in human tumors with a missense mutation in the tetramerization domain. Int. J. Cancer, *78:* 372–376, 1998.
43. Teitz, T., Wei, T., Valentine, M. B., Vanin, E. F., Grenet, J., Valentine, V. A., Behm, F. G., Look, A. T., Lahti, J. M., and Kidd, V. J. Caspase 8 is deleted or silenced preferentially in childhood neuroblastomas with amplification of MYCN. Nat. Med., *6:* 529–535, 2000.
44. Pu, Q., Bianchi, P., and Bezwoda, W. R. Alkylator resistance in human B lymphoid cell lines: (I). Melphalan accumulation, cytotoxicity, interstrand-DNA-crosslinks, cell cycle analysis, and glutathione content in the melphalan-sensitive B-lymphocytic cell line (WIL2) and in the melphalan-resistant B-CLL cell line (WSU-CLL). Anticancer Res., *20:* 2561–2568, 2000.
45. Calvert, P., Yao, K. S., Hamilton, T. C., and O'Dwyer, P. J. Clinical studies of reversal of drug resistance based on glutathione. Chem.-Biol. Interact., *111–112:* 213–224, 1998.
46. Ishikawa, T., Bao, J. J., Yamane, Y., Akimaru, K., Frindrich, K., Wright, C. D., and Kuo, M. T. Coordinated induction of MRP/GS-X pump and γ-glutamylcysteine synthetase by heavy metals in human leukemia cells. J. Biol. Chem., *271:* 14981–14988, 1996.
47. Capoulade, C., Bressac-de Paillerets, B., Leffere, J., Ronsin, M., Feunteun, J., Tursz, T., and Wiels, J. Overexpression of MDM2, due to enhanced translation, results in inactivation of wild-type p53 in Burkitt's lymphoma cells. Oncogene, *16:* 1603–1610, 1998.
48. Keleti, J., Quezado, M. M., Abaza, M. M., Raffeld, M., and Tsokos, M. The MDM2 oncoprotein is overexpressed in rhabdomyosarcoma cell lines and stabilizes wild-type p53 protein. Am. J. Pathol., *149:* 143–151, 1996.
49. Peng, Y., Chen, L., Li, C., Lu, W., Agrawal, S., and Chen, J. Stabilization of the MDM2 oncoprotein by mutant p53. J. Biol. Chem., *276:* 6874–6878, 2001
50. Havre, P. A., Yuan, J., Hedrick, L., Cho, K. R., and Glazer, P. M. p53 inactivation by HPV16 E6 results in increased mutagenesis in human cells. Cancer Res., *55:* 4420–4424, 1995.
51. Tsang, N. M., Nagasawa, H., Li, C., and Little, J. B. Abrogation of p53 function by transfection of *HPV16 E6* gene enhances the resistance of human diploid fibroblasts to ionizing radiation. Oncogene, *10:* 2403–2408, 1995.
52. Meyn, M. S., Strasfeld, L., and Allen, C. Testing the role of p53 in the expression of genetic instability and apoptosis in ataxia-telangiectasia. Int. J. Radiat. Biol., *66:* S141–S149, 1994.
53. Seeger, R. C., Brodeur, G. M., Sather, H., Dalton, A., Siegel, S. E., Wong, K. Y., and Hammond, D. Association of multiple copies of the *N-myc* oncogene with rapid progression of neuroblastomas. N. Engl. J. Med., *313:* 1111–1116, 1985.
54. Kaghad, M., Bonnet, H., Yang, A., Creancier, L., Biscan, J. C., Valent, A., Minty, A., Chalon, P., Lelias, J. M., Dumont, X., Ferrara, P., McKeon, F., and Caput, D. Monoallelically expressed gene related to p53 at 1p36, a region frequently deleted in neuroblastoma and other human cancers. Cell, *90:* 809–819, 1997.
55. Keshelava, N., Zuo, J. J., Widyarame, N. S., Triche, T. J., and Reynolds, C. P. p53 mutations and loss of p53 function confer multidrug resistance in neuroblastoma. Med. Pediatr. Oncol., *35:* 563–568, 2000.
56. Tweddle, D., Malcolm, A., Bown, N., Pearson, A., and Lunec, J. Evidence for the development of p53 mutations after cytotoxic therapy in a neuroblastoma cell line. Cancer Res., *61:* 8–13, 2001.
57. Wen, W. H., Bernstein, L., Lescallett, J., Beazer-Barclay, Y., Sullivan-Halley, J., White, M., and Press, M. F. Comparison of TP53 mutations identified by oligonu-

cleotide microarray and conventional DNA sequence analysis. Cancer Res., *60:* 2716–2722, 2000.

58. Ahrendt, S. A., Decker, P. A., Doffek, K., Wang, B., Xu, L., Demeure, M. J., Jen, J., and Sidransky, D. Microsatellite instability at selected tetranucleotide repeats is associated with p53 mutations in non-small cell lung cancer. Cancer Res., *60:* 2488–2491, 2000.
59. Maurer, B. J., Melton, L., Billups, C., Cabot, M. C., and Reynolds, C. P. Synergistic cytotoxicity in solid tumor cell lines between *N*-(4-Hydroxyphenyl)retinamide and modulators of ceramide metabolism. J. Natl. Cancer Inst., *92:* 1897–1909, 2000.
60. Anderson, C. P., Keshelava, N., Satake, N., Meek, W. H., and Reynolds, C. P. Synergism of buthionine sulfoximine and melphalan against neuroblastoma cell lines derived after disease progression. Med. Pediatr. Oncol., *35:* 659–662, 2000.
61. Cheung, N. V., and Yu, A. L. Immunotherapy of neuroblastoma. *In:* G. M. Brodeur, T. Sawada, Y. Tsuchida, and P. A.Voute (eds.), Neuroblastoma, pp. 1541–1546. Amsterdam: Elsevier Science, 2000.
62. Lavarino, C., Pilotti, S., Oggionni, M., Gatti, L., Perego, P., Bresciani, G., Pierotti, M. A., Scambia, G., Ferrandina, G., Fagotti, A., Mangioni, C., Lucchini, V., Vecchione, F., Bolis, G., Scarfone, G., and Zunino, F. *p53* gene status, and response to platinum/paclitaxel-based chemotherapy in advanced ovarian carcinoma. J. Clin. Oncol., *18:* 3936–3945, 2000.
63. King, T. C., Akerley, W., Fan, A. C., Moore, T., Mangray, S., Hsiu, C. M., and Safran, H. p53 mutations do not predict response to paclitaxel in metastatic nonsmall cell lung carcinoma. Cancer (Phila.), *89:* 769–773, 2000.

[CANCER RESEARCH 62, 1458–1461, March 1, 2002]

Enhanced Photodynamic Therapy Efficacy with Inducible Suicide Gene Therapy Controlled by the grp Promoter[1]

Marian C. Luna, Xinke Chen, Sam Wong, Janet Tsui, Natalie Rucker, Amy S. Lee, and Charles J. Gomer[2]

Clayton Center for Ocular Oncology, Childrens Hospital Los Angeles [M. C. L., S. W., J. T., C. J. G.] and Departments of Pediatrics [C. J. G.], Radiation Oncology [C. J. G.], and Biochemistry and Molecular Biology [X. C., A. S. L.], Keck School of Medicine, University of Southern California, Los Angeles, California 90027

ABSTRACT

Photodynamic therapy (PDT) is a promising cancer treatment involving the administration of a tumor-localizing photosensitizer followed by the photochemical generation of cytotoxic singlet oxygen. PDT elicits strong transcriptional activation of a variety of genes including stress response genes belonging to the glucose-regulated protein (grp) family. Oxidative stress and hypoxia can activate GRP-78, and both of these physiological insults occur in treated tissue during and/or after PDT. In the current study, we evaluated the grp promoter as a PDT-inducible molecular switch for controlled expression of the herpes simplex virus-thymidine kinase (*HSV-tk*) suicide gene in mouse mammary adenocarcinoma (TSA) cells and tumors stably transduced with the G1NaGrpTk retroviral expression vector. We also examined whether PDT-inducible expression of HSV-tk, together with systemic administration of ganciclovir, could enhance the tumoricidal responsiveness of PDT. Inducible expression of HSV-tk was observed after PDT in stably transduced TSA cells grown in culture and in TSA tumors growing in BALB/c mice. We also observed enhanced tumoricidal activity in mice with TSA tumors containing the G1NaGrpTk expression vector treated with PDT plus ganciclovir when compared with either treatment alone. Our results confirm that the grp promoter was able to effectively function as a molecular switch for the inducible expression of the HSV-tk gene after exposure to PDT.

INTRODUCTION

PDT[3] is a localized cancer treatment involving the systemic administration of a tumor-localizing photosensitizer followed by focal light activation (1, 2). This procedure results in the photochemical generation of cytotoxic singlet oxygen within target tissue. The photosensitizer, Photofrin, is approved by the Food and Drug Administration for PDT treatment of endobronchial and esophageal carcinomas (1). PDT clinical trials using PH as well as a variety of second-generation photosensitizers are showing promise in treating malignancies of the brain, peritoneal cavity, skin, bladder, and head and neck, as well as for nononcological disorders such as age-related macular degeneration and psoriasis (1, 2). Initial treatment responses after PDT are routinely positive; however, recurrences can occur, and therefore methods to improve PDT responsiveness are needed.

Positive clinical results have encouraged an expanded mechanistic analysis of cellular and tissue responses associated with PDT as well as the identification of *in vitro* and *in vivo* targets of PDT-mediated cytotoxicity (3). Mitochondria, lysosomes, and the plasma membrane are all identified as subcellular PDT targets (2). PDT is an efficient and rapid inducer of apoptosis and necrosis (4). PDT is also a strong activator of genes encoding for transcription factors, cytokines, and stress-induced proteins (5–8). Members of both the heat shock protein and GRP families are overexpressed after PDT. These proteins function as chaperones of nascent proteins and are also involved in protecting cells by binding to denatured proteins and assisting in proper refolding (7, 8).

Numerous preclinical studies indicate that PDT induces both direct tumor cell kill and vascular damage (2, 3, 9). Vascular damage within tumor tissue is accompanied by tumor tissue hypoxia (10, 11). Likewise, photochemical depletion of oxygen occurs during light illumination at high dose rates (10, 12). Therefore, PDT results in both oxidative stress and hypoxia within target tissue.

The current study builds upon our observation that PDT is an effective inducer of GRP expression and directly examines the effectiveness of the *grp78* promoter to drive inducible gene expression after PDT (8). Several inducible gene expression strategies are being examined for potential therapeutic applications. These procedures allow for temporal and spatial regulation of therapeutic gene activation, which minimizes potential systemic toxicity of cytotoxic gene products. Promising preclinical gene therapy studies have combined radiotherapy together with the radiation-inducible egr-1 promoter to induce therapeutic gene expression (13). We and others have shown that hyperthermia and/or PDT can induce selective and temporal expression of heterologous genes under the control of the heat shock protein promoter (14–16). Recent experiments have also shown strong inducible expression of transgenes under the control of the grp78 promoter or multiple copies of the hypoxic response element in hypoxic tumor tissue (17, 18). We have attempted to take advantage of the fact that both PDT-mediated oxidative stress and PDT-mediated tumor tissue hypoxia can transcriptionally activate GRP-78 (19). We hypothesized that combining PDT with inducible gene therapy using the grp78 promoter to drive selective expression of HSV-tk would improve tumor treatment responses.

MATERIALS AND METHODS

Drugs and Reagents. The photosensitizer Photofrin porfimer sodium was a gift from QLT PhotoTherapeutics, Inc. (Vancouver, British Columbia, Canada) and Axcan Scandipharm, Inc. (Birmingham, AL). The drug was dissolved in 5% dextrose in water to make a 2.5-mg/ml stock solution. Ganciclovir was obtained from Roche Laboratories, Inc. (Nutley, NJ). A 50-mg/ml stock solution of GCV was diluted with normal saline to obtain a 10-mg/ml working solution. The calcium ionophore A-23187 was obtained from Calbiochem (La Jolla, CA), and a stock solution was prepared in ethanol at a concentration of 1 mg/ml.

Cell Culture and *in Vivo* Tumor Models. The TSA mouse mammary adenocarcinoma cell line was used in all *in vitro* and *in vivo* experiments (20). Cells were grown as a monolayer in DMEM supplemented with 4.5 mg/ml glucose, 10% FCS, 2 mM glutamine, and 1% penicillin-streptomycin-neomycin. TSA cells transduced with the G1NaGrpTk vector were maintained in the same culture conditions along with 600 mg/ml of G418. Mammary carcinomas were generated by injection of 10^6 TSA cells or TSA cells infected with the

Received 10/12/01; accepted 1/4/02.

The costs of publication of this article were defrayed in part by the payment of page charges. This article must therefore be hereby marked *advertisement* in accordance with 18 U.S.C. Section 1734 solely to indicate this fact.

[1] This investigation was performed in conjunction with the Clayton Foundation for Research and was supported in part by USPHS Grants RO-1 CA-31230, RO-1 CA-27607, and PO-1 CA59318 from the NIH, Office of Naval Research Grant N000014-91-J-4047 from the Department of Defense, United States Army Medical Research Grant BC981102 from the Department of Defense, the Neil Bogart Memorial Fund of the T. J. Martell Foundation for Leukemia, Cancer and AIDS Research, Susan Komen Breast Cancer Grant BCTR 2000359, and the Las Madrinas Endowment for Experimental Therapeutics in Ophthalmology.

[2] To whom requests for reprints should be addressed, at Childrens Hospital Los Angeles, Mail Stop 67, 4650 Sunset Boulevard, Los Angeles, CA 90027. Phone: (323) 669-2335; Fax: (323) 669-0742; E-mail: cgomer@chla.usc.edu.

[3] The abbreviations used are: PDT, photodynamic therapy; GCV, ganciclovir; grp, glucose regulated protein; HSV, herpes simplex virus; tk, thymidine kinase; PH, Photofrin porfimer sodium.

G1NaGrpTk-inducible expression vector in the hind right flank of 8–12-week-old female BALB/c mice.

Treatment Protocols. *In vitro* photosensitization experiments involved seeding 2×10^6 cells into 100-mm plastic Petri dishes and incubating overnight in complete growth medium to allow for cell attachment. PDT treatments included incubating cells in the dark at 37°C for 16 h with PH (25 μg/ml) in medium containing 5% FCS. Cells were then incubated for an additional 30 min in growth media containing 10% FCS and rinsed in medium without serum. The cells were then exposed to graded doses of red light (570–650 nm) generated by a parallel series of red Milar-filtered 30 W fluorescent bulbs and delivered at a dose rate of 0.35 mW/cm^2 (14). Cell protein was collected at various time intervals after treatment.

In vivo PDT tumor treatments were performed as reported previously on tumors measuring 6 mm in diameter (21). Mice were randomly placed in groups receiving either no treatment, PDT alone, PDT plus GCV, or GCV alone. PDT included an i.v. injection of PH (5 mg/kg), followed 24 h later with tumor-localized laser irradiation using an argon-pumped dye laser emitting red light at 630 nm. A nonthermal light dose rate of 75 mW/cm^2 and a total light dose of 200 J/cm^2 were used for all *in vivo* PDT treatments. GCV was administered as a daily 100 mg/kg i.p. injection starting 1 h before PDT light exposure. After treatment, tumors were measured three times/week. Cures were defined as being disease free for at least 40 days after PDT. Previous studies in our laboratory have shown that mouse tumor responses observed 40 days after PDT treatment remain constant when analyzed at 90 days.

Western Blot Analysis. HSV-tk expression was monitored by Western immunoblot analysis as described previously (14). Control and treated cells were scraped off Petri dishes and transferred to 15-ml tubes. Cell pellets were lysed in SDS loading buffer (4% SDS, 10% glycerol, 4% 2-mercaptoethanol, 0.125 M Tris base, and 0.02% bromphenol blue, pH 6.8). Tumors from treated mice were collected at various times after treatment and homogenized with a Polytron in 1× commercial lysis buffer (Promega Corp., Madison WI). Protein concentrations were determined using Bio-Rad protein analysis solution (Bio-Rad, Hercules, CA). Protein samples (30 μg) were size separated on 10% discontinuous polyacrylamide gels and transferred overnight to nitrocellulose membranes. Filters were blocked for 1 h with 5% nonfat milk and then incubated for 2 h with either rabbit polyclonal anti-TK antibody (provided by W. Summers, Yale University, New Haven, CT) or mouse monoclonal anti-actin antibody (clone C-4; ICN, Aurora, OH). Filters were then incubated with antirabbit or antimouse IgG (Sigma Chemical Co., St. Louis, MO), and the resulting complexes were visualized by enhanced chemiluminescence autoradiography (Amersham Life Science, Chicago, IL).

Statistical Analysis. The PDT treatment response data were evaluated using the log-rank test.

RESULTS AND DISCUSSION

Goals of the present study were to document whether PDT could induce selective expression of an HSV-tk transgene that was under the control of the grp promoter and to determine whether such gene expression could enhance PDT effectiveness. A variety of gene therapy strategies offer potential clinical benefits in the treatment of solid tumors, including the combination of conventional tumor treatments with gene therapy (13–18). Improvements in PDT responsiveness may also be obtained by combining this physical treatment with spatially controlled therapeutic gene therapy. The suicide gene HSV-tk, in combination with the prodrug GCV, has been studied extensively in preclinical and clinical gene therapy studies (22). Replicating DNA is the primary target for GCV in tumors expressing HSV-tk. Nucleoside analogues such as GCV are phosphorylated by HSV-tk. This leads to DNA incorporation of the phosphorylated GCV during S-phase and subsequent cytotoxicity by inhibiting DNA chain elongation. Cell death is most often apoptotic and independent of p53 status (23). A bystander effect for HSV-tk plus GCV results in cytotoxicity to HSV-tk-negative cells as well as to HSV-tk-positive cells (23). This phenomenon helps to compensate for the low transfer rate of genes into target tumor tissue. Numerous other cytotoxic gene products or prodrugs are also being examined in preclinical and clinical gene therapy trials. However, the nonselective toxicity of the therapeutic gene products being examined often necessitates that one minimize the level of systemic gene expression (15). Constitutive expression of some therapeutic genes can induce uncontrolled toxicity to normal tissue as well as to targeted tissue. Likewise, gene therapy expression vectors can leak out of tissue after direct injection. Therefore, interest in methods to minimize systemic toxicity using spatially inducible expression systems has increased.

We have performed proof of principle experiments using tumor cells stably transduced with the HSV-tk suicide gene controlled by the grp promoter. GRPs are stress-inducible proteins localized to the endoplasmic reticulum (24). These calcium-binding proteins serve as chaperones and assist in the folding and assembly of nascent proteins. The grp78 promoter has been shown to be highly inducible under glucose starvation conditions and within the environment of large solid tumors (17). The grp promoter has several unique characteristics, which suggested that it might also be an effective inducible promoter to study with PDT. GRPs are transcriptionally activated by both oxidative stress and hypoxia (8, 19). PDT produces both photochemically generated singlet oxygen and tumor tissue hypoxia secondary to vascular damage (1). The 695-bp *grp-78* promoter fragment inserted into the G1NaGrpTk retroviral construct used in this study contains three copies of the endoplasmic reticulum stress response elements, a TATA element, as well as binding sites for CCAAT, Sp1, and cyclic AMP-responsive element binding protein transcription factors (17, 24). Synthetic endoplasmic reticulum stress response element consisting of two units of a 19-bp sequence motif (CCAAT)N9(CCACG) are responsive to glucose starvation (25). The removal of the noninducible elements is currently being examined in the context of further enhancing the selective inducibility of the grp promoter.

Our first set of experiments examined the *in vitro* effectiveness of PDT to induce expression of HSV-tk under the transcriptional control of the grp promoter (23). Fig. 1 shows Western analysis results demonstrating that PDT efficiently induced HSV-tk expression in TSA cells stably transduced with the G1NA grp-Tk retroviral vector. The PDT doses (0–630 J/m^2) used in these experiments induced from 0 to 80% cytotoxicity, as measured by a clonogenic assay (data not shown). Fig. 1*A* shows HSV-tk expression results for transduced cells collected 12 h after exposure to increasing PDT doses. The calcium ionophore, A-23187, functions as a strong transcriptional activator of *grp-78* and served as a positive control for *in vitro* inducibility of HSV-tk under the control of the grp promoter. *In vitro* PDT doses corresponding to 20–50% survival (*i.e.*, 315–420 J/m^2) were associated with considerable HSV-tk expression. Higher PDT doses resulted in reduced HSV-tk expression, probably because of the severity of the PDT cytotoxic response. Minimal constitutive HSV-tk expression was observed in untreated transduced cells. Likewise, HSV-tk expression was not initiated by PH incubation alone. Kinetic analysis of HSV-tk expression is shown in Fig. 1*B* for transduced cells exposed to a PDT light dose of 315 J/m^2. This PDT dose resulted in 20–30% lethality. HSV-tk expression was observed from 8 to 36 h after treatment.

The second set of experiments examined the *in vivo* efficiency of PDT to function as a molecular switch for the inducible expression of HSV-tk. Stably transduced TSA cells were injected into the hind flank of BALB/c mice and produced reproducible solid tumors amenable to PDT. PDT treatments were started when tumors reached 6 mm in diameter. Fig. 2*A* shows HSV-tk expression 12 h after PDT doses ranging from 50 to 350 J/cm^2. PDT produced significant HSV-tk expression over a large range of light doses. The exceptionally strong *in vivo* inducible expression of HSV-tk may be related to the fact that PDT induces both oxidative stress and tumor tissue hypoxia (3, 9–11). Both of these stress conditions can activate GRP-78 (8, 19). Fig. 2*B*

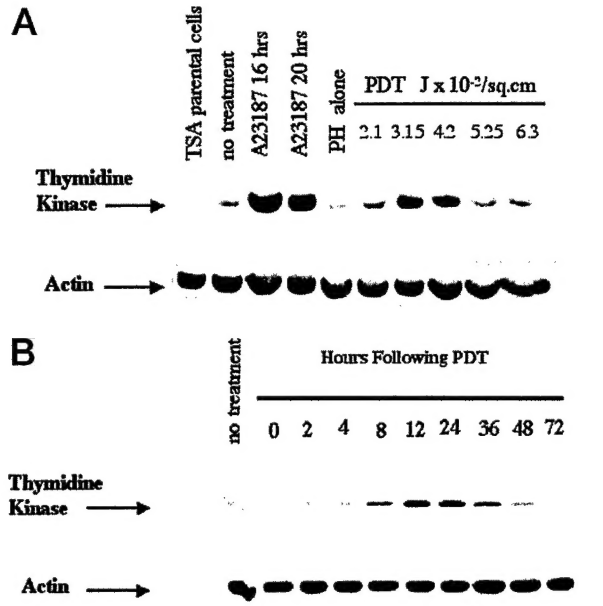

Fig. 1. Inducible expression of HSV-tk is observed in TSA G1NaGrpTk cells after exposure to PDT. Cell lysates were assayed for tk and actin levels by Western immunoblot analysis. *A*, transduced cells were exposed to increasing PDT doses ($0-6.3 \times 10^{-2}$ J/cm^2) and collected 12 h after treatment. Transduced cells exposed to the calcium ionophore A23187 for either 16 or 20 h served as a positive control for grp promoter activation and TK expression. Nontransduced parental TSA cells did not exhibit TK expression. *B*, transduced cells were exposed to a 3.15×10^{-2} J/cm^2 PDT dose and collected at increasing time intervals (0–72 h) after treatment. Expression of actin was used to monitor protein loading.

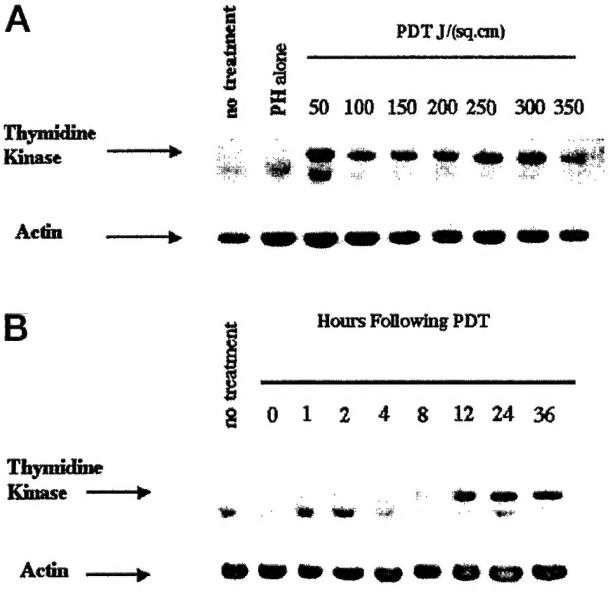

Fig. 2. Inducible expression of HSV-tk is observed in TSA G1NaGrpTk tumors after *in vivo* PDT treatment. Tumor lysates were assayed for TK and actin levels by Western immunoblot analysis. Localized PDT was performed on tumors measuring 6 mm in diameter. *A*, tumors were exposed to increasing doses of PDT (5 mg/kg PH; 0–350 J/cm^2) and collected 12 h after treatment. *B*, for TK kinetic analysis, tumors were exposed to a 100 J/cm^2. PDT dose and tumor lysates were collected at increasing time intervals (0–36 h) after treatment. Expression of actin was used to monitor protein loading.

shows the kinetics of PDT-inducible HSV-tk expression in treated tumor tissue. Expression is observed within 12 h of treatment and continues to be observed 36 h after treatment. PDT elicits rapid hemorrhagic necrosis in tumor tissue, and therefore, analysis of HSV-tk expression at time intervals longer than 36 h was not possible because of the lack of removable tissue (2, 3). Nevertheless, HSV-tk expression in any remaining viable tumor cells would likely occur at time periods longer than 36 h because of the prolonged hypoxia induced by PDT (1, 3). These experiments demonstrate a strong and prolonged expression of a therapeutic transgene under the control of the grp promoter.

We next examined the therapeutic efficacy of the PDT-inducible gene therapy in BALB/c mice transplanted with s.c. tumors derived from stably transduced TSA cells. Tumors were again treated when they reached 6 mm in diameter. Fig. 3 shows tumor response data for mice treated with PDT alone, GCV alone, or a combination of PDT plus GCV. The PDT dose (5 mg/kg, 200 J/cm^2) was chosen because: (*a*) it elicited a positive inducible HSV-tk expression in tumor tissue as shown in Fig. 2; and (*b*) it produces a 50% cure rate in this tumor model when used alone. We have shown previously that this tumor response level allows for effective evaluation of combination therapies involving PDT and antiangiogenic therapy (26). A standard multiday administration regimen of GCV was used (17, 20). GCV by itself did not result in any cures in the transduced TSA tumors, probably because of the minimal level of hypoxia in these 6-mm lesions. PDT alone resulted in a 50% tumor cure rate, whereas the combination of PDT and GCV resulted in 100% cures. The combination of PDT plus PDT-inducible gene therapy showed a significantly enhanced tumor response compared with PDT alone ($P = 0.0066$). Treatment of nontransduced parental tumors with GCV did not affect PDT sensitivity (data not shown). These results indicate that HSV-tk gene expression under the control of the grp promoter was effective at enhancing the tumoricidal response of PDT when the prodrug GCV was added to the treatment regimen.

PDT-responsive, promoter-mediated gene activation has been demonstrated previously using the heat shock protein promoter (14). The results of the current study extend these observations and demonstrate the effectiveness of PDT to activate an HSV-tk gene controlled by the grp promoter. This study also illustrates the feasibility of using PDT-controlled, HSV-tk suicide gene therapy in the treatment of solid tumors. Clinically relevant PDT doses and treatment parameters were used in this study, suggesting that PDT-inducible gene therapy could be expected to function within current clinical treatment protocols. Studies are in progress to evaluate the *in vivo* responsiveness of PDT-mediated gene therapy after direct injection of adenoviral expression vectors.

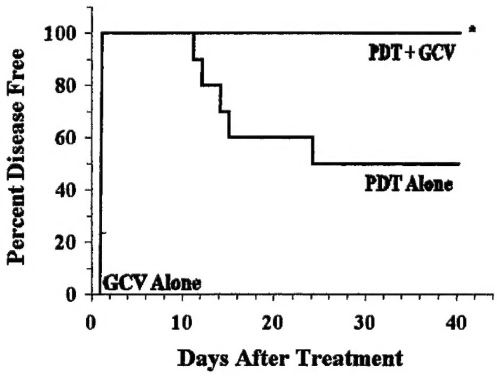

Fig. 3. Inducible gene therapy using the grp promoter to drive expression of the HSV-tk suicide gene enhances the tumoricidal action of PDT. Treatment of TSA G1NaGrpTk tumors with a combination of PDT and GCV resulted in increased tumor cures compared with PDT treatment alone. BALB/c mice with 6-mm diameter TSA G1NaGrpTk tumors were exposed to either PDT + GCV (10 daily injections of GCV (100 mg/kg per dose) commencing 1 h before a single PDT treatment (5 mg/kg PH, 200 J/cm^2; $n = 13$); PDT alone (the identical PDT treatment without GCV; $n = 10$), or GCV alone (10 daily injections of GCV; $n = 8$). Mice were monitored for tumor recurrences three times per week for 40 days. *, statistically significant difference in percentage of cures between PDT alone *versus* PDT + GCV ($P = 0.0066$).

ACKNOWLEDGMENTS

We thank QLT PhotoTherapeutics, Inc., Vancouver, British Columbia, Canada and Axcan Scandipharm, Inc., Birmingham, AL for the generous gift of Photofrin; William C. Summers, Yale University, for providing HSV-tk antibody; Earl Leonard for assistance with statistical analysis; and Angela Ferrario for helpful discussions.

REFERENCES

1. Dougherty, T. J., Gomer, C. J., Henderson, B. W., Jori, G., Kessel, D., Korbelik, M., Moan, J., and Peng, Q. Photodynamic Therapy. J. Natl. Cancer Inst., *90.* 889–905, 1998.
2. Fisher, A. M. R., Murphree, A. L., and Gomer, C. J. Clinical and preclinical photodynamic therapy. Lasers Surg. Med., *17:* 2–31, 1995.
3. Henderson, B. W., and Dougherty, T. J. How does photodynamic therapy work? Photochem. Photobiol., *55:* 145–157, 1992.
4. Oleinick, N. L., and Evans, H. E. The photobiology of photodynamic therapy: cellular targets and mechanisms. Radiat. Res., *150:* S146–S156, 1998.
5. Luna, M. C., Wong, S., and Gomer, C. J. Photodynamic therapy mediated induction of early response genes. Cancer Res., *53:* 1374–1380, 1994.
6. Gollnick, S. O., Liu, X., Owczarczak, B., Musser, D. A., and Henderson, B. W. Altered expression of interleukin 6 and interleukin 10 as a result of photodynamic therapy *in vivo*. Cancer Res., *57:* 3904–3909, 1997.
7. Gomer, C. J., Ryter, S., Ferrario, A., Rucker, N., Wong, S., and Fisher, A. Photodynamic therapy mediated oxidative stress can induce heat shock proteins. Cancer Res., *56:* 2355–2360, 1996.
8. Gomer, C. J., Ferrario, A., Rucker, N., Wong, S., and Lee, A. Glucose regulated protein (GRP-78) induction and cellular resistance to oxidative stress mediated by porphyrin photosensitization. Cancer Res., *51:* 6574–6579, 1991.
9. Fingar, V. H., Wieman, T. J., Wiehle, S. A., and Cerrito, P. B. The role of microvascular damage in photodynamic therapy: the effect of treatment on vessel constriction, permeability, and leukocyte adhesion. Cancer Res., *52:* 4914–4921, 1992.
10. Sitnik, T. M., Hampton, J. A., and Henderson, B. W. Reduction of tumor oxygenation during and after photodynamic therapy *in vivo*: effects of fluence rate. Br. J. Cancer, *77:* 1386–1394, 1998.
11. van Geel, I. P. J., Oppelaar, H., Rijken, P. F. J. W., Bernsen, H. J. J. A., Hagemeier, N. E. M., van der Kogel, A. L., Hodgkiss, R. J., and Stewart, F. A. Vascular perfusion and hypoxic areas in RIF-1 tumours after photodynamic therapy. Br. J. Cancer, *73:* 288–293, 1996.
12. Foster, T. H., Murant, R. S., Byrant, R. G., Knox, R. S., Gibson, S. L., and Hilf, R. Oxygen consumption and diffusion effects in photodynamic therapy. Radiat. Res., *126:* 296–303, 1991.
13. Hallahan, D. E., Mauceri, H. J., Seung, L. P., Dunphy, E. J., Wayne, J. D., Hanna, N. N., Toledano, A., Hellman, S., Kufe, D. W., and Weichselbaum, R. R. Spatial and temporal control of gene therapy using ionizing radiation. Nat. Med., *1:* 786–791, 1995.
14. Luna, M., Ferrario, A., Wong, S., Fisher, A. M. R., and Gomer, C. J. Photodynamic therapy mediated oxidative stress as a molecular switch for the temporal expression of genes ligated to the human heat shock promoter. Cancer Res., *60:* 1637–1644, 2000.
15. Huang, Q., Hu, J. K., Lohr, F., Zhang, L., Braun, R., Lanzen, J., Little, J. B., Dewhirst, M. W., and Li, C-Y. Heat-induced gene expression as a novel targeted cancer gene therapy strategy. Cancer Res., *60:* 3435–3439, 2000.
16. Blackburn, R. V., Galoforo, S. S., Corry, P. M., and Lee, Y. J. Adenoviral-mediated transfer of a heat-inducible double suicide gene into prostate carcinoma cells. Cancer Res., *58:* 1358–1362, 1998.
17. Gazit, G., Hung, G., Chen, X., Anderson, W. F., and Lee, A. S. Use of the glucose starvation inducible grp-78 promoter in suicide gene therapy of murine fibrosarcoma. Cancer Res., *59:* 3100–3106, 1999.
18. Dachs, G. U., Patterson, A. V., Firth, J. D., Ratcliffe, P. J., Townsend, K. M., Stratford, I. J., and Harris, A. L. Targeting gene expression to hypoxic tumor cells. Nat. Med., *3:* 515–520, 1997.
19. Koonig, A. C., Auger, E. A., Chen, E. Y., and Giaccia, A. J. The regulation of GRP78 and messenger RNA levels by hypoxia is modulated by protein kinase C activators and inhibitors. Radiat. Res., *138:* S60–S63, 1994.
20. Chen, X., Zhang, D., Dennert, G., Hung, G., and Lee, A. S. Eradication of murine mammary adenocarcinoma through HSV-tk expression directed by the glucose-starvation inducible grp78 promoter. Breast Cancer Res. Treat., *59:* 81–90, 2000.
21. Ferrario, A., Kessel, D., and Gomer, C. J. Metabolic properties and photosensitizing responsiveness of mono-L-aspartyl chlorin e6 in a mouse tumor model. Cancer Res., *52:* 2890–2893, 1992.
22. Moolten, F. L., and Wells, J. M. Curability of tumors bearing herpes thymidine kinase genes transferred by retroviral vectors. J. Natl. Cancer Inst., *82:* 297–300, 1990.
23. Mesnil, M., and Yamasaki, H. Bystander effect in herpes simplex virus-thymidine kinase/ganciclovir cancer gene therapy. Role of gap-junctional intercellular communication. Cancer Res., *60:* 3989–3999, 2000.
24. Lee, A. S. The glucose regulated proteins: stress induction and clinical applications. Trends Biochem. Sci., *26:* 504–510, 2001.
25. Roy, B., and Lee, A. S. The mammalian endoplasmic reticulum stress response element consists of an evolutionarily conserved tripartite structure and interacts with a novel stress-inducible complex. Nucleic Acids Res., *27:* 1437–1443, 1999.
26. Ferrario, A., von Tiehl, K. F., Rucker, N., Schwartz, M. A., Gill, P. S., and Gomer, C. J. Antiangiogenic treatment enhances photodynamic therapy responsiveness in a mouse mammary carcinoma. Cancer Res., *60:* 4066–4069, 2000.